#16

AEDC-TR-77-117

cy 3

INFLUENCES OF SWAY BRACES AND MOUNTING GAPS ON THE STATIC AERODYNAMIC LOADING OF EXTERNAL STORES

R. E. Dix
ARO, Inc., a Sverdrup Corporation Company

PROPULSION WIND TUNNEL FACILITY
ARNOLD ENGINEERING DEVELOPMENT CENTER
AIR FORCE SYSTEMS COMMAND
ARNOLD AIR FORCE STATION, TENNESSEE 37389

February 1978

Final Report for Period October 1, 1976 - September 30, 1977

Approved for public release; distribution unlimited.

Prepared for

AIR FORCE ARMAMENT LABORATORY/DLJC
EGLIN AIR FORCE BASE, FLORIDA 32542

APPROVAL STATEMENT

This report has been reviewed and approved.

Alexander F. Money

ALEXANDER F. MONEY
Project Manager, Research Division
Directorate of Test Engineering

Approved for publication:

FOR THE COMMANDER

Marion L. Laster

MARION L. LASTER
Director of Test Engineering
Deputy for Operations

REPORT DOCUMENTATION PAGE		READ INSTRUCTIONS BEFORE COMPLETING FORM
1. REPORT NUMBER AEDC-TR-77-117	2. GOVT ACCESSION NO.	3. RECIPIENT'S CATALOG NUMBER
4. TITLE (and Subtitle) INFLUENCES OF SWAY BRACES AND MOUNTING GAPS ON THE STATIC AERODYNAMIC LOADING OF EXTERNAL STORES		5. TYPE OF REPORT & PERIOD COVERED Final Report - October 1, 1976 - September 30, 1977
		6. PERFORMING ORG. REPORT NUMBER
7. AUTHOR(s) R. E. Dix, ARO, Inc., a Sverdrup Corporation Company		8. CONTRACT OR GRANT NUMBER(s)
9. PERFORMING ORGANIZATION NAME AND ADDRESS Arnold Engineering Development Center/DOT Air Force Systems Command Arnold Air Force Station, Tennessee 37389		10. PROGRAM ELEMENT, PROJECT, TASK AREA & WORK UNIT NUMBERS Program Element 62602F
11. CONTROLLING OFFICE NAME AND ADDRESS Arnold Engineering Development Center/DOS Arnold Air Force Station Tennessee 37389		12. REPORT DATE February 1978
		13. NUMBER OF PAGES 137
14. MONITORING AGENCY NAME & ADDRESS(if different from Controlling Office)		15. SECURITY CLASS. (of this report) UNCLASSIFIED
		15a. DECLASSIFICATION/DOWNGRADING SCHEDULE N/A

16. DISTRIBUTION STATEMENT (of this Report)

Approved for public release; distribution unlimited.

17. DISTRIBUTION STATEMENT (of the abstract entered in Block 20, if different from Report)

18. SUPPLEMENTARY NOTES

Available in DDC

19. KEY WORDS (Continue on reverse side if necessary and identify by block number)

F-4C aircraft
sway braces
external stores
aerodynamic characteristics
aerodynamic loading
captive tests
trajectories
transonic flow
wind tunnel tests

20. ABSTRACT (Continue on reverse side if necessary and identify by block number)

As the scale factor applied in the design of wind tunnel models is reduced, many details of the configuration being simulated are customarily omitted. A series of experiments was conducted in the Aerodynamic Wind Tunnel (4T) of the Propulsion Wind Tunnel Facility at the Arnold Engineering Development Center to evaluate the effect on captive store loading of model details such as sway braces and mounting gaps existing between store and aircraft

DD FORM 1 JAN 73 1473 EDITION OF 1 NOV 65 IS OBSOLETE

20. ABSTRACT (Continued)

components. Six components of aerodynamic loads acting on both pylon- and rack-mounted stores in the captive position were measured, a limited number of store separation trajectories was predicted using the captive trajectory system, and a brief comparison of wind tunnel and in-flight measurements of captive loads was made. It was determined that the effects of mounting gaps or flow ventilation passages were generally small, but that sway braces can significantly influence both captive loads and separation trajectories. It was also observed that better agreement between wind tunnel and in-flight measurements of captive store loading resulted when mounting gaps and sway braces were simulated on the wind-tunnel models.

AFSC
Arn-ld AFS Tenn

PREFACE

The work reported herein was conducted by the Arnold Engineering Development Center (AEDC), Air Force Systems Command (AFSC), at the request of the Air Force Armament Laboratory (AFATL), under Program Element 62602F. The monitor of the project was Lt. Norman O. Speakman, AFATL (DLJC). The results were obtained by ARO, Inc., AEDC Division (a Sverdrup Corporation Company), operating contractor for the AEDC, AFSC, Arnold Air Force Station, Tennessee, under ARO Project Number P34A-K6A. Analysis of the data was completed in August 1977, and the manuscript was submitted for publication on November 2, 1977.

CONTENTS

	Page
1.0 INTRODUCTION	7
2.0 EXPERIMENTAL APPARATUS	
2.1 Test Facility	7
2.2 Models	8
2.3 Instrumentation	10
3.0 DESCRIPTION OF TESTS	
3.1 Flow Conditions and Test Procedures	10
3.2 Corrections	11
3.3 Precision of Measurements	11
4.0 DISCUSSION OF RESULTS	
4.1 Pylon-Mounted Stores	11
4.2 Rack-Mounted Stores	13
5.0 CONCLUSIONS	14
REFERENCES	15

ILLUSTRATIONS

Figure	
1. Pylon-Mounted Store with Thermographic Paint Pattern for Heat-Transfer Measurements in Flight	17
2. Schematic Illustration of a Typical Model Installation in Tunnel 4T	19
3. Schematic Illustration of the Captive Trajectory System (CTS)	20
4. Outline Drawing of the 1/20-Scale Model of the F-4C Aircraft	21
5. Details of the Models of the F-4C Pylons	22
6. Details of the Simulated Sway Braces for the Left Inboard Pylon (LIB)	23
7. Details of the Model of the Triple Ejector Rack	24
8. Photograph of the Detailed and Simplified Triple Ejector Rack Models	25
9. Internal Bracket-Support Balance/Store Installations	26
10. Outline Drawings of the Store Models	28
11. Locations of the Store Models on the Left Inboard Pylon	29

Figure Page

12. Effect of a Ventilated Supporting Bracket in the Presence of Pylon Sway Braces on the Static Aerodynamic Loads Acting on an Unstable Pylon-Mounted Store 30
13. Effect of Pylon Sway Braces in the Presence of a Ventilated Supporting Bracket on the Static Aerodynamic Loads Acting on an Unstable Pylon-Mounted Store 42
14. Isolated Effect of a Ventilated Supporting Bracket on the Static Aerodynamic Loads Acting on a Stable Pylon-Mounted Store 54
15. Isolated Effect of Pylon Sway Braces on the Static Aerodynamic Loads Acting on a Stable Pylon-Mounted Store 66
16. Combined Effects of Both a Ventilated Supporting Bracket and Pylon Sway Braces on the Static Aerodynamic Loads Acting on a Stable Pylon-Mounted Store 78
17. Isolated Effect of a Ventilated Supporting Bracket and Triple Ejector Rack Model on the Static Aerodynamic Loads Acting on a Stable, Triple Ejector Rack-Mounted Store 90
18. Isolated Effect of Triple Ejector Rack Sway Braces on the Static Aerodynamic Loads Acting on a Stable Triple Ejector Rack-Mounted Store 102
19. Combined Effects of Both a Ventilated Supporting Bracket and Triple Ejector Rack and Triple Ejector Rack Sway Braces on the Static Aerodynamic Loads Acting on a Stable Triple Ejector Rack-Mounted Store 114

TABLES

1. Miscellaneous Dimensions of Store Models 126
2. Uncertainty Intervals in Force and Moment Coefficients for Store Models 127

Page

APPENDIXES

A. EFFECT OF SWAY BRACES ON STORE SEPARATION TRAJECTORIES . . .129

B. COMPARISON OF FLIGHT TEST DATA WITH WIND TUNNEL DATA INCLUDING SWAY BRACES 132

NOMENCLATURE 134

1.0 INTRODUCTION

Ground testing of flight-rated vehicles and articles (whether on sleds, in wind tunnels, environmental chambers, or other laboratory facilities) is often accomplished with small models scaled from the full-size body. For most experiments involving the use of models, costs are an important consideration. Consequently, for economy, it is customary to omit many small features of the full-size body from the model. Beyond a fundamental resemblance, therefore, faithful geometric similitude is often a goal rather than a fact.

A recent series of experiments, conducted in the Propulsion Wind Tunnel (PWT) facility of the Arnold Engineering Development Center (AEDC), was designed to investigate both the necessity and feasibility of simulating certain small physical features associated with the installation of stores on the exterior of an aircraft. Specifically, the investigation was limited to the influence exerted on the static aerodynamic loading of a captive store by the presence of two features of store-to-aircraft installations: sway braces and openings through which flow could pass between closely spaced items such as stores, racks, and pylons. An indication of the potential effect of sway braces emerged during a recent flight test in which thermographic paint was used to obtain heat-transfer information for a store (Ref. 1). Photographs of the store taken before and after a flight are presented in Figs. 1a and b, respectively. The phase of the paint changed from solid to liquid during the flight, and flowed from the concentric-ring pattern applied before the flight to a pattern conforming to streamlines of the air deflected around the sway brace pads and the nose of the pylon. Ultimate development of the flow over the store was clearly influenced by the presence of the sway braces. Although the flight data applied only to pylon-mounted stores, the scope of the wind tunnel experiments discussed herein was broadened to include a rack-mounted configuration as well as two pylon-mounted stores. The experiments were conducted with 1/20-scale models of contemporary configurations (rather than simplified shapes) to place the results in immediate context.

2.0 EXPERIMENTAL APPARATUS

2.1 TEST FACILITY

Experiments were conducted in the Aerodynamic Wind Tunnel (4T) of the PWT, a closed-circuit design in which continuous flow can be maintained at various density settings. Mach number in the free stream can be set at any value from 0.1 to 1.3. Nozzle blocks can be installed to provide discrete Mach numbers of 1.6 and 2.0. Stagnation pressure can be maintained at any value from 300 to 3,700 psfa. The test section is 4-ft square and 12.5-ft long with perforated, variable porosity (0.5- to 10-percent open) walls.

It is completely enclosed in a plenum chamber from which the air can be evacuated, allowing part of the tunnel airflow to be removed through the perforated walls of the test section.

Models are supported in the test section with a conventional strut-sting system. A model can be pitched from approximately -12 to 28 deg with respect to the centerline of the tunnel. A capability of rolling a model from -180 to 180 deg about the centerline of the sting is also available. An illustration of a typical model installed for testing is presented in Fig. 2.

A second support system is available in the wind tunnel, and is used primarily for studies of trajectories of stores separating from aircraft, i.e., the captive trajectory system (CTS). Using the CTS, a store can be moved in six degrees of freedom with respect to the aircraft. Instruments monitoring tunnel flow conditions and relative position and attitude of all models, together with a strain-gage balance mounted within the store model, provide the input information for a digital computer that performs calculations resulting in electrical commands to servo systems that move the store model. A schematic illustration of the CTS is provided in Fig. 3.

2.2 MODELS

2.2.1 Aircraft

Since a model was available from the experiments described in Refs. 2 and 3, the F-4C was selected as parent aircraft. (An outline drawing of the F-4C model is presented in Fig. 4.) Throughout the experiments, the tail surfaces of the F-4C were omitted. Also, airflow was allowed into the engine intakes of the model, through internal ducting, and out through cruise-configuration exhaust ports. Since the CTS was used during the series of experiments for some trajectory predictions, the aircraft model was installed inverted in the test section.

2.2.2 Pylons

All wing pylons and a centerline weapons adaptor were installed throughout the experiments; however, store models were mounted on the left inboard pylon (LIB) only. Details of the pylon models are presented in Fig. 5.

To evaluate the effect of sway braces on captive store loading, appropriately scaled sway braces for the model pylon were fabricated as separate components that could be attached and removed without affecting the store model. Dimensions and location of the pylon sway braces are presented in Fig. 6.

2.2.3 Triple Ejector Rack

For experiments involving the smaller, rack-mounted store configuration, a model of the triple ejector rack (TER), USAF version 9A, was used. (A drawing of the TER model is presented in Fig. 7.) Captive store loads were recorded for the store model mounted on TER station 1 (bottom station) only. Throughout the experiments, dummy models of the same store configuration were mounted on the "shoulder" stations, 2 and 3.

Both sway braces and mounting gaps were simulated on the TER model. Just as for the pylon model, the scaled sway braces were fabricated with a provision for easy installation and removal. To determine the effect of the mounting gaps that exist between the ejector racks and the body of the triple suspension assembly, slots approximating the actual gaps were cut into the model at appropriate locations, as in Fig. 7. Wax was used when required to seal the slots. The sway brace and ventilating slot features had not been included in previous models of the TER. (A photograph of the "detailed" TER model is presented in Fig. 8, in which the sway braces and slots are indicated, with an older simplified TER model alongside for comparison.)

2.2.4 Internal Balance-Supporting Brackets

Two typical bracket-supported installations are illustrated in Fig. 9. The store model is securely fastened to one end of a six-component strain-gage balance. The other end of the balance is firmly supported by a rigid bracket protruding through the upper surface of the store model and attached to the pylon or rack. To allow unrestricted reaction of the store model (and hence the balance) to aerodynamic loading, the opening in the upper surface of the store model was made large enough to ensure a clearance of approximately 0.050 in. around the bracket.

Separation between the upper surface of a store model and the lower surface of the pylon was set at 0.125 in., approximating the nominal gap maintained between store and aircraft models during dual-support experiments. The 0.125-in. gap, corresponding to a full-size gap of 2.5 in., was about twice a typical value, but large enough to allow study of the effect of the presence of a solid internal balance-supporting bracket in the wind tunnel. Separation for the rack-mounted store model was a more realistic 0.04 in. (0.8 in. full scale).

In the exposed portion of the balance-supporting bracket, a slotted opening was cut through the solid blade to simulate the opening existing in full-size installations between forward and aft suspension lugs. To reestablish a solid surface as necessary during the experiments, the slot was filled with a putty that could be easily removed. The slots are depicted in Fig. 9.

2.2.5 Stores

During the process of selecting store configurations for the investigation, stores were classified as either pylon-mounted (relatively large stores normally carried one per pylon), or rack-mounted (relatively small stores, carried in clusters on multiple suspension devices). Two pylon-mounted configurations were selected, the unstable Black Crow gun pod, and the stable M-118 bomb. Only one rack-mounted store configuration was used, the stable MK 83 low-drag bomb. Sketches of the store models are shown in Fig. 10, and characteristic dimensions and mass properties are presented in Table 1. The store models were supported with the longitudinal axis parallel to the lower surface of the pylon, i.e., with a 1-deg nose-down attitude with respect to the waterline of the aircraft model. Respective locations of the store models on the left inboard pylon are presented in Fig. 11.

2.3 INSTRUMENTATION

Conventional strain-gage balances were used to sense the aerodynamic forces acting on the store models. The six conventional components of forces and moments were resolved. Balance wiring was routed from the store model through channels in the support bracket into the aircraft and thence to appropriate signal processing equipment. The gravimetric angle of attack of the F-4C aircraft model was sensed with an oil-damped pendulum fitted with strain gages and mounted in the aircraft model.

3.0 DESCRIPTION OF TESTS

3.1 FLOW CONDITIONS AND TEST PROCEDURES

Aerodynamic forces and moments acting on the store models were measured at nominal free-stream Mach numbers of 0.6, 0.7, 0.8, 0.9, 1.1, and 1.2. Reynolds number was maintained at approximately 3.5 x 10^6 per foot throughout the tests.

During the tests, flow conditions were established before the attitude of the model was set. Then, a pitch-pause technique was used, in which the attitude of the aircraft model was set and maintained for approximately 3 sec at each value of a specified sequence of attitudes. Data were recorded at the end of a pause, after which the model attitude was changed to the next sequential value. After completing a sequence of attitudes at a fixed Mach number, flow conditions were changed to establish the next specified Mach number, and the pitch-pause sequence was repeated.

3.2 CORRECTIONS

Calibrations of the balance for deflections of the mounting point of the store model as a function of impressed load were used to identify contributions of balance flexibility to the attitude of the store model. The calibration data were used in the data reduction equations to derive the correct gravimetric attitude of the store model.

3.3 PRECISION OF MEASUREMENTS

Uncertainty intervals (including 95 percent of the calibration data) for the basic flow parameters, i.e., p_{t_∞} and M_∞, were estimated from both repeated calibrations of the instrumentation and the repeatability and uniformity of the free-stream flow in the test section during calibration of the tunnel. Uncertainty intervals for the instrumentation systems were estimated from repeated calibrations of the systems using secondary standards with accuracies traceable to the National Bureau of Standards. Uncertainty intervals for values of forces and moments derived from the output of the balance gages were determined from a root-mean-square analysis of the calibration data from the balance. Values of the above uncertainties and estimates of instrument bias were combined using the Taylor series method of error propagation to determine the precision of the force and moment coefficients. Values of the uncertainty intervals for the force and moment coefficients for the models included in the study are presented in Table 2. For all flow conditions, the uncertainty interval was ±0.15 deg for the angle of attack, and ±0.004 for Mach number.

4.0 DISCUSSION OF RESULTS

4.1 PYLON-MOUNTED STORES

In Figs. 12 through 16, the effects of using ventilated supporting brackets and simulated sway braces are presented for the Black Crow and M-118 store configurations. On the left-hand page of each figure, two curves are presented as a function of the angle of attack of the store model. One curve represents values of the coefficient of the specified static aerodynamic load component acting on the store model as installed with a specified physical feature, either vents or sway braces. The other curve represents data for the same configuration of the store model installed without the physical feature. Presented on the opposite page is the incremental effect on the load component coefficient of using the specified physical feature, i.e., the difference between values of the load component coefficient obtained with the feature and without the feature.

Because of the manner in which the experiments were conducted, it was possible to isolate the effects of ventilating slots and sway braces for the loads acting on the M-118 and the MK 83. However, data were not recorded for one of the store/pylon configurations necessary to allow isolation of the two effects for the Black Crow.

The effect of ventilating the internal balance-supporting bracket (in the presence of the sway braces) is presented for the Black Crow in Fig. 12. Bands of diagonal lines on the graphs delineate the precision of the data. Normal-force coefficient is relatively unaffected for all conditions except extreme negative angles of attack and supersonic Mach numbers, for which an increase occurs. It appears that the presence of the vent permits a three-dimensional flow alleviation on the upper surface of the store. More negative pitching-moment coefficients, corresponding to the increased normal-force coefficients, indicate negligible shift in the center of pressure from a position aft of the cg of the store. Side-force coefficient is unaffected by the presence of the vent, but yawing-moment coefficient is affected at the higher angles of attack at all Mach numbers. Such a condition is associated with a shift in the lateral center of pressure. It is clear that axial-force and rolling-moment coefficients are unaffected by the presence of the ventilating slot.

In Fig. 13, the effect of adding sway braces to the pylon (in the presence of the vented bracket) is presented. A slight effect upon the normal-force and yawing-moment coefficients at high angles of attack is noted. Axial-force and rolling-moment coefficients acting on the Black Crow are unaffected by the presence of sway braces.

For the M-118, the isolated effects of the ventilated bracket are presented in Fig. 14. As in the case of the Black Crow, the significant effects are upon the normal-force, pitching-moment, and yawing-moment coefficients. Unlike the Black Crow, however, the rolling-moment coefficient is affected, indicating a different flow pattern over the fins of the stable M-118 because of the slot. Likewise, in Fig. 15, where the isolated effects of the presence of sway braces are presented, it is clear that the primary effect is again on the normal-force, pitching-moment, and yawing-moment coefficients. Sway braces, however, influence the side-force coefficient more than the vented bracket. The relationships between changes in normal-force and pitching-moment coefficients and in side-force and yawing-moment coefficients are insufficiently clear to justify more than a general estimate of the effects of the vented bracket and the sway braces: the flow pattern over the store is altered by either feature so as to produce different moments, but with little change in forces; hence, a shift in center of pressure is the likely result of the simulation of these features. However, axial force is unaffected by the presence of either a ventilated bracket or sway braces.

The combined effects of both the vented bracket and sway braces are presented in Fig. 16 for the M-118. From these graphs, it is possible to deduce that the effects of the vent and the sway braces cannot be superimposed to predict the effect of the two features simulated simultaneously. By choosing a Mach number and angle of attack for which the force or moment coefficient increments are greater than the uncertainty of the measurement, it can be seen that it is not consistently possible to add the independently measured vent and sway brace effects to produce the value of the effect of the combined simulation. Above 4-deg angle of attack of the store, significant effects on normal-force and side-force coefficients exist at all Mach numbers. Pitching-and yawing-moment coefficients may be affected at any angle of attack, depending on Mach number. Axial-force and rolling-moment coefficients are virtually unaffected by simulating both the ventilation provided by lug suspension and the sway braces.

Measurable effects upon the aerodynamic loading of captive, pylon-mounted stores can be generated as a result of simulating flow passages and/or sway braces. However, the conditions for which the largest effects occur are generally unimportant, i.e., either the Mach number is unrealistically high or the angle of attack is likewise too great.

4.2 RACK-MOUNTED STORES

Effects of simulating two physical details existing on a TER - the openings between various components and surfaces through which flow may pass and the sway braces on all three stations for mounting stores - are presented in Figs. 17 through 19 for the MK 83 store configuration. The isolated effects of simulating the flow passages, or vents, on the TER are presented in Fig. 17. Normal-, side-, and axial-force and rolling-moment coefficients are unaffected. Only the pitching- and yawing-moment coefficients are altered, and then, with any significance, only at the higher Mach numbers for a few moderate angles of attack. No net change in total force results, but the corresponding moments are affected. For these cases, it is probable that regions of low flow velocity are relieved by the vents, with a concomitant alteration of the pressure distribution over the store model.

The isolated effects of sway braces are presented in Fig. 18. Clearly, the effects of simulating sway braces are significant. Not only are there significant differences in normal-force coefficient at all conditions and in side-force coefficient at supersonic Mach numbers, but there is also an increase in axial-force coefficient at all subsonic Mach numbers. Rolling-moment coefficient is essentially unaffected. Both pitching- and yawing-moment coefficients are substantially affected, especially in the low angle-of-attack range in which many trim condition store releases are initiated. It should be noted that the effects of vents, or flow passages, discussed above, although measurable, are not at all as severe as the effects of sway braces, especially in the conventional range of Mach number and angle of attack.

Comparing Fig. 19, in which the effects of simultaneously simulating vents and sway braces are presented, with Figs. 17 and 18, in which the isolated effects of the vents and sway braces are presented, respectively, it is clear that, just as for the pylon-mounted stores, the effects are not totally independent. Since the combined vent and sway brace installation more closely simulates the full-size configuration, and since the effects of simulating the features are so large in certain cases, it appears advisable to include the vents and sway braces on models of any scale, whenever physically possible.

Two additional indications of the effects and advisability of simulating sway braces and vents for wind tunnel experiments can be gained from an examination of separation trajectories for the store configurations considered herein, and a comparison of wind tunnel and flight test results for one of the same configurations. Some separation trajectory data are presented in Appendix A, and a brief comparison of wind tunnel and flight test data sets is presented in Appendix B.

5.0 CONCLUSIONS

In a series of wind tunnel experiments conducted with 1/20-scale models, static aerodynamic loads acting on captive stores were measured both with and without two physical features not normally simulated for models of such small size: mounting gaps between adjacent components through which flow can pass, and sway braces. The effects on captive store loading were evaluated for both pylon- and TER-mounted stores carried by a contemporary fighter aircraft on under-wing pylons. As a result of an analysis of the data, the following conclusions can be made:

1. The simulation of vents between adjacent hardware components exert measurable but minor influence on the pitching- and yawing-moment coefficients acting on both pylon- and TER-mounted captive store models at low-to-moderate angles of attack and transonic Mach numbers. Negligible effect on normal- and side-force coefficients results from the simulation of vents.

2. Sway braces can exert a measurable influence on the normal-force, pitching-moment, and yawing-moment coefficients acting on pylon-mounted stores. However, for TER-mounted stores, the influence of sway braces is considerably more significant for all load components except rolling-moment coefficient.

3. Rolling-moment is unaffected by the presence of either sway braces or vents, for both pylon- and rack-mounted stores.

4. The effects of simulating flow passages and sway braces are not independent, i.e., the effects become coupled when both features are simulated simultaneously.

5. There is evidence to indicate that, for both pylon-and TER-mounted stores, predictions of separation trajectories obtained by using the CTS can be significantly different when sway braces are simulated.

6. For at least one store, better agreement between flight test measurements and wind tunnel measurements of the static aerodynamic loads acting on the captive store resulted when sway braces were simulated on the wind tunnel model.

REFERENCES

1. Matthews, R. K. and Key, J. C. "Comparison of Wind-Tunnel and Flight-Test Heat-Transfer Measurements on a Pylon-Mounted Store." Journal of Aircraft, Vol. 14, No. 6, June 1977, pp. 565-568.

2. Dix, R. E. "Comparison of Two Methods Used to Measure Aerodynamic Loads Acting on Captive Store Models in Wind Tunnel Tests." AEDC-TR-76-122 (AD-A030208), September 1976.

3. Dix, R. E. "Evaluation of an Internal Balance-Supporting Bracket Simulating Lug Suspension for Captive Stores in Wind Tunnel Tests." AEDC-TR-76-117 (AD A030 603), October 1976.

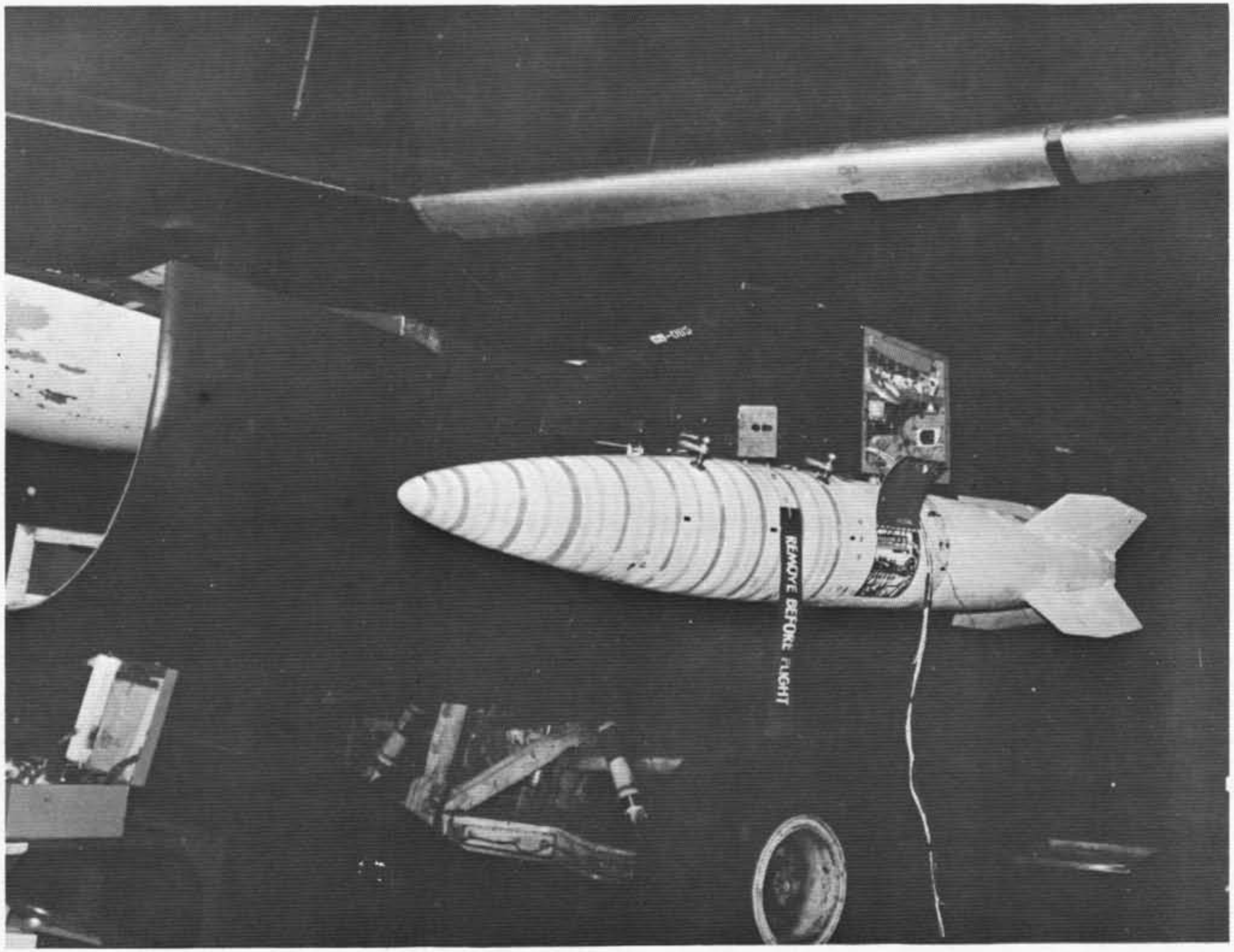

a. Preflight

Figure 1. Pylon-mounted store with thermographic paint pattern for heat-transfer measurements in flight.

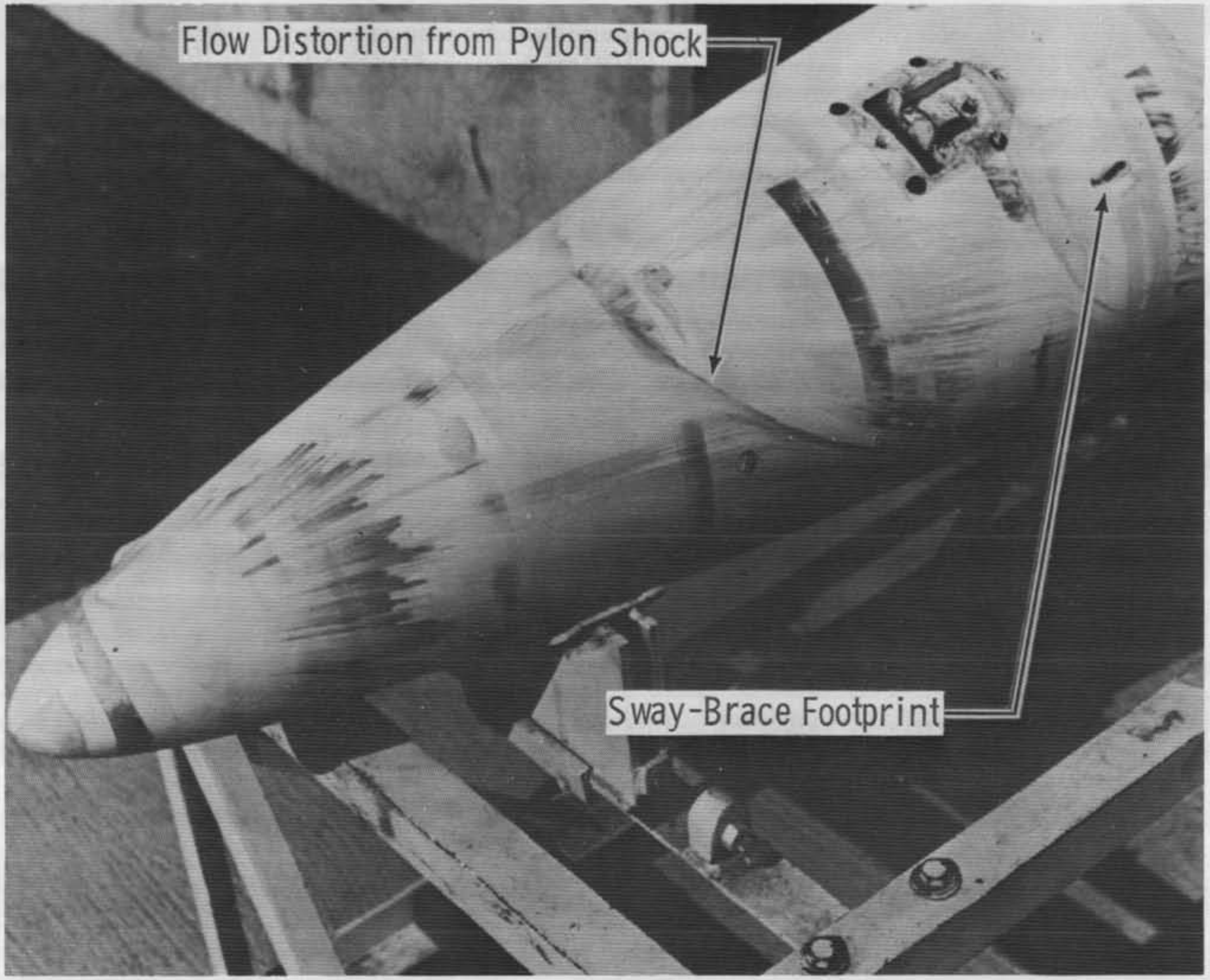

b. Postflight
Figure 1. Concluded.

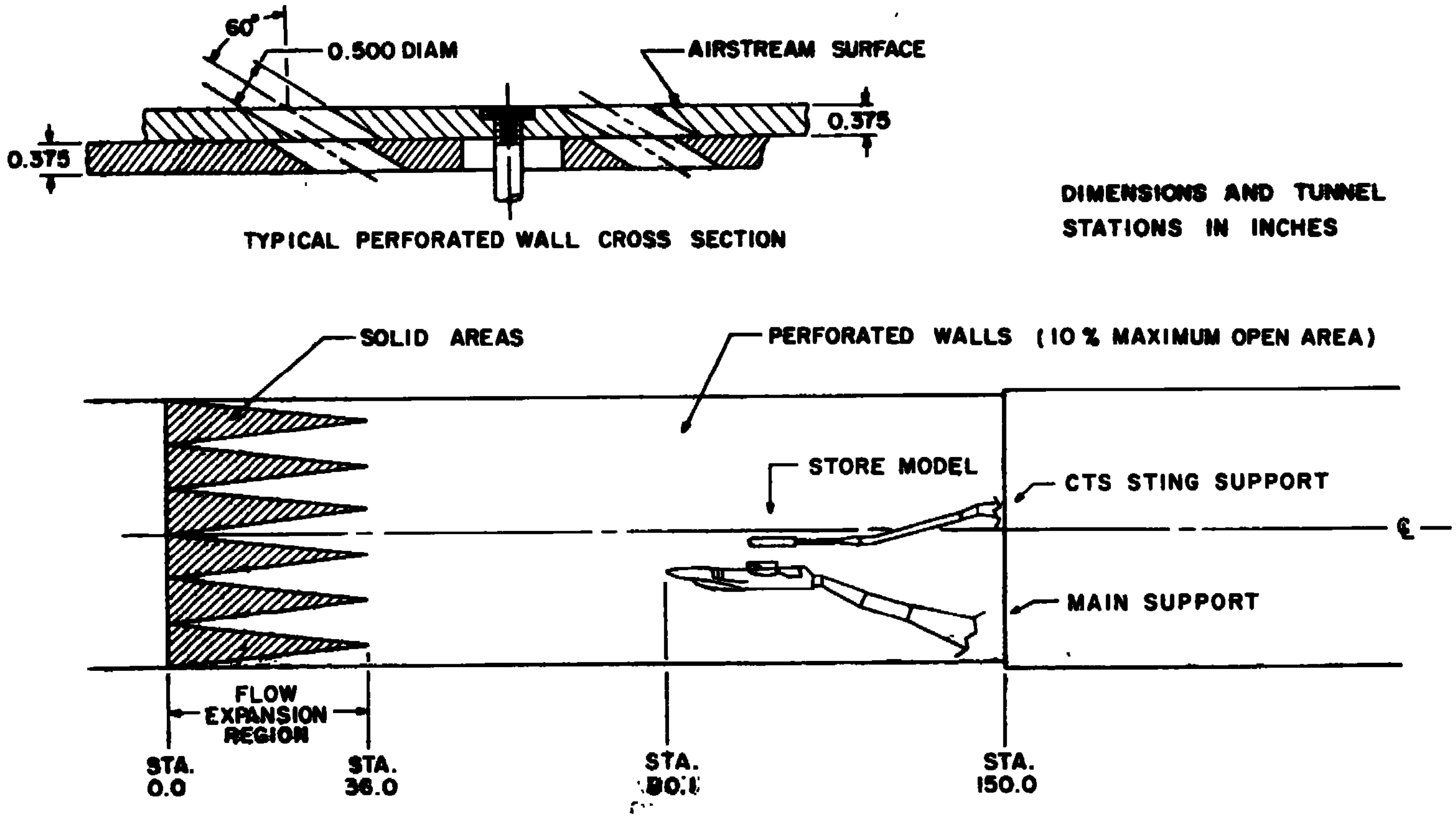

Figure 2. Schematic illustration of a typical model installation in Tunnel 4T.

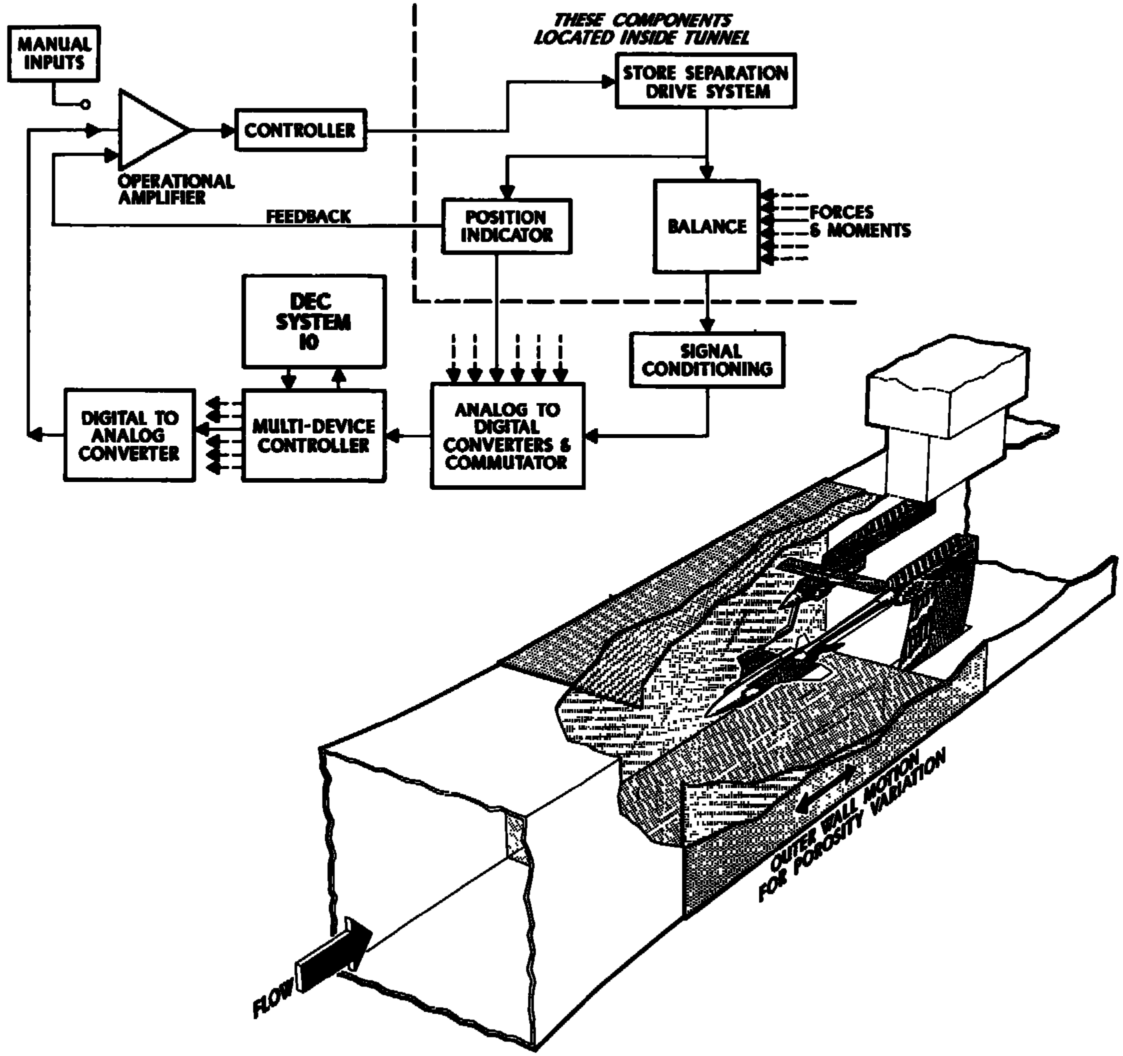

Figure 3. Schematic illustration of the captive trajectory system (CTS).

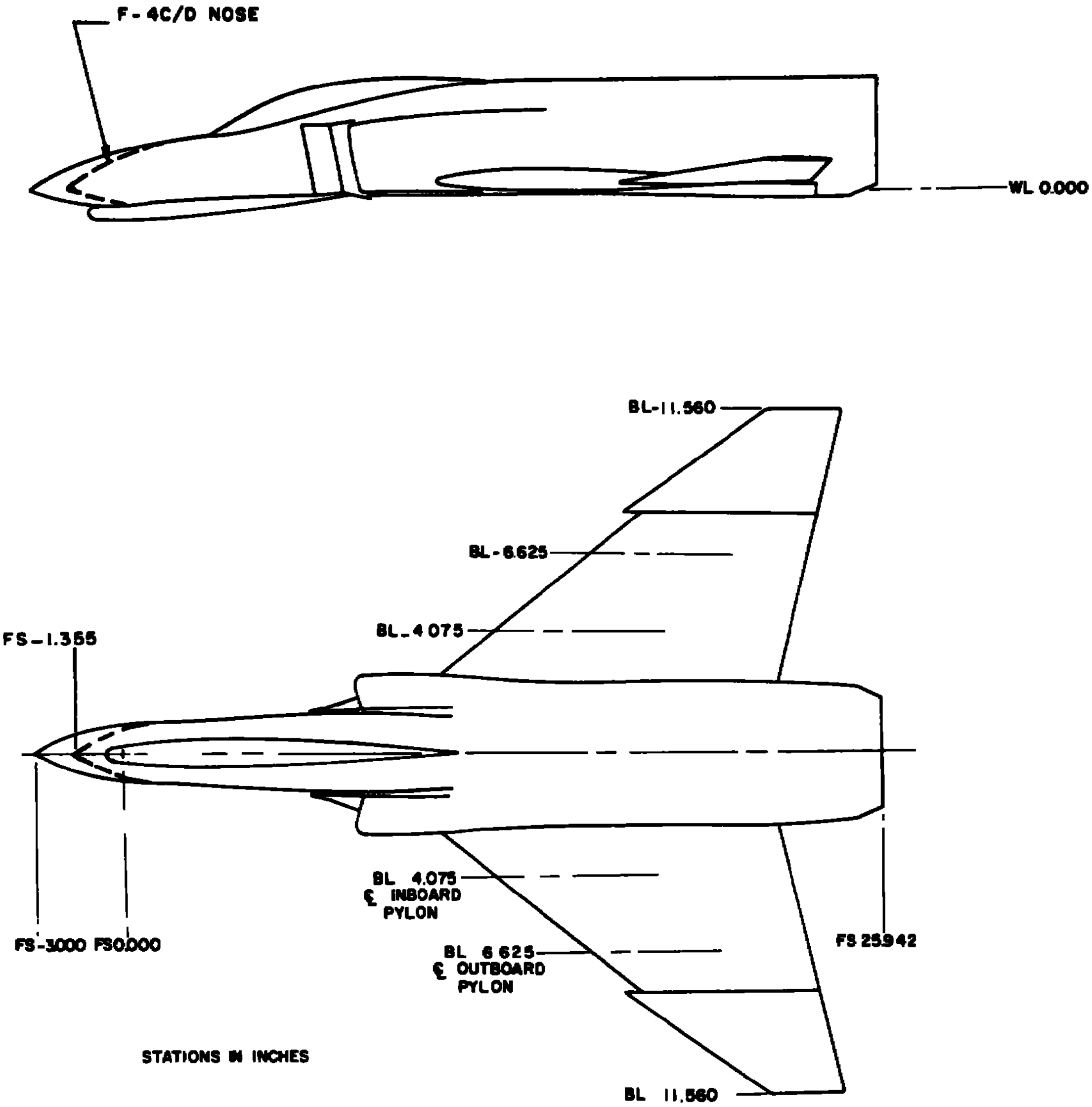

Figure 4. Outline drawing of the 1/20-scale model of the F-4C aircraft.

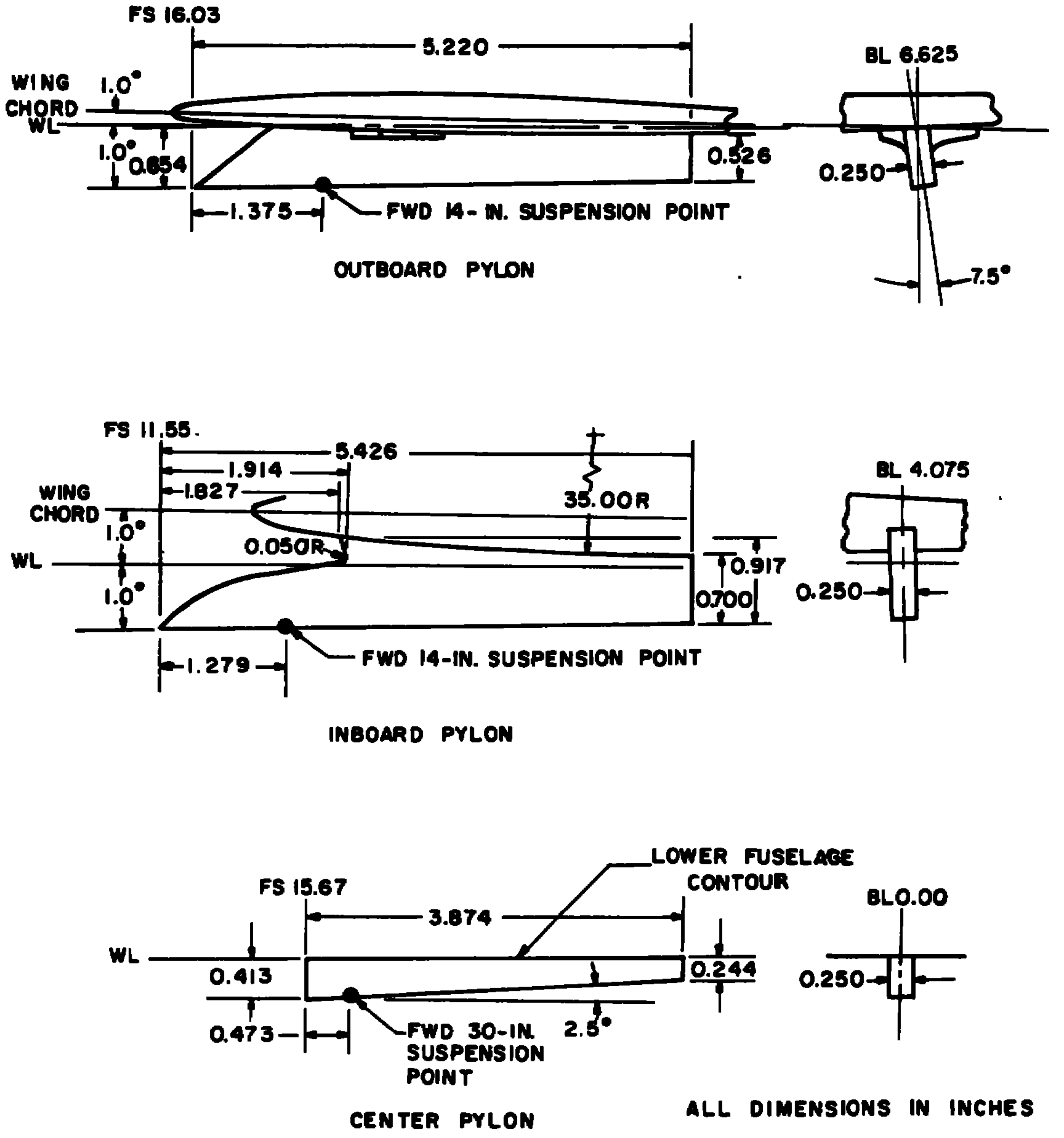

Figure 5. Details of the models of the F-4C pylons.

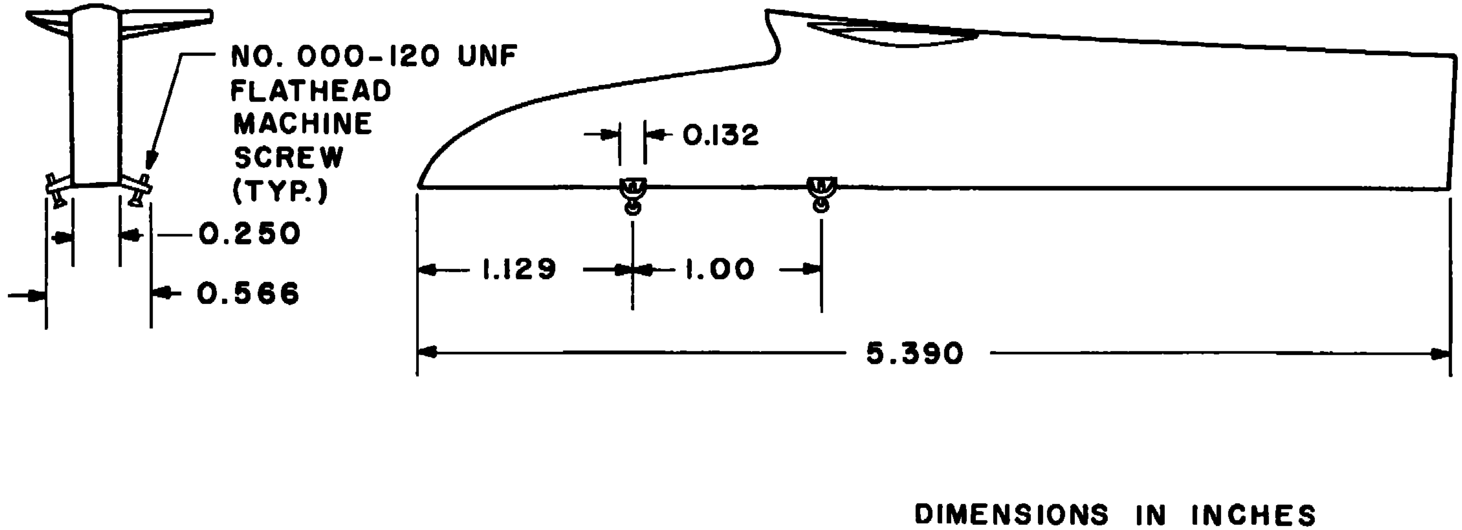

Figure 6. Details of the simulated sway braces for the left inboard pylon (LIB).

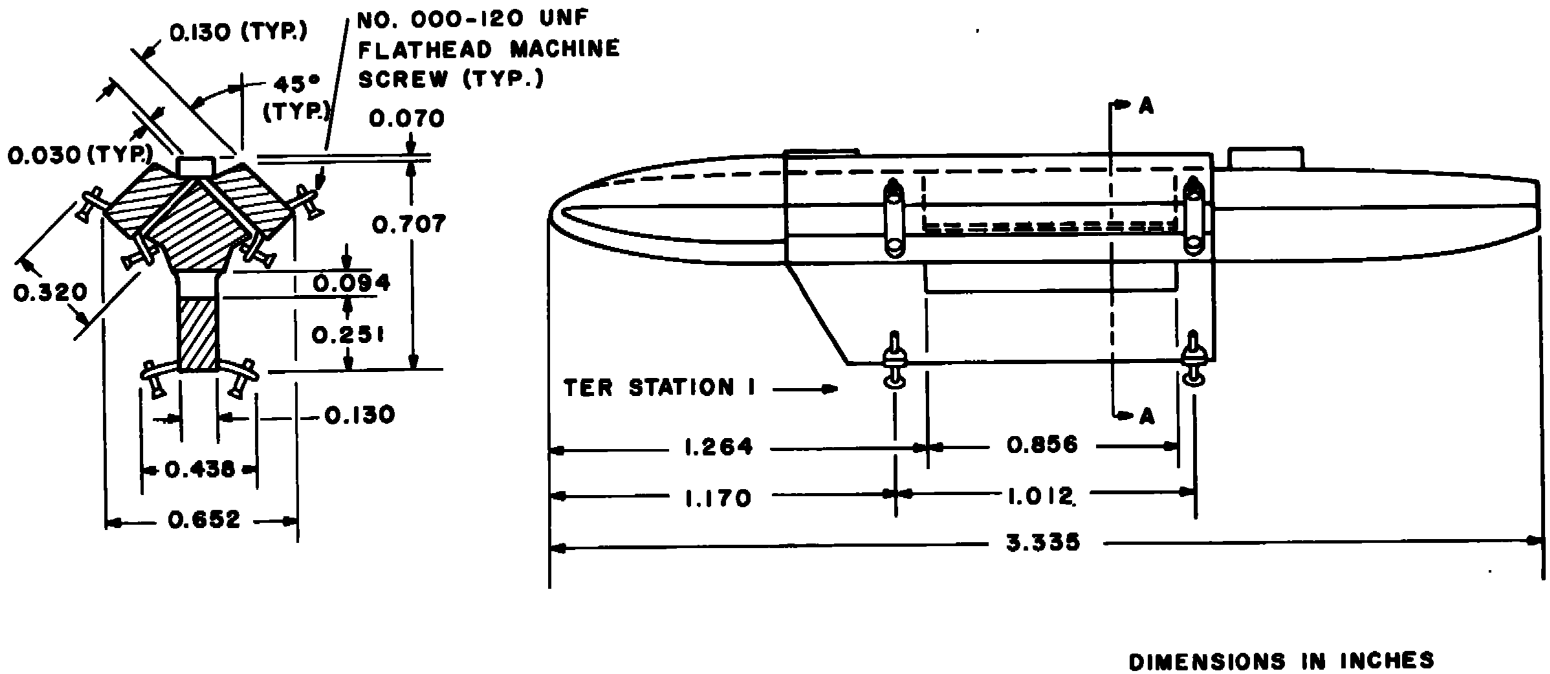

Figure 7. Details of the model of the triple ejector rack.

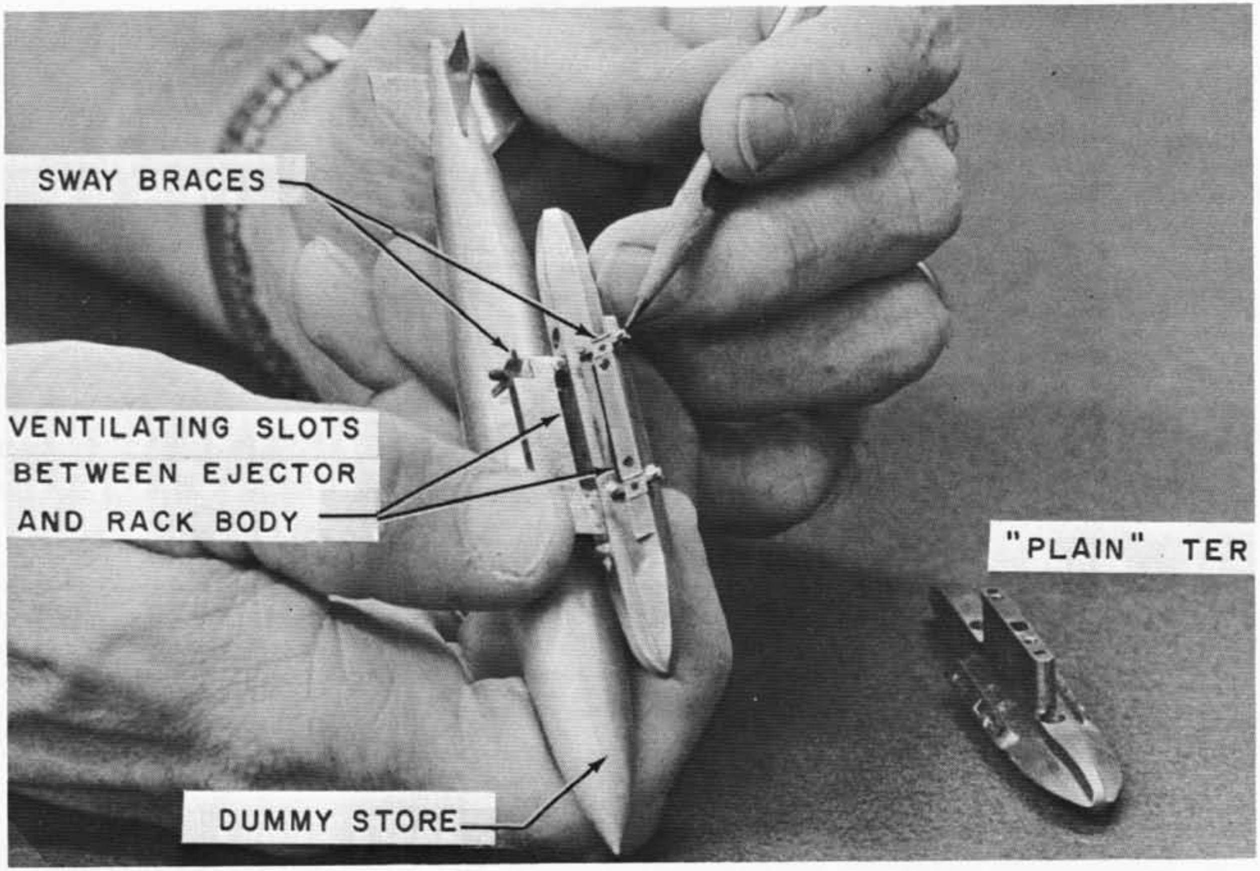

Figure 8. Photograph of the detailed and simplified triple ejector rack models.

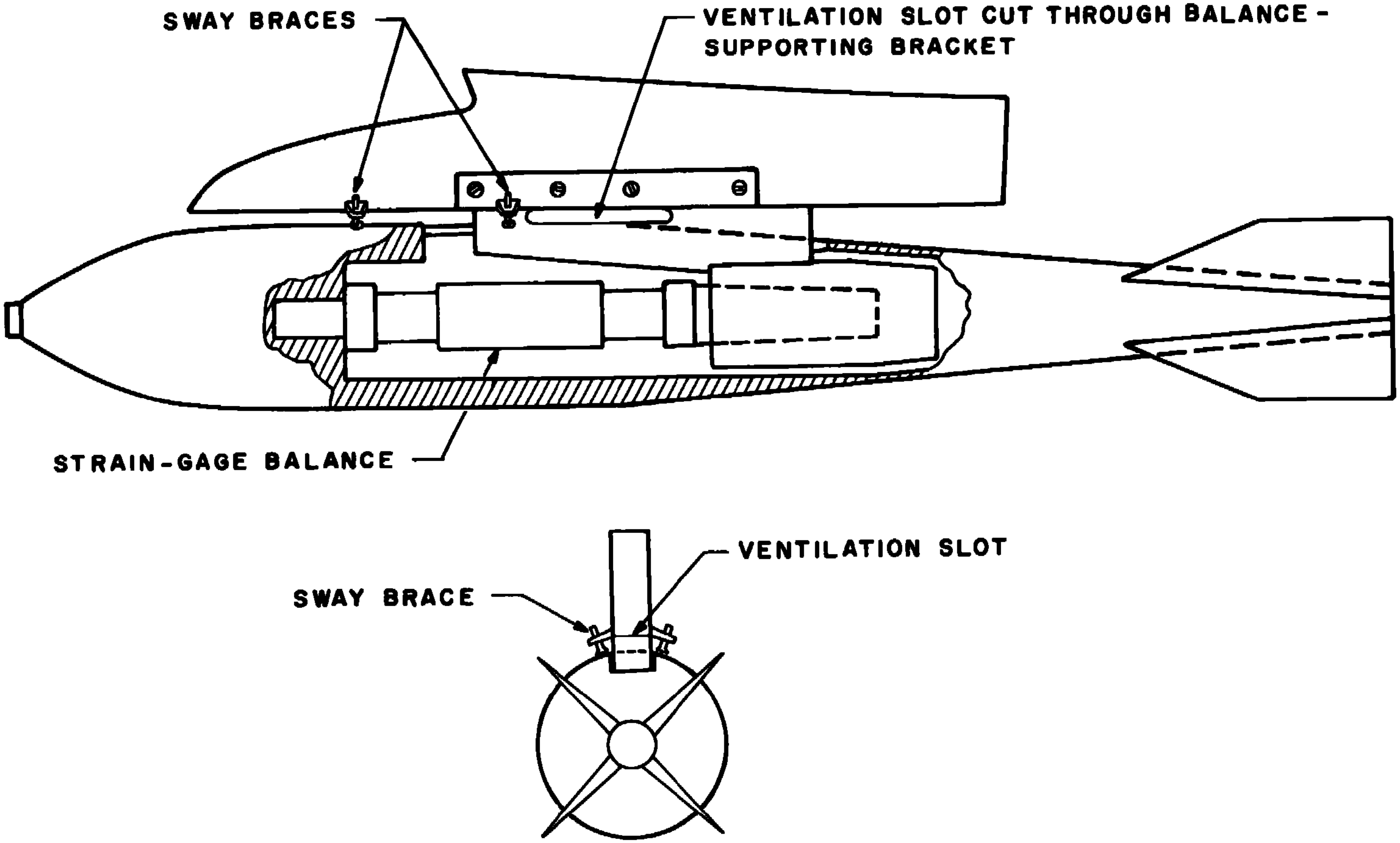

a. Pylon mount

Figure 9. Internal bracket-support balance/store installations.

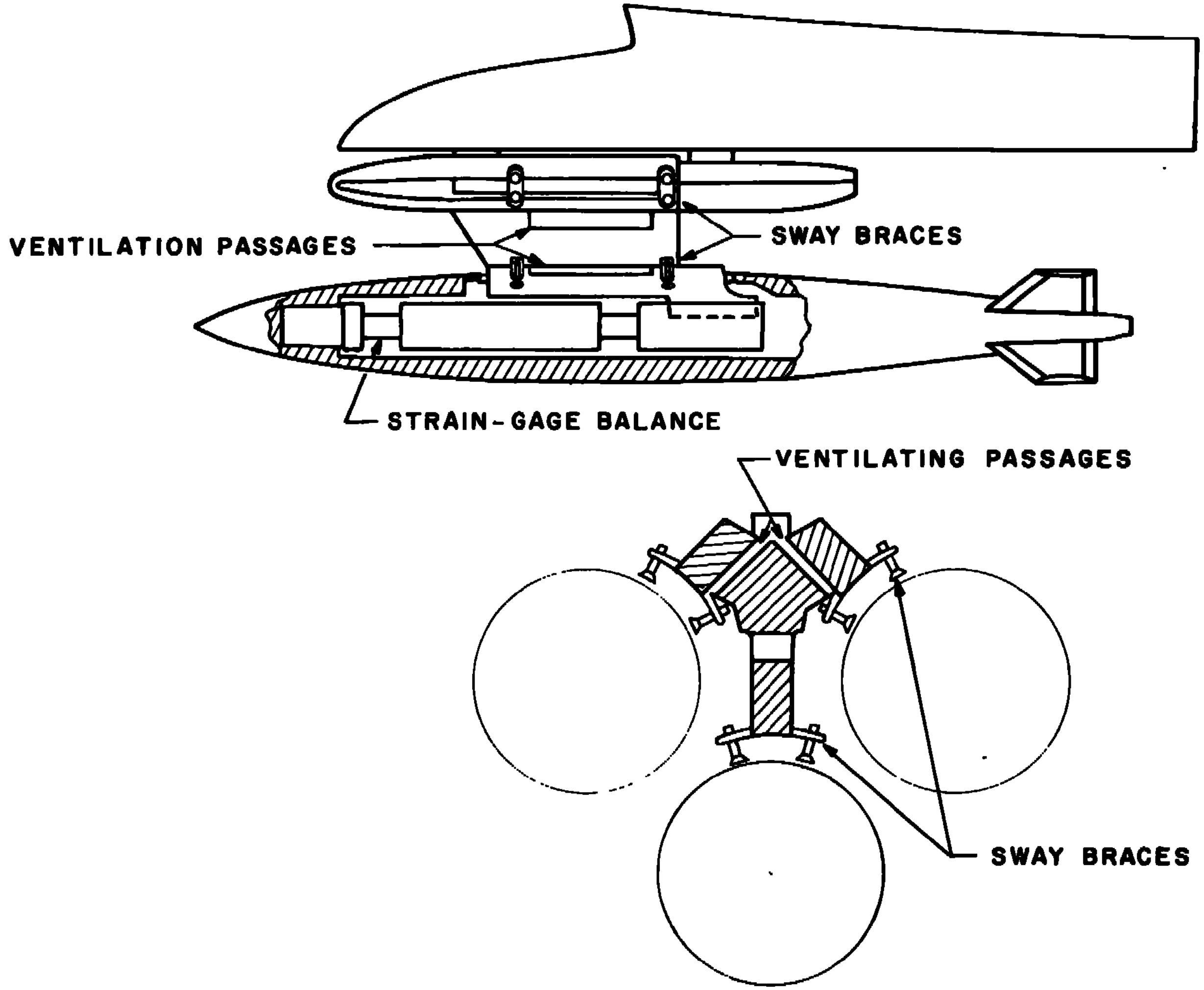

b. Rack mount
Figure 9. Concluded.

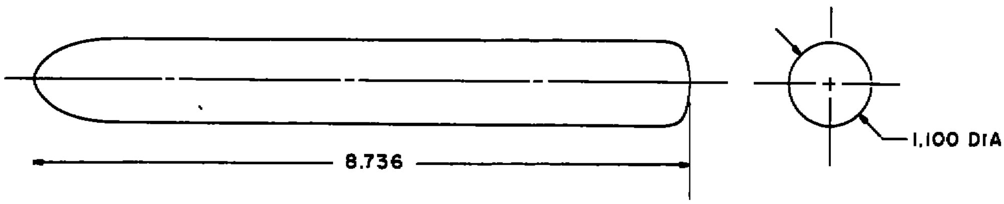

a. Black crow

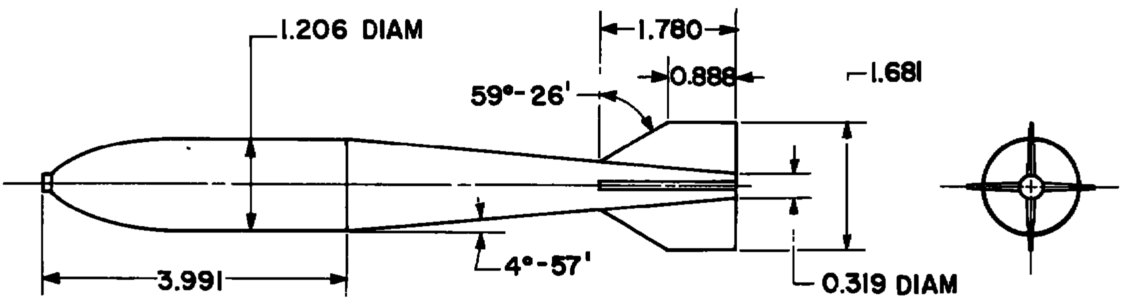

b. M-118

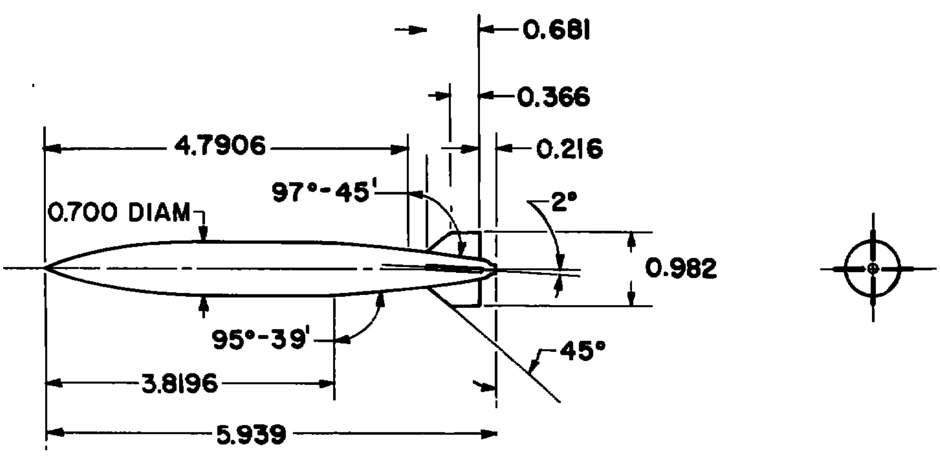

c. MK 83

Figure 10. Outline drawings of the store models.

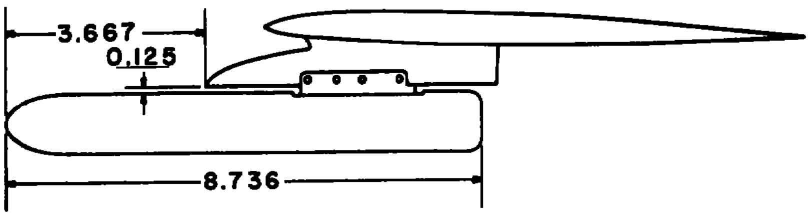

a. Black crow

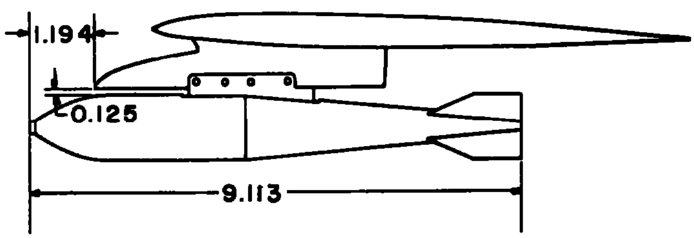

b. M-118

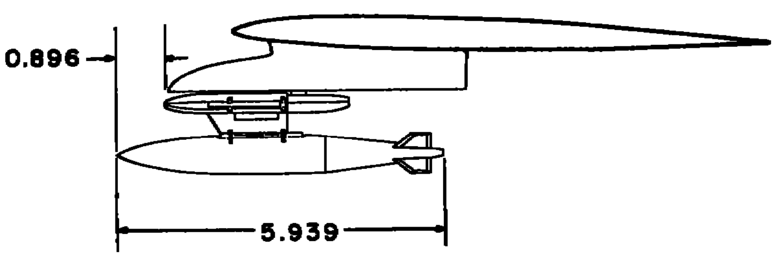

DIMENSIONS IN INCHES

c. MK 83

Figure 11. Locations of the store models on the left inboard pylon.

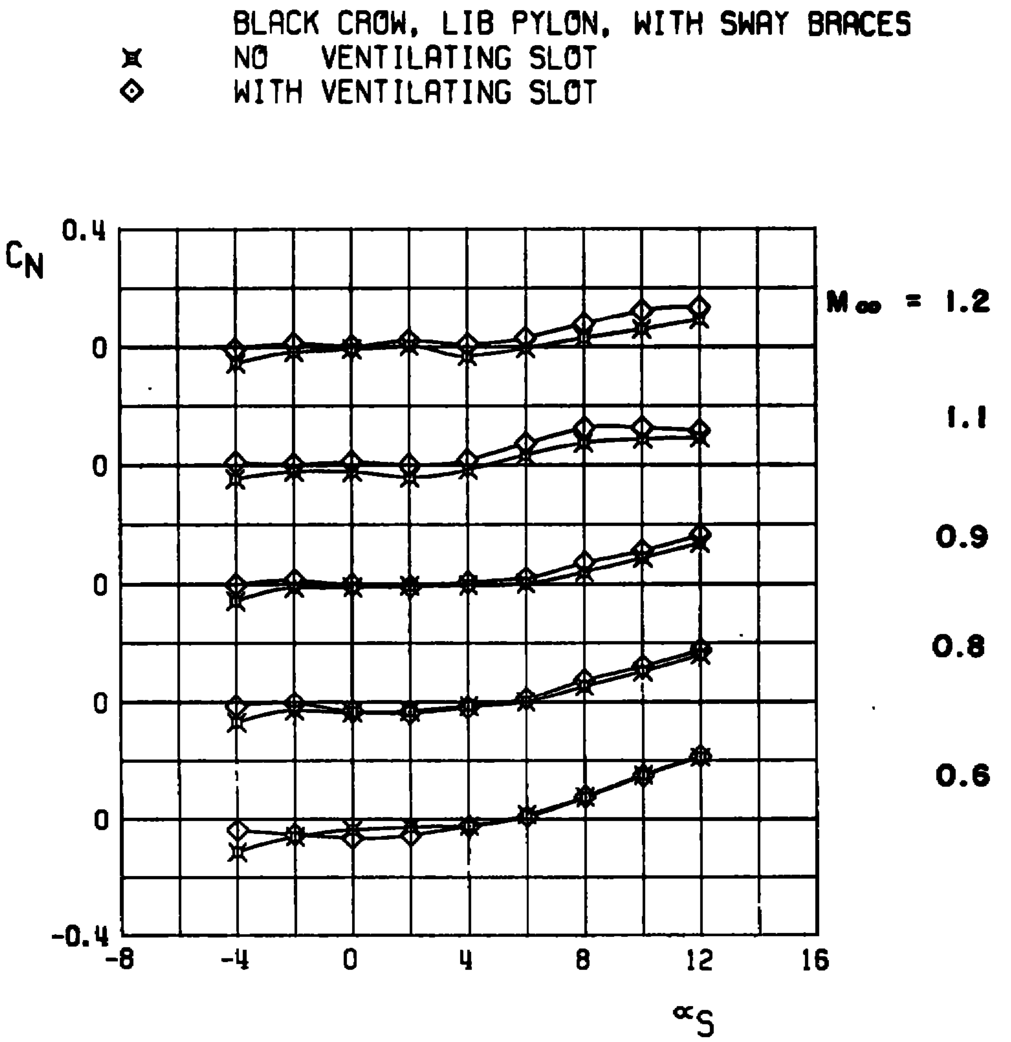

a. Normal-force coefficient

Figure 12. Effect of a ventilated supporting bracket in the presence of pylon sway braces on the static aerodynamic loads acting on an unstable pylon-mounted store.

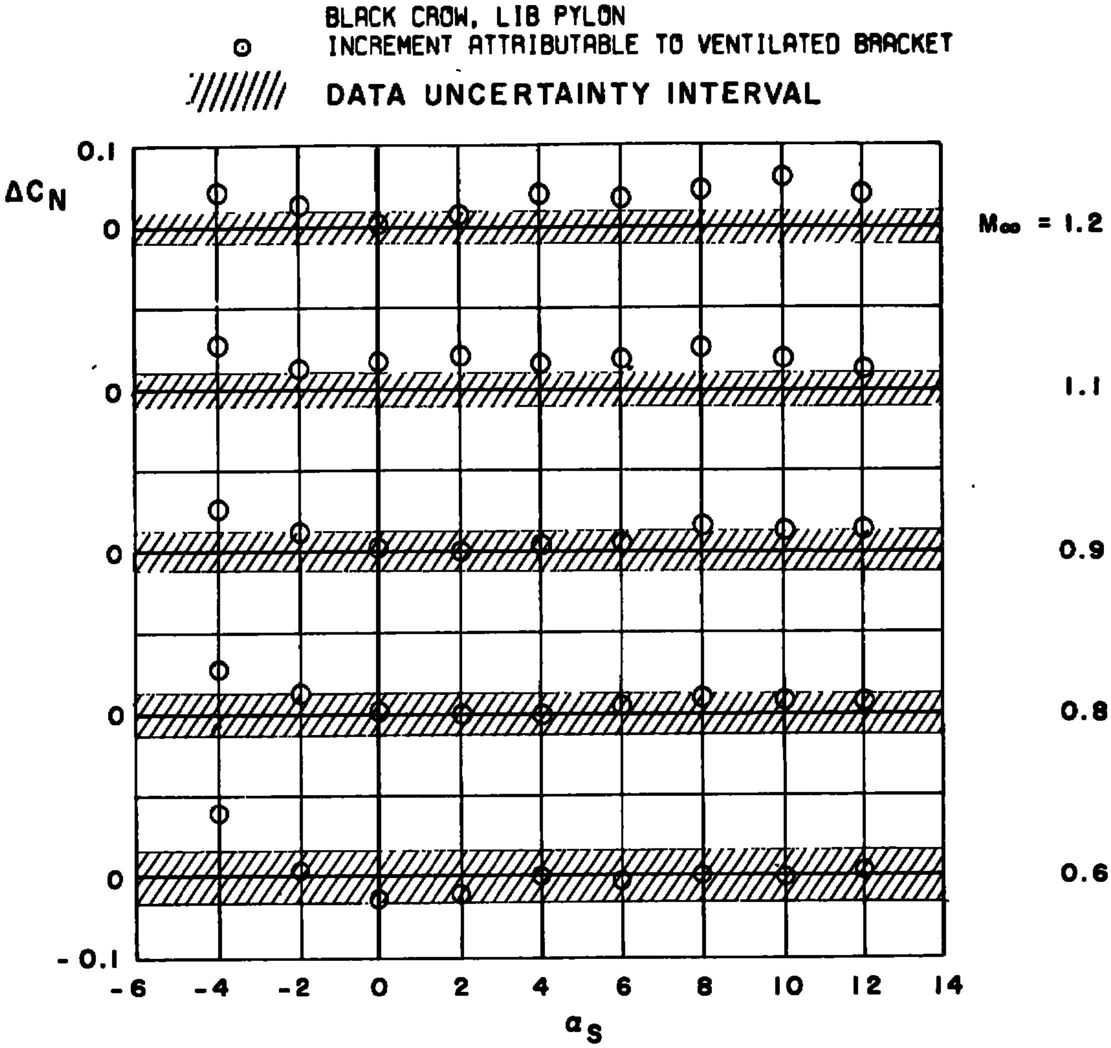

b. Increment in normal-force coefficient
Figure 12. Continued.

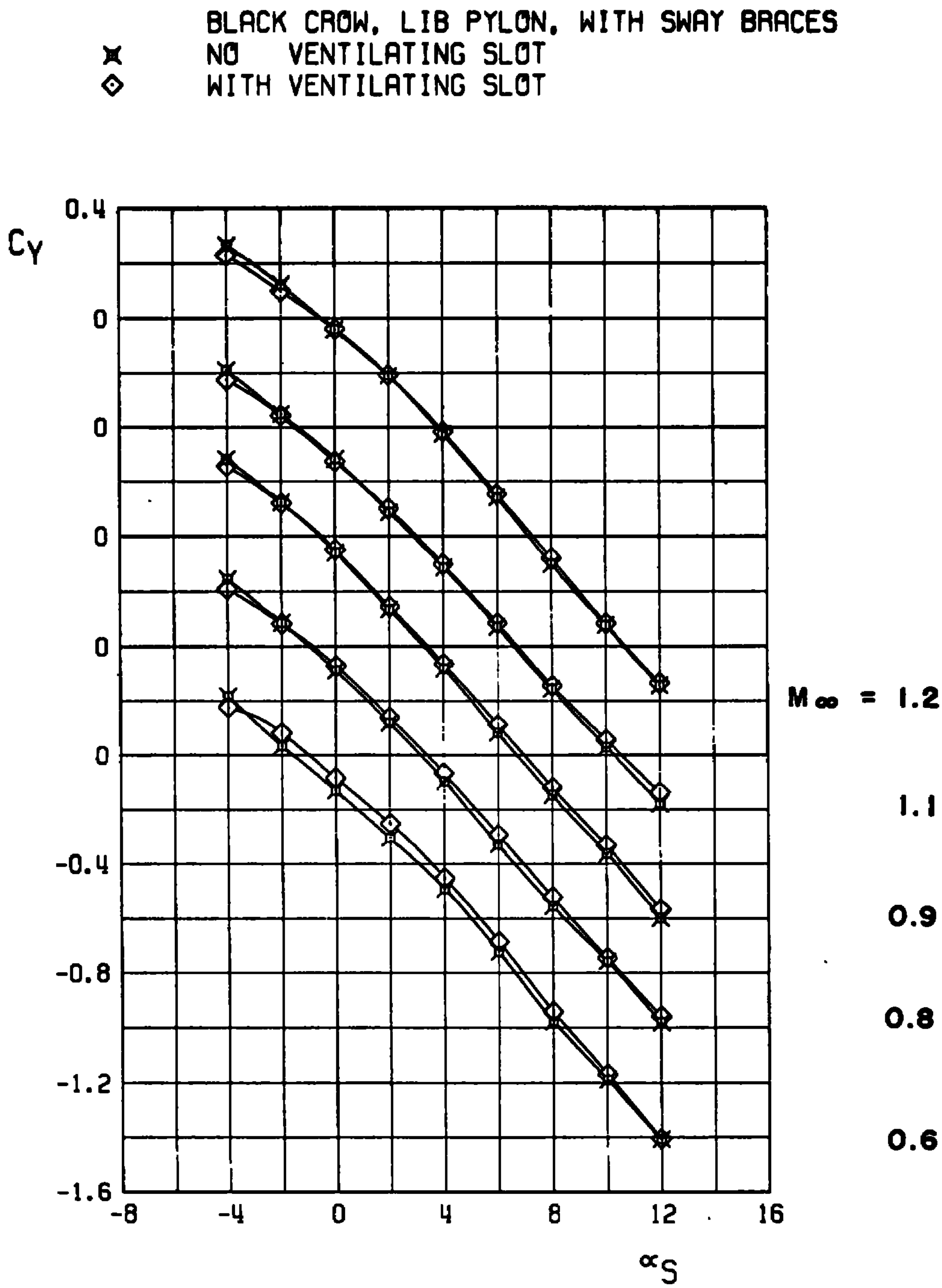

c. Side-force coefficient
Figure 12. Continued.

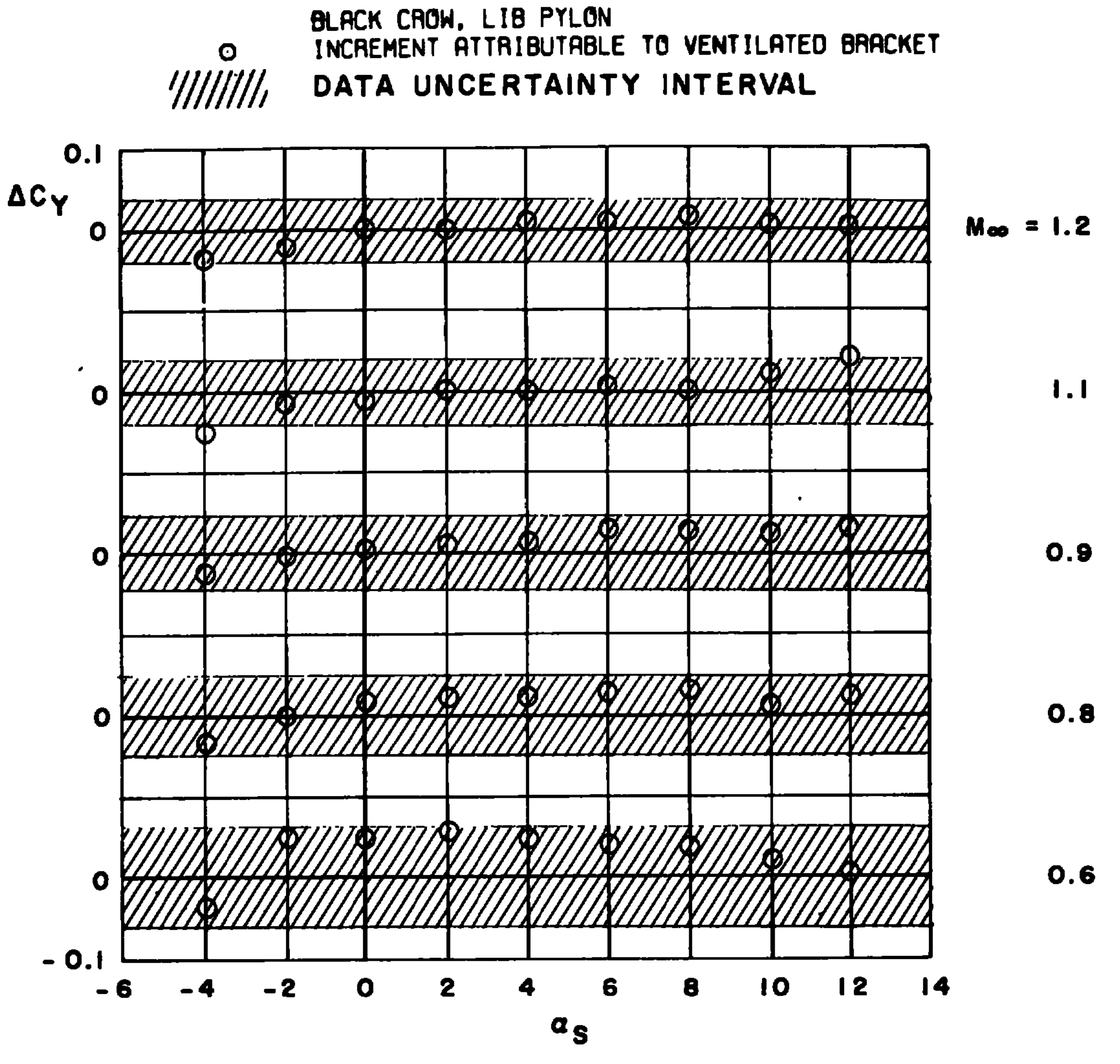

d. Increment in side-force coefficient
Figure 12. Continued.

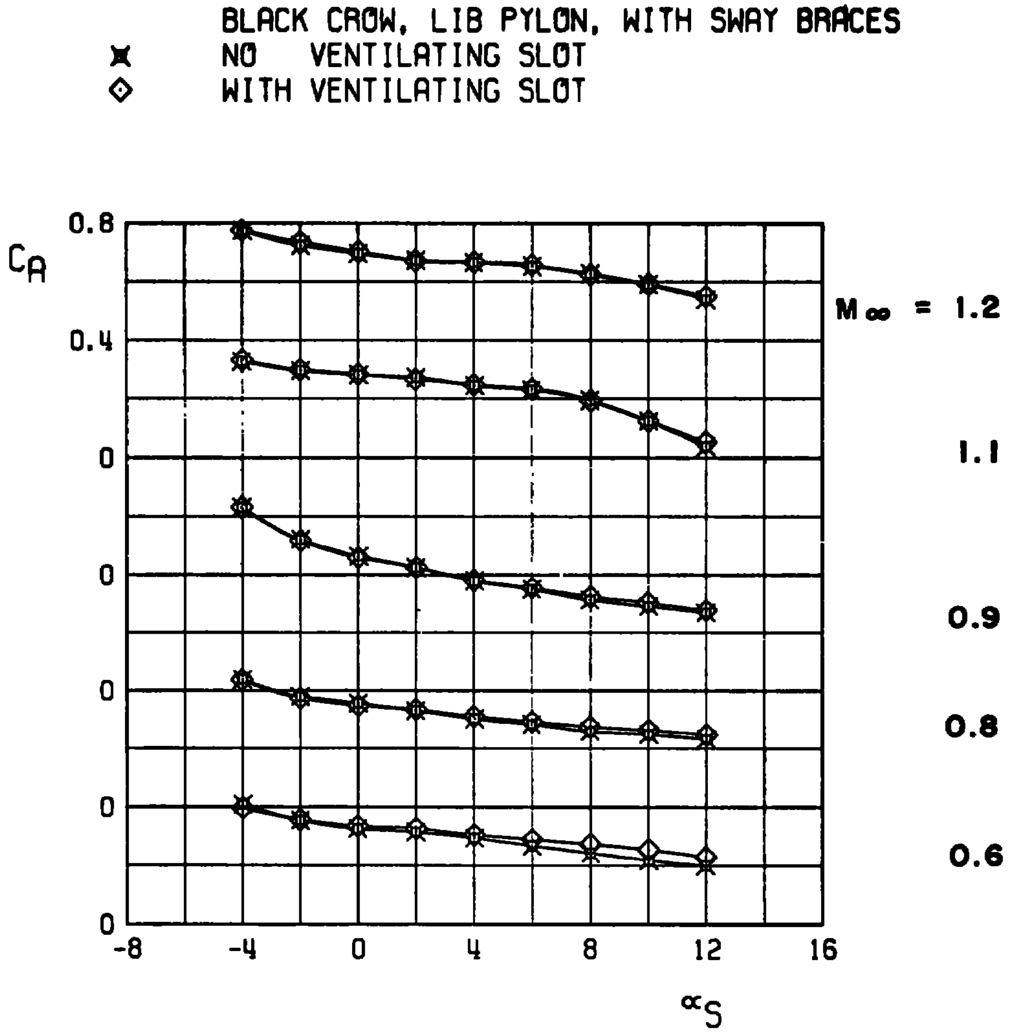

e. Axial-force coefficient
Figure 12. Continued.

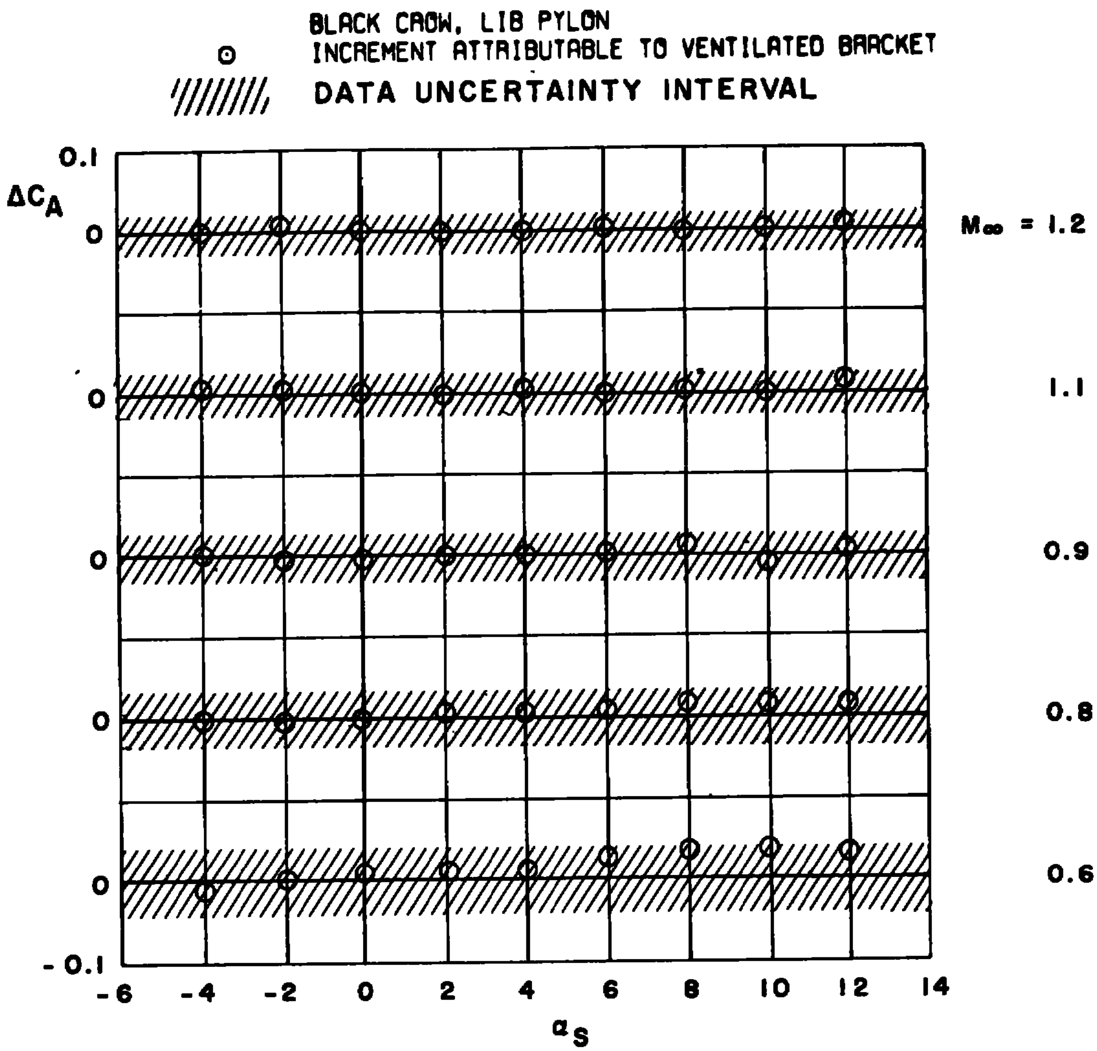

f. Increment in axial-force coefficient
Figure 12. Continued.

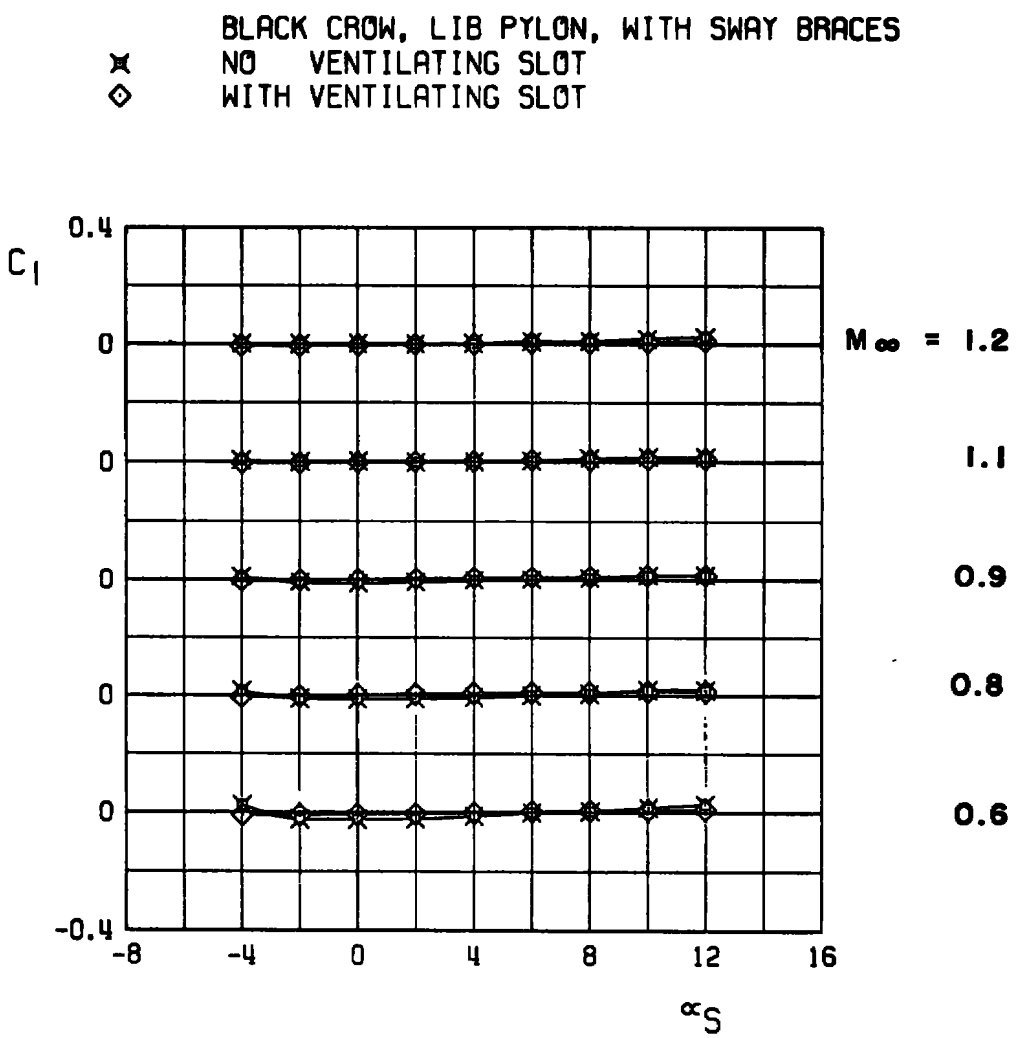

g. Rolling-moment coefficient
Figure 12. Continued.

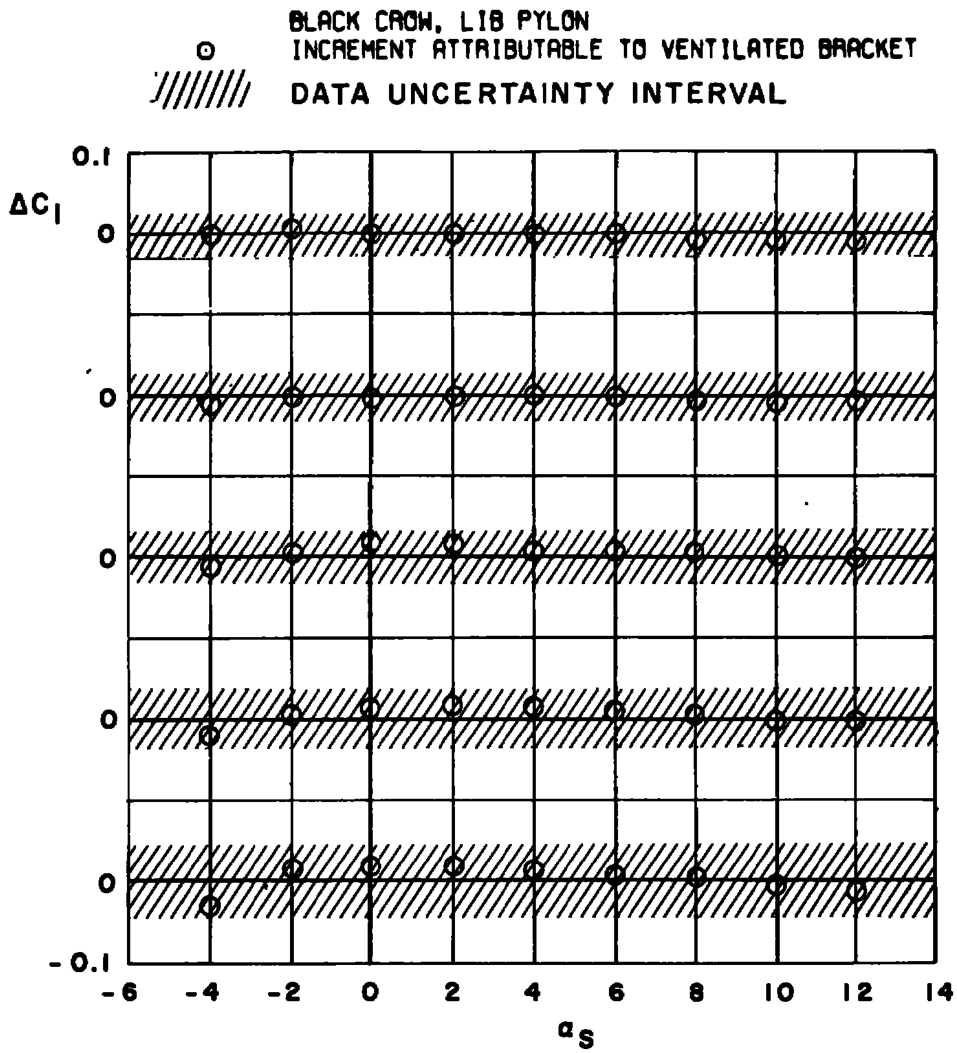

h. Increment in rolling-moment coefficient
Figure 12. Continued.

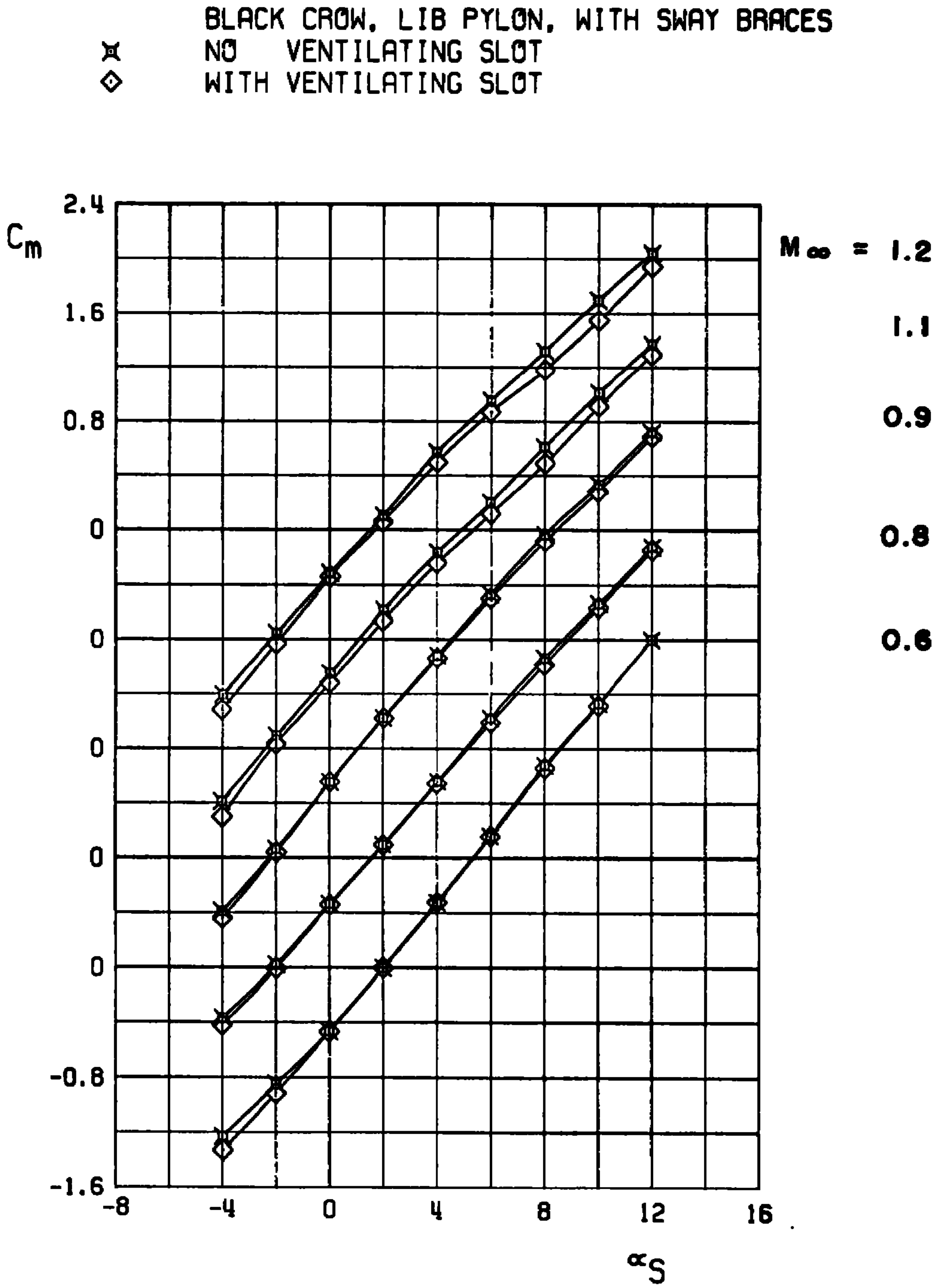

i. Pitching-moment coefficient
Figure 12. Continued.

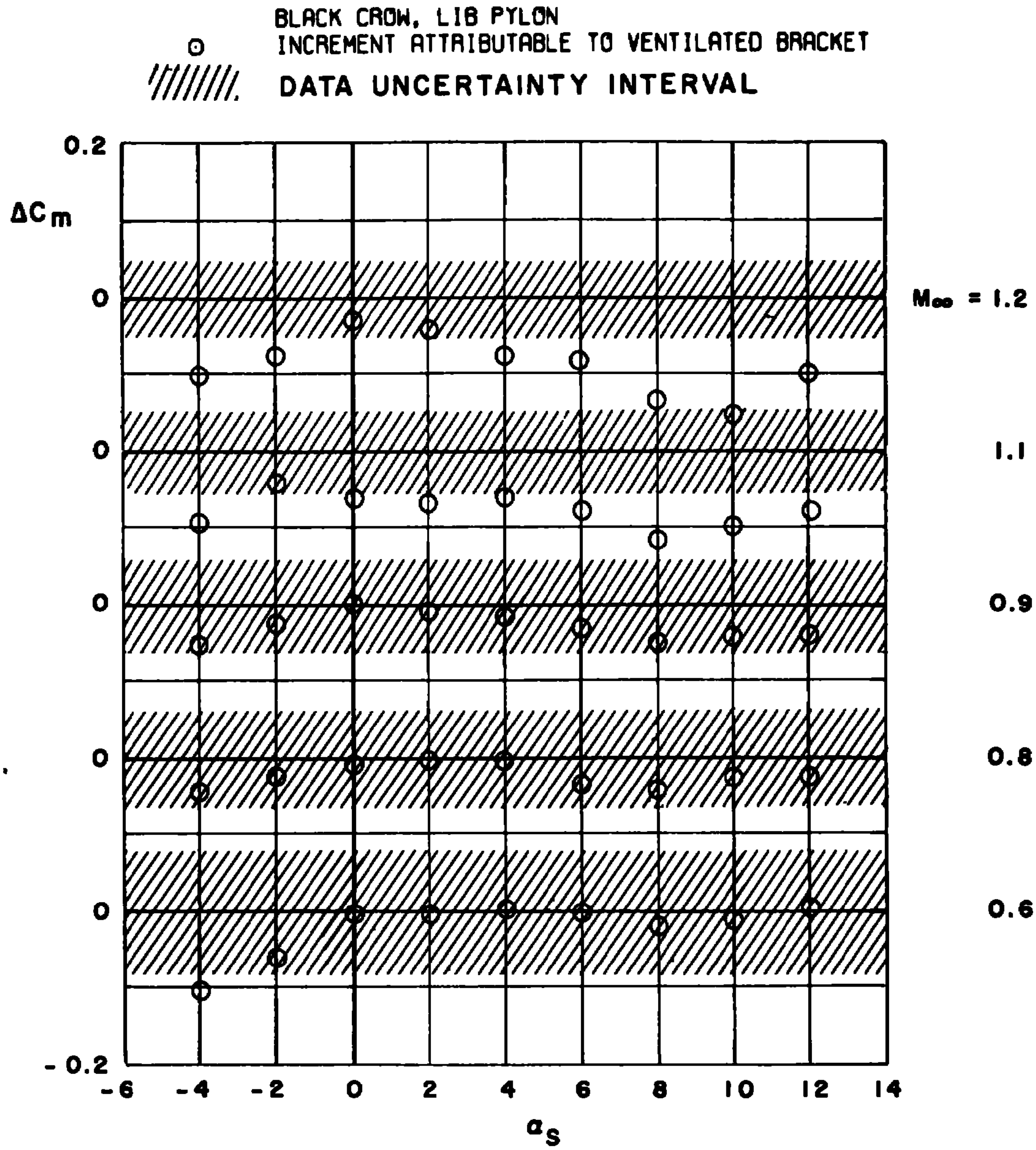

j. Increment in pitching-moment coefficient
Figure 12. Continued.

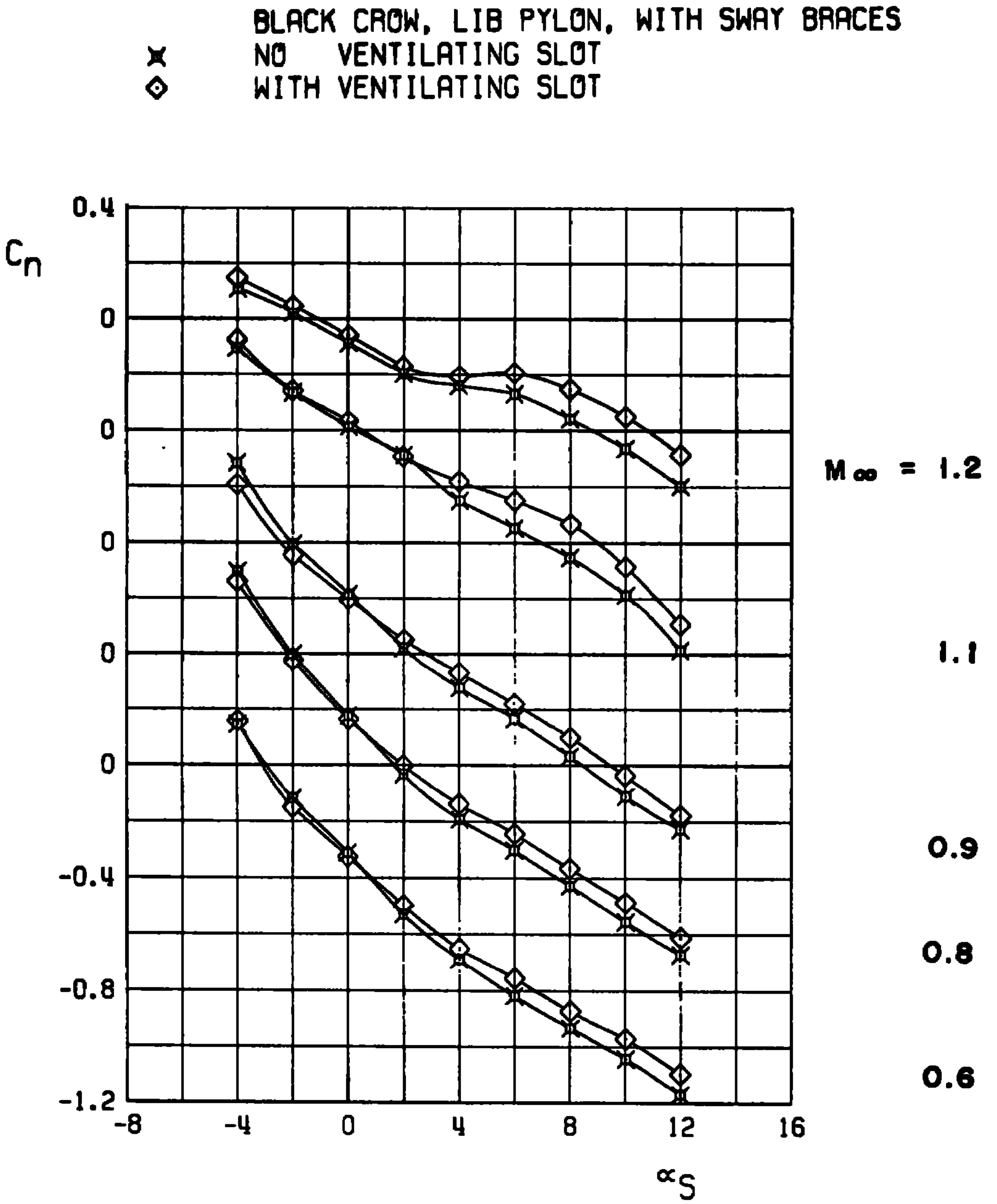

k. Yawing-moment coefficient
Figure 12. Continued.

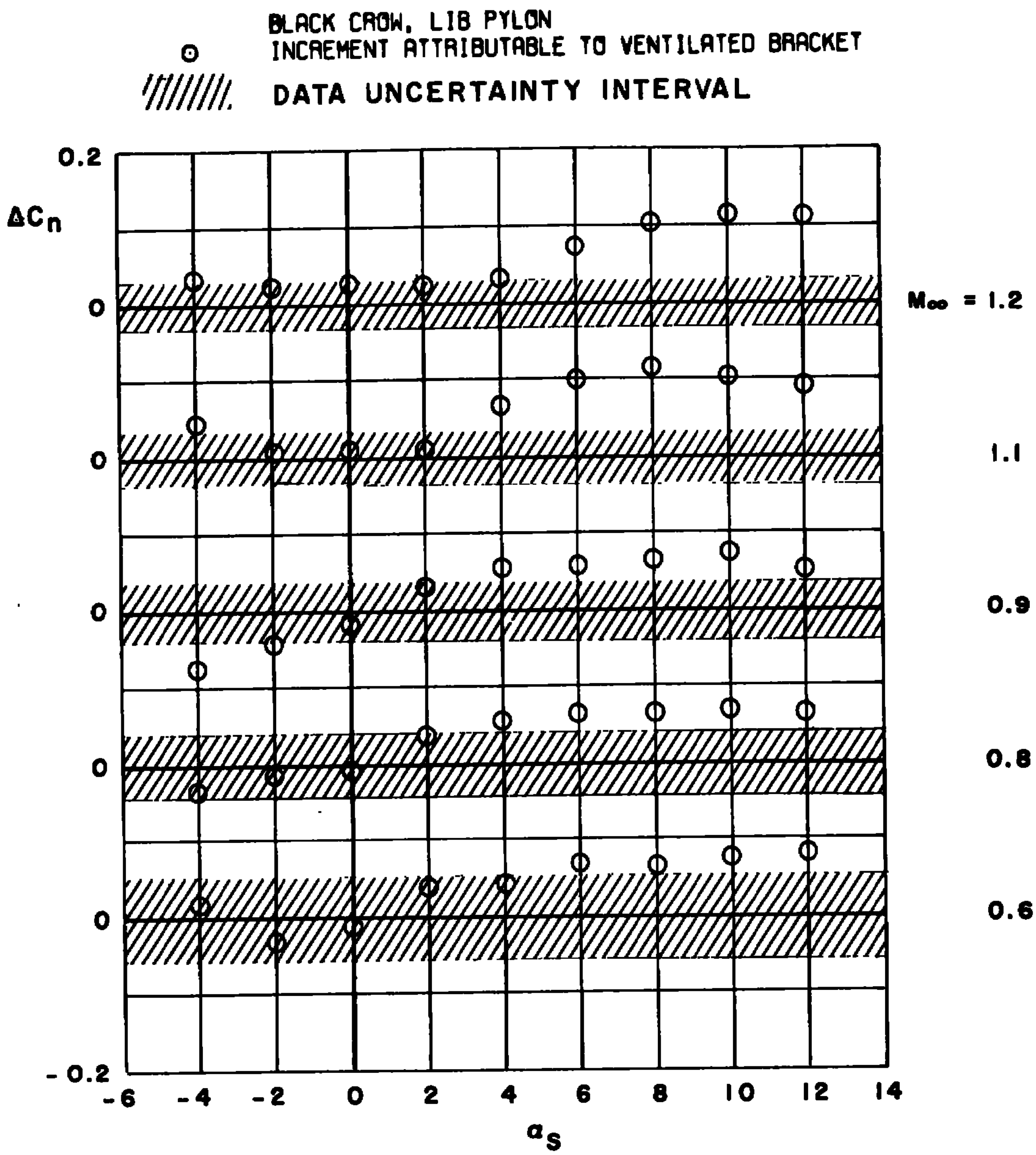

I. Increment in yawing-moment coefficient
Figure 12. Concluded.

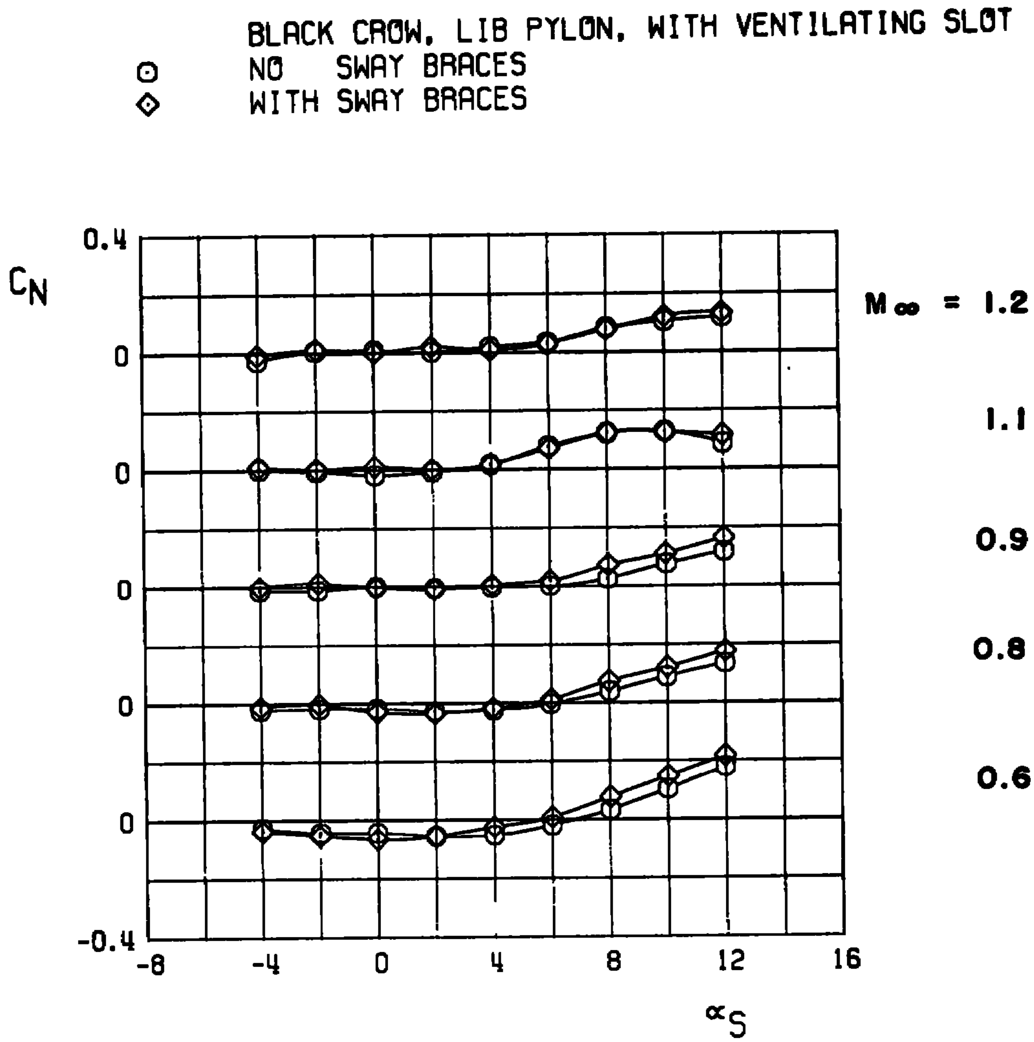

a. Normal-force coefficient

Figure 13. Effect of pylon sway braces in the presence of a ventilated supporting bracket on the static aerodynamic loads acting on an unstable pylon-mounted store.

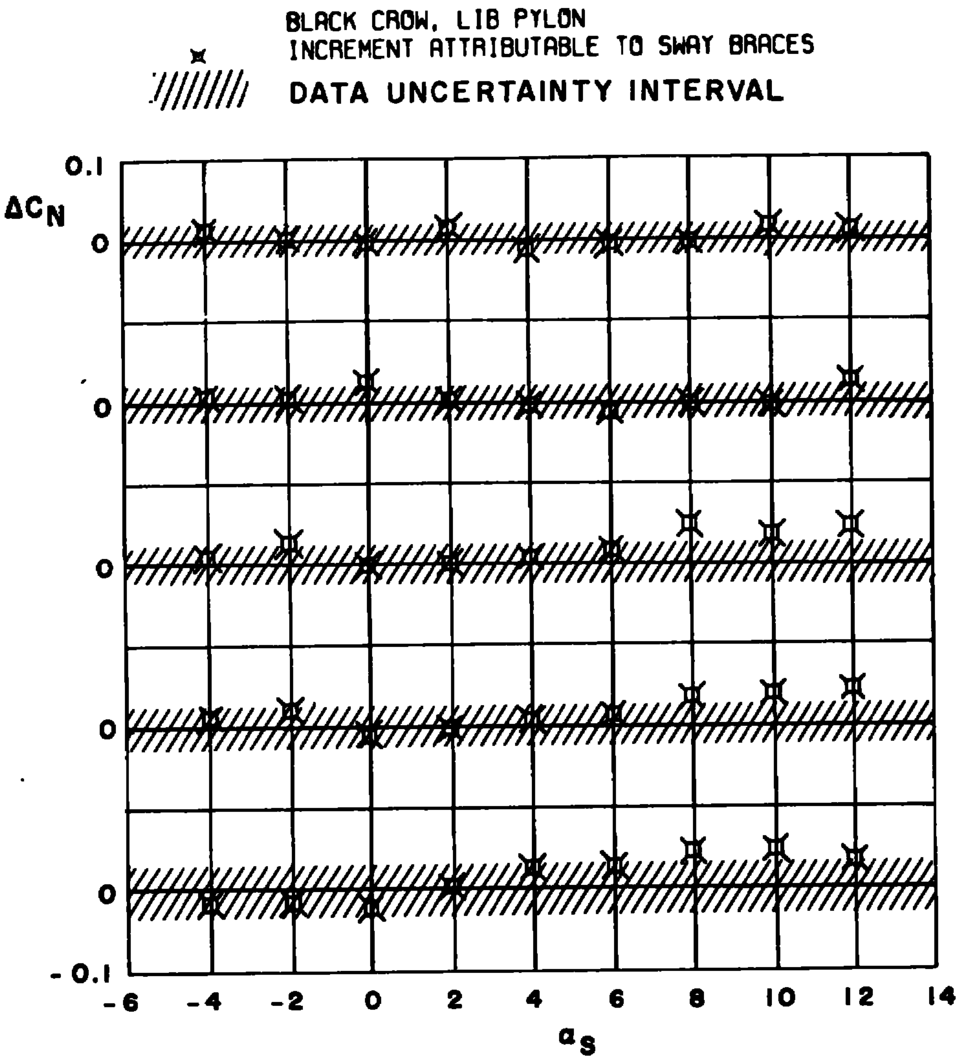

b. Increment in normal-force coefficient
Figure 13. Continued.

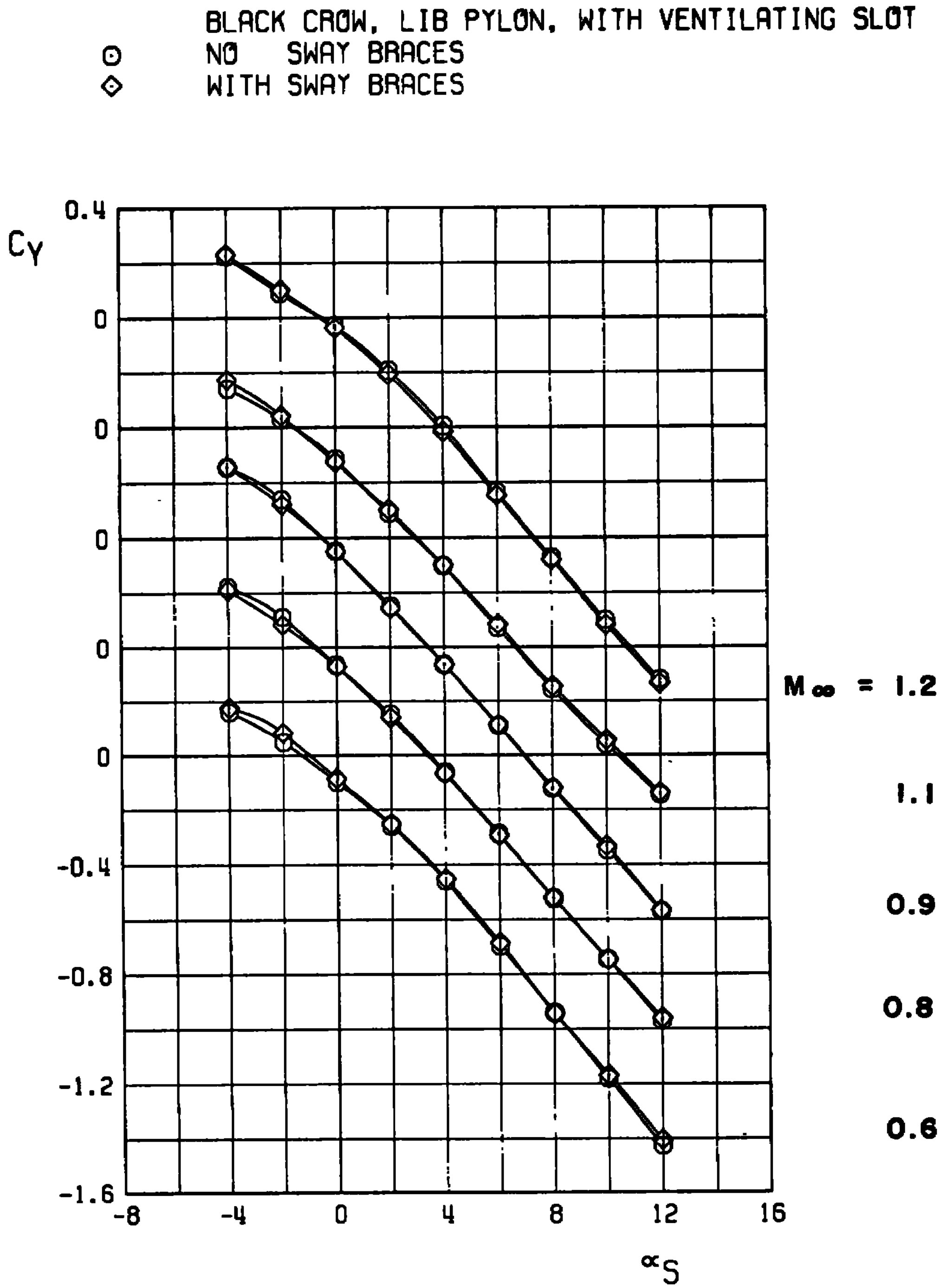

c. Side-force coefficient
Figure 13. Continued.

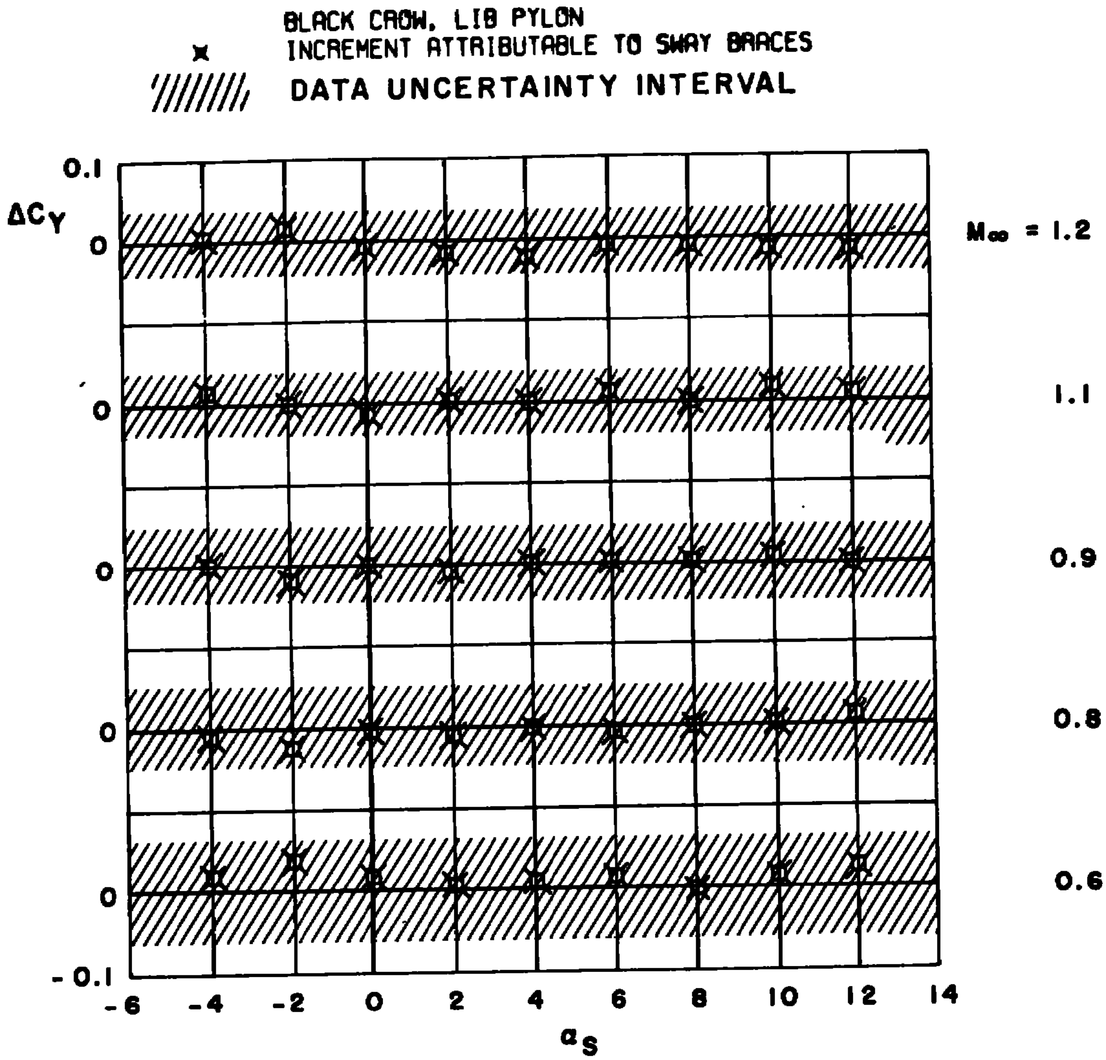

d. Increment in side-force coefficient
Figure 13. Continued.

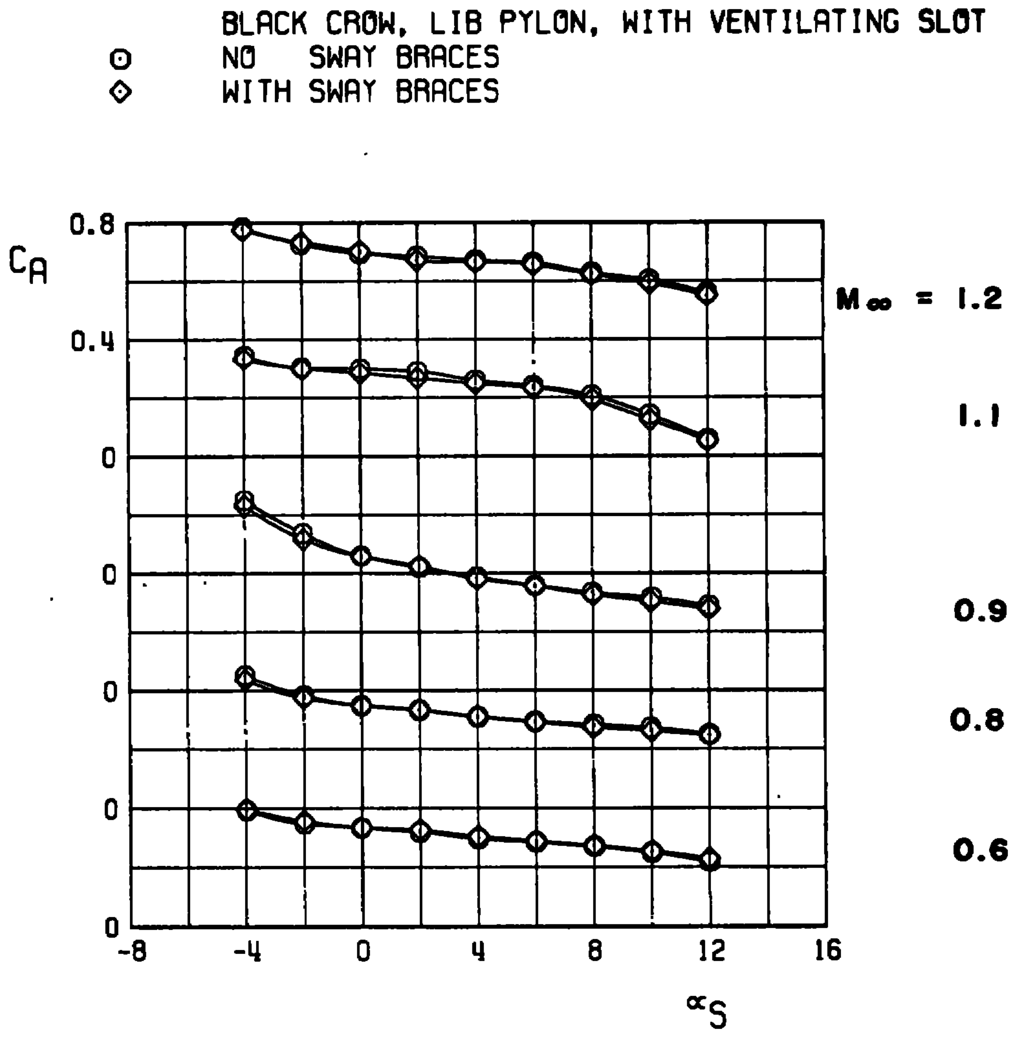

e. Axial-force coefficient
Figure 13. Continued.

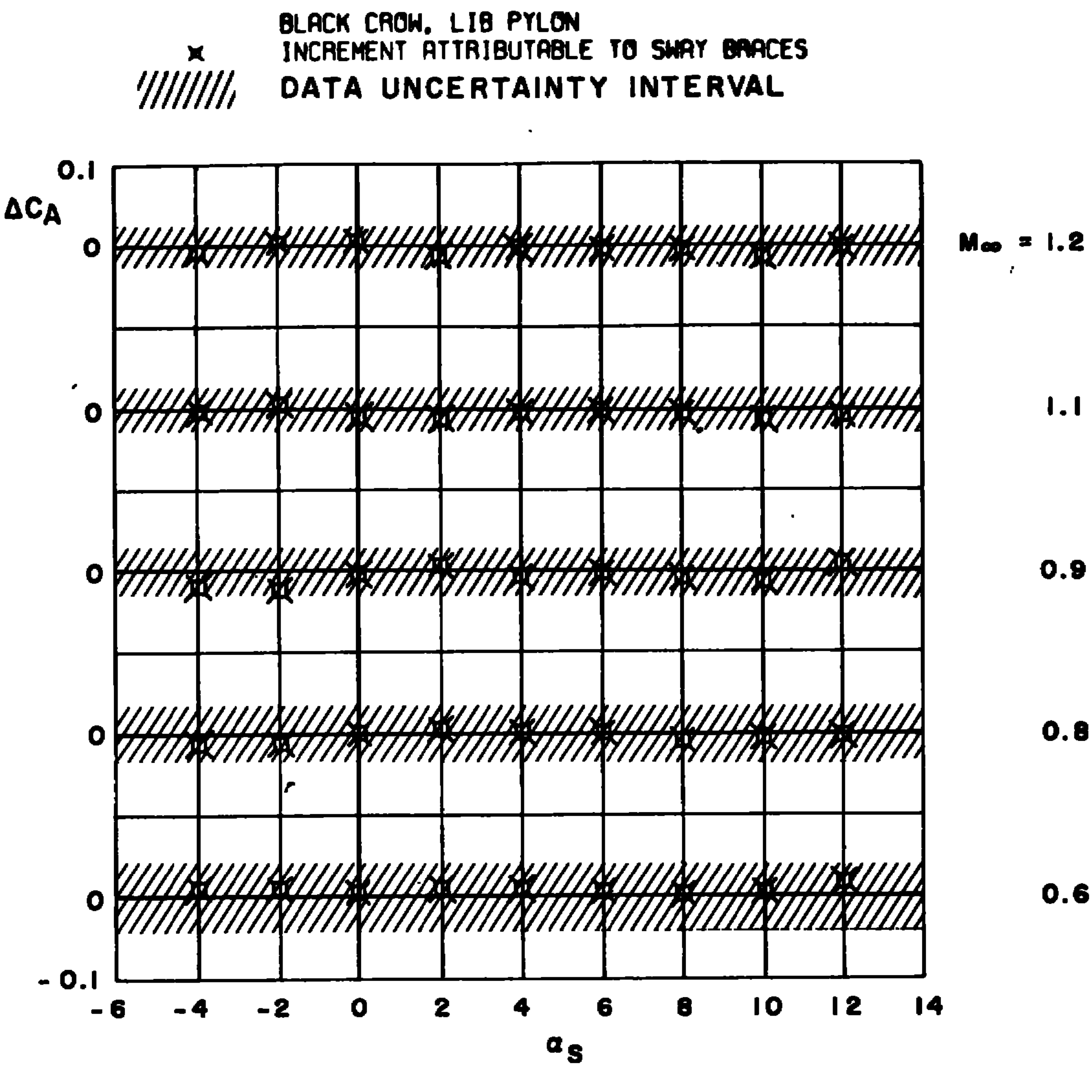

f. Increment in axial-force coefficient
Figure 13. Continued.

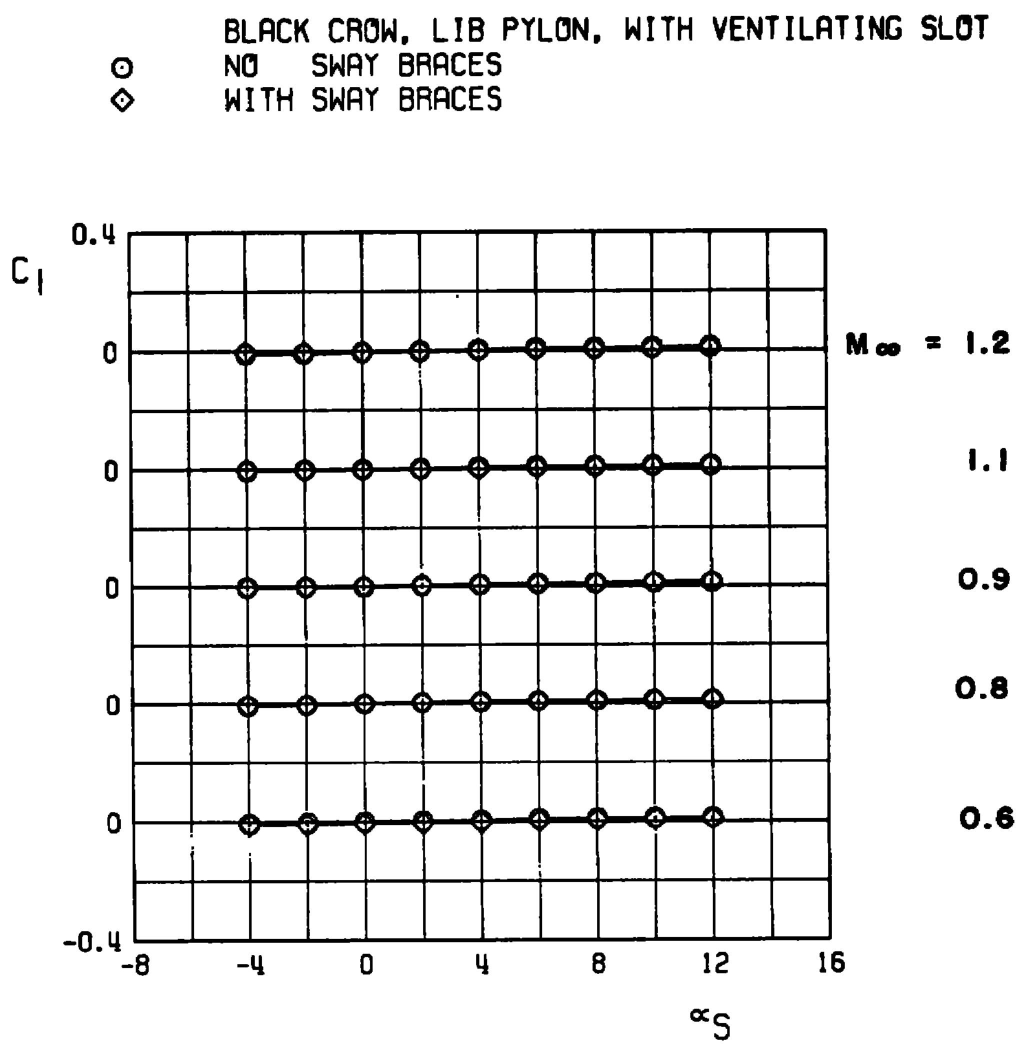

g. Rolling-moment coefficient
Figure 13. Continued.

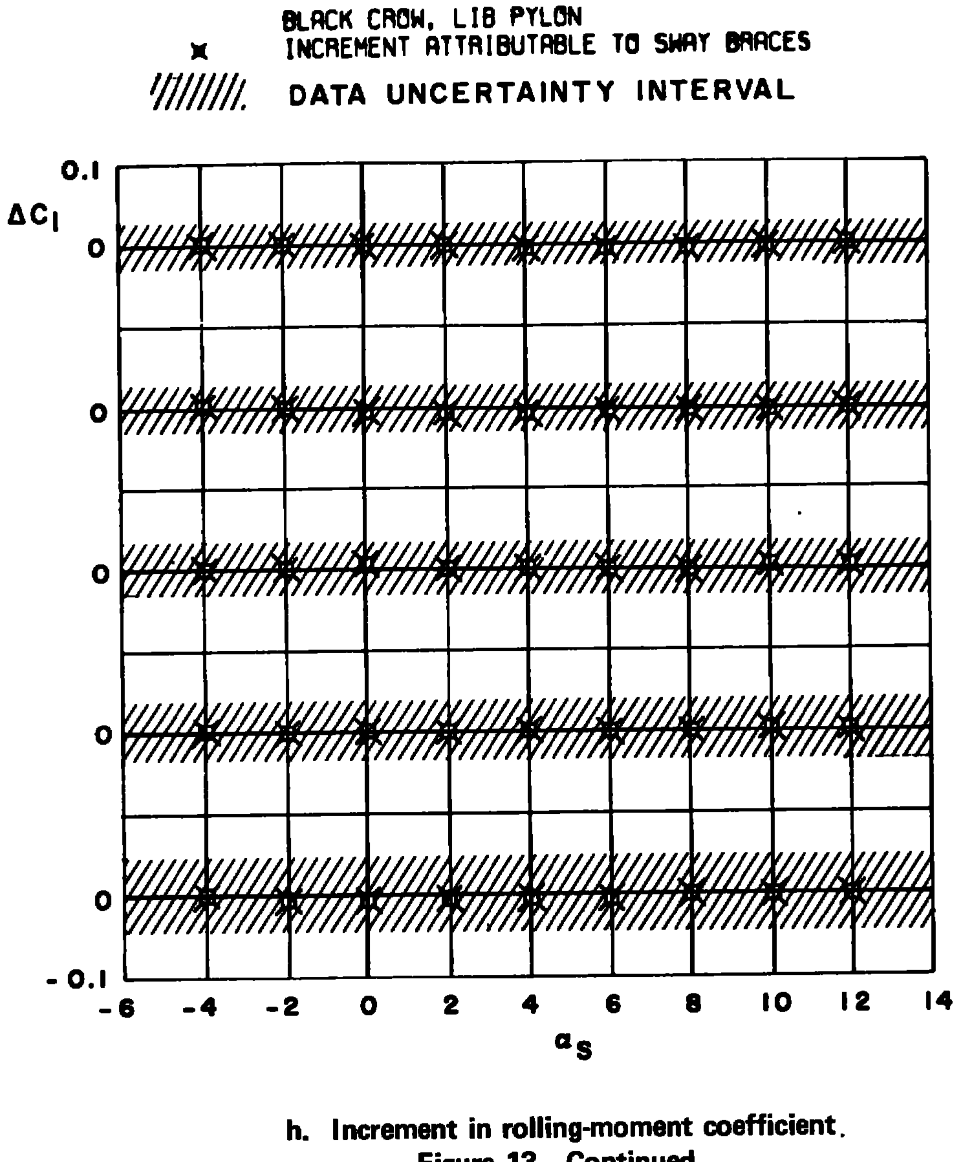

h. Increment in rolling-moment coefficient.
Figure 13. Continued.

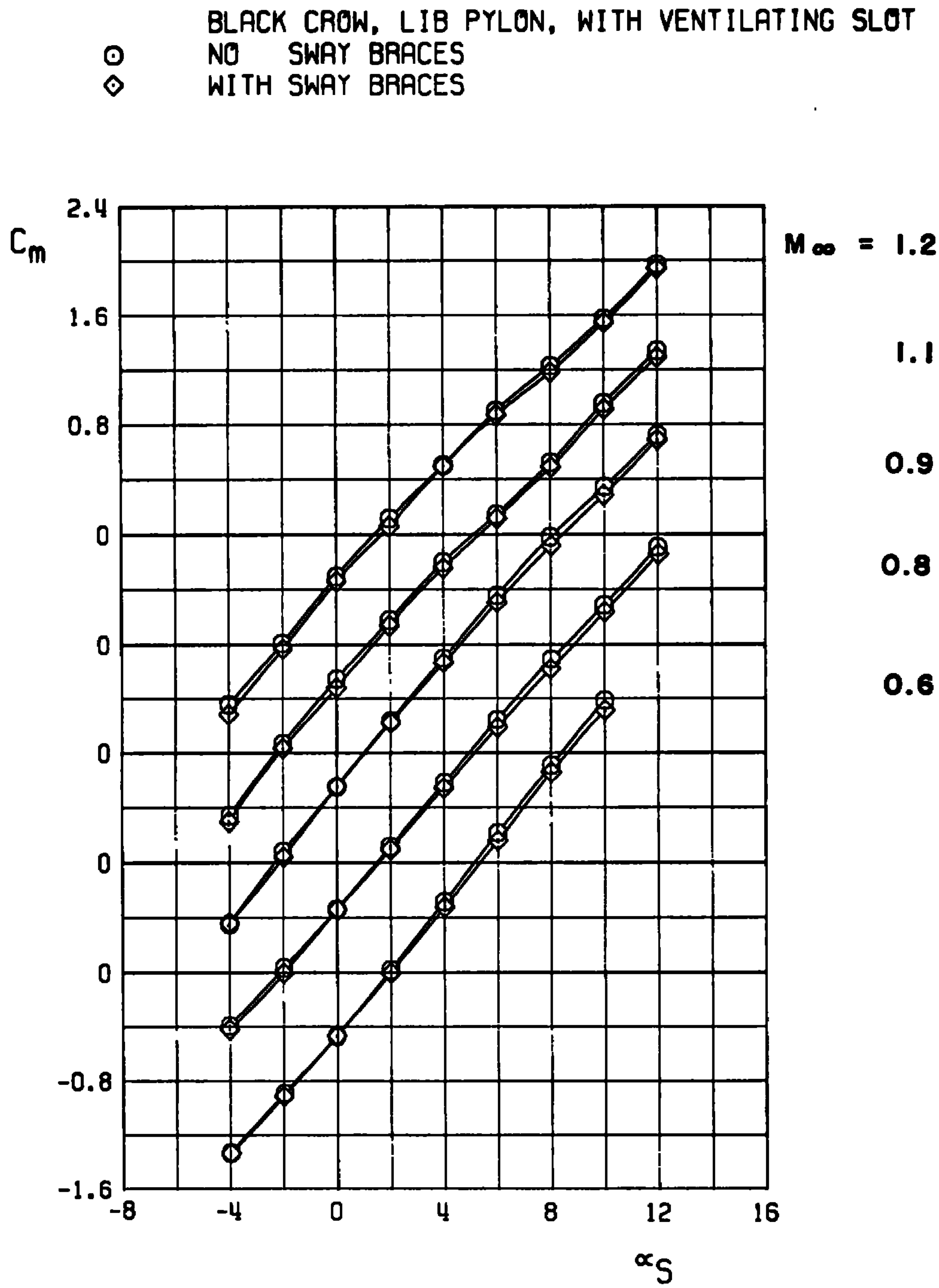

i. Pitching-moment coefficient
Figure 13. Continued.

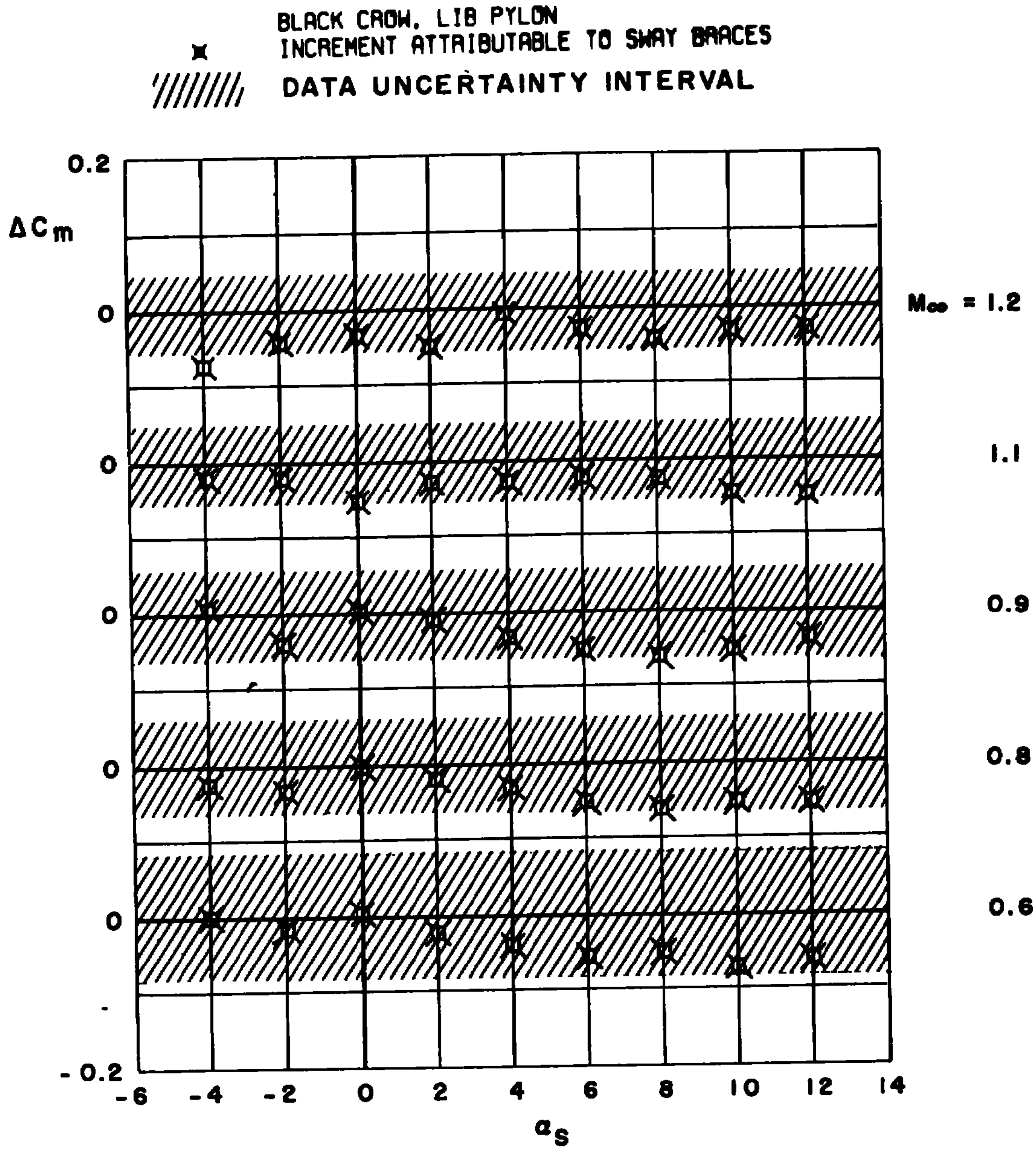

j. Increment in pitching-moment coefficient
Figure 13. Continued.

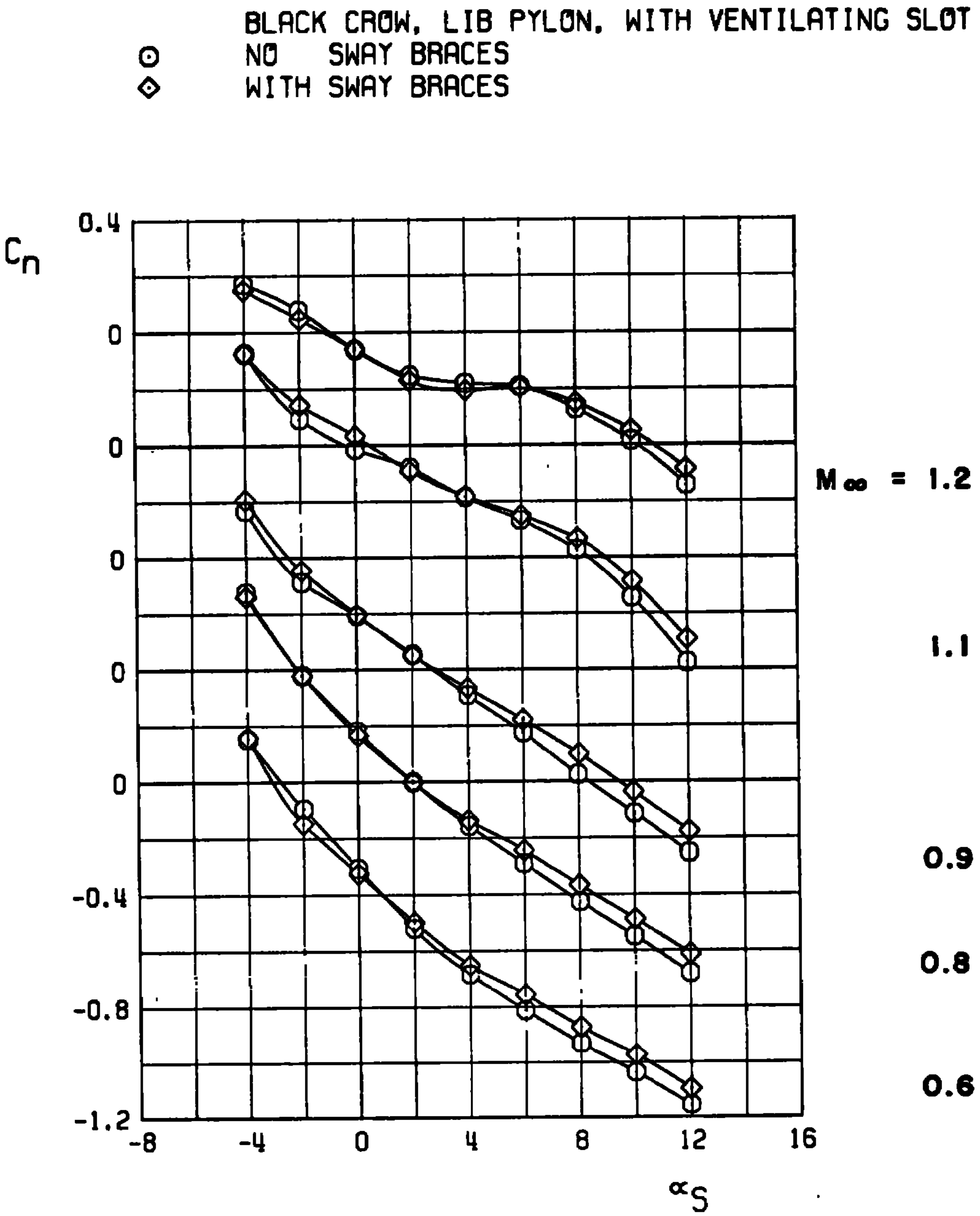

k. Yawing-moment coefficient
Figure 13. Continued.

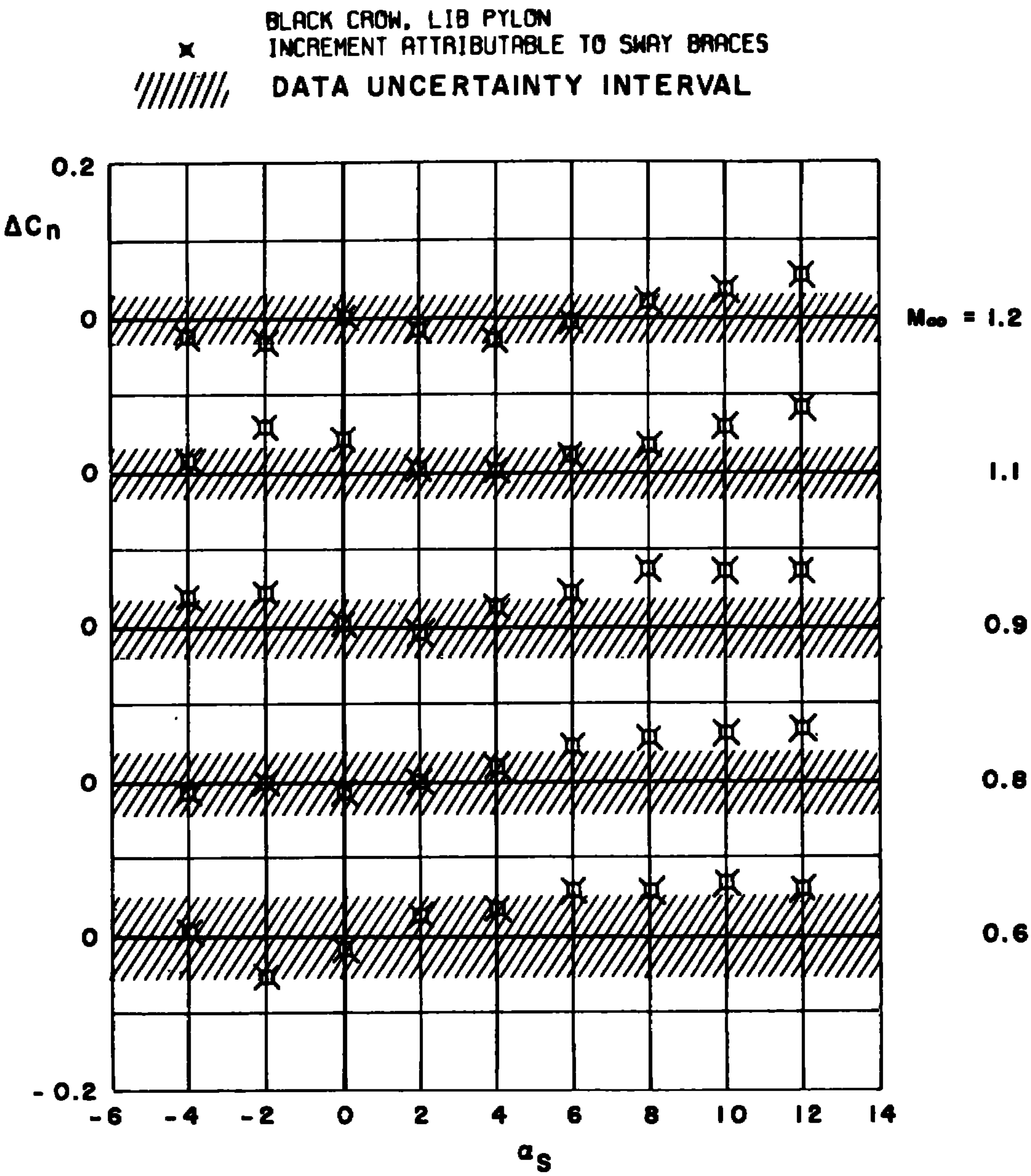

I. Increment in yawing-moment coefficient
Figure 13. Concluded.

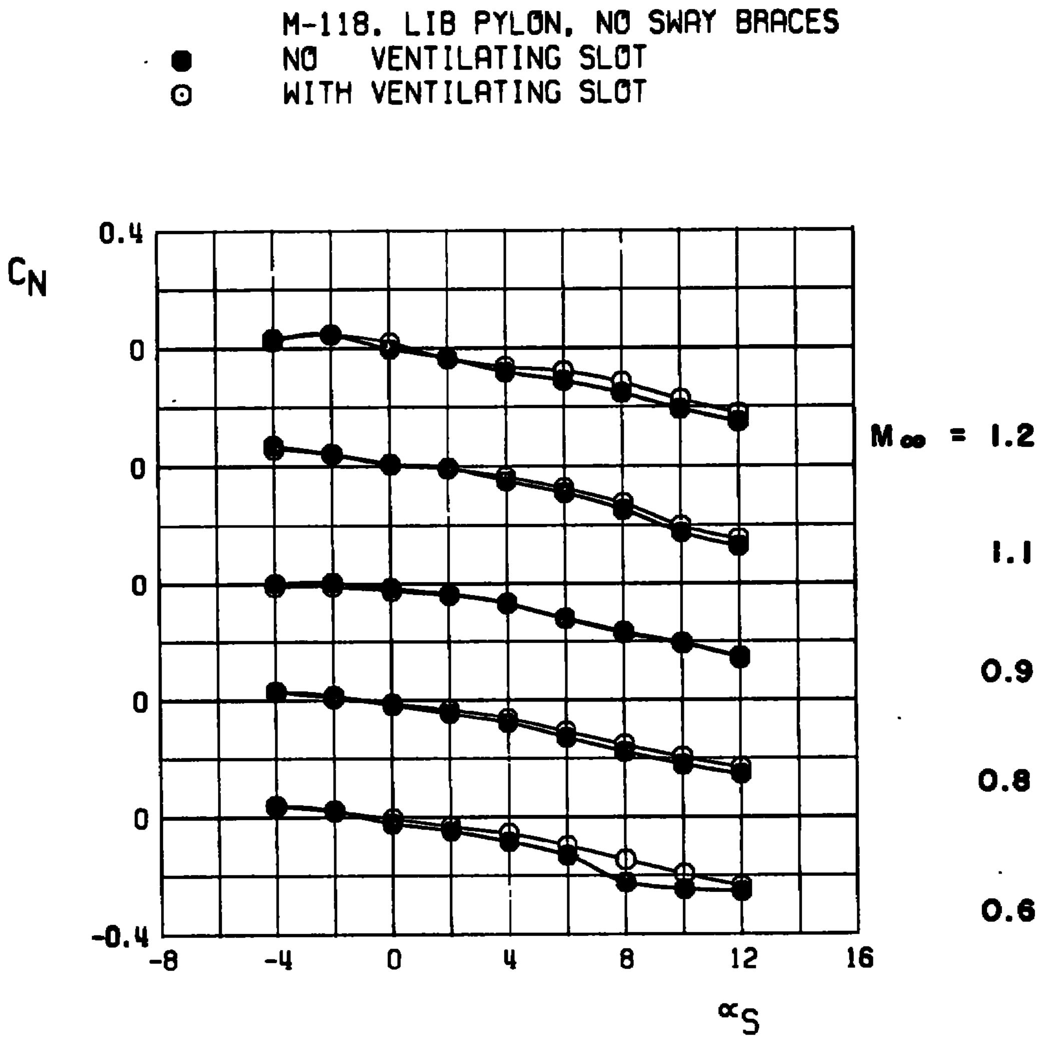

a. Normal-force coefficient

Figure 14. Isolated effect of a ventilated supporting bracket on the static aerodynamic loads acting on a stable pylon-mounted store.

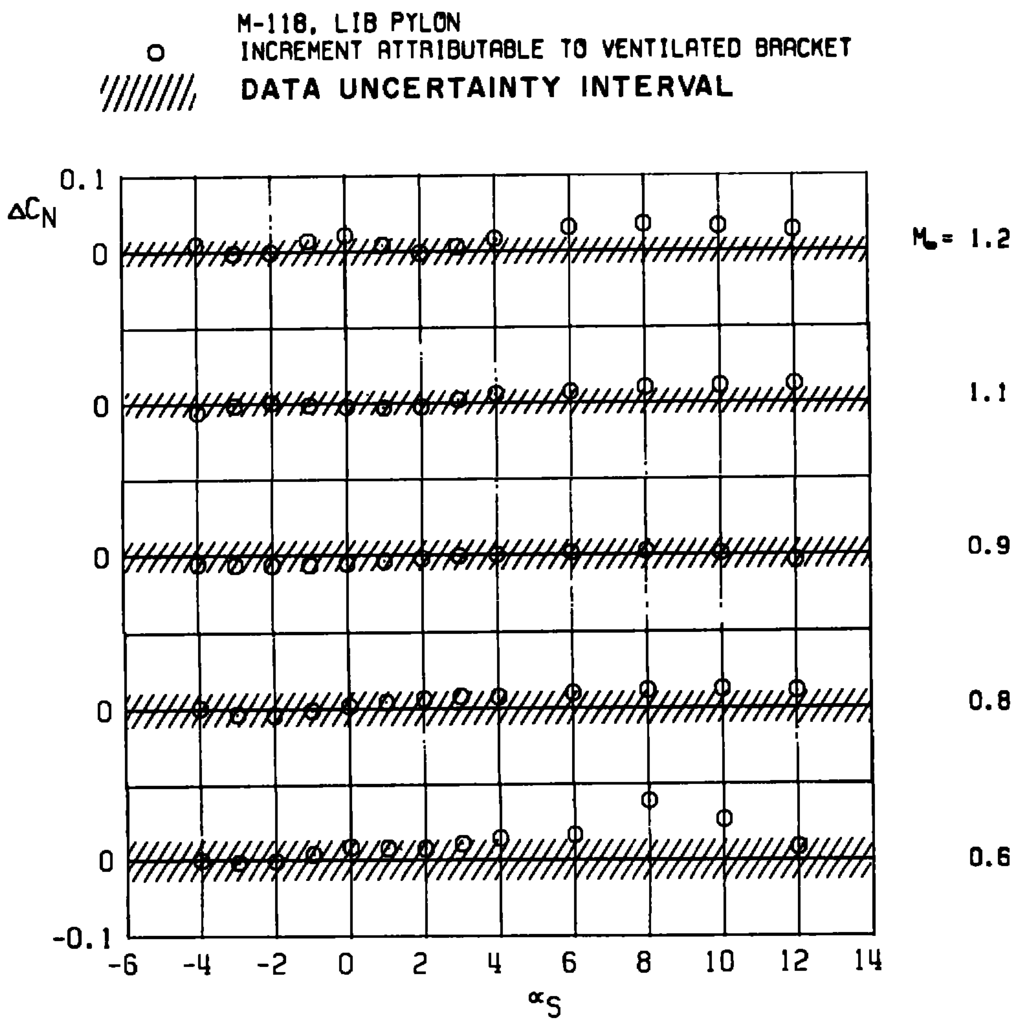

b. Increment in normal-force coefficient
Figure 14. Continued.

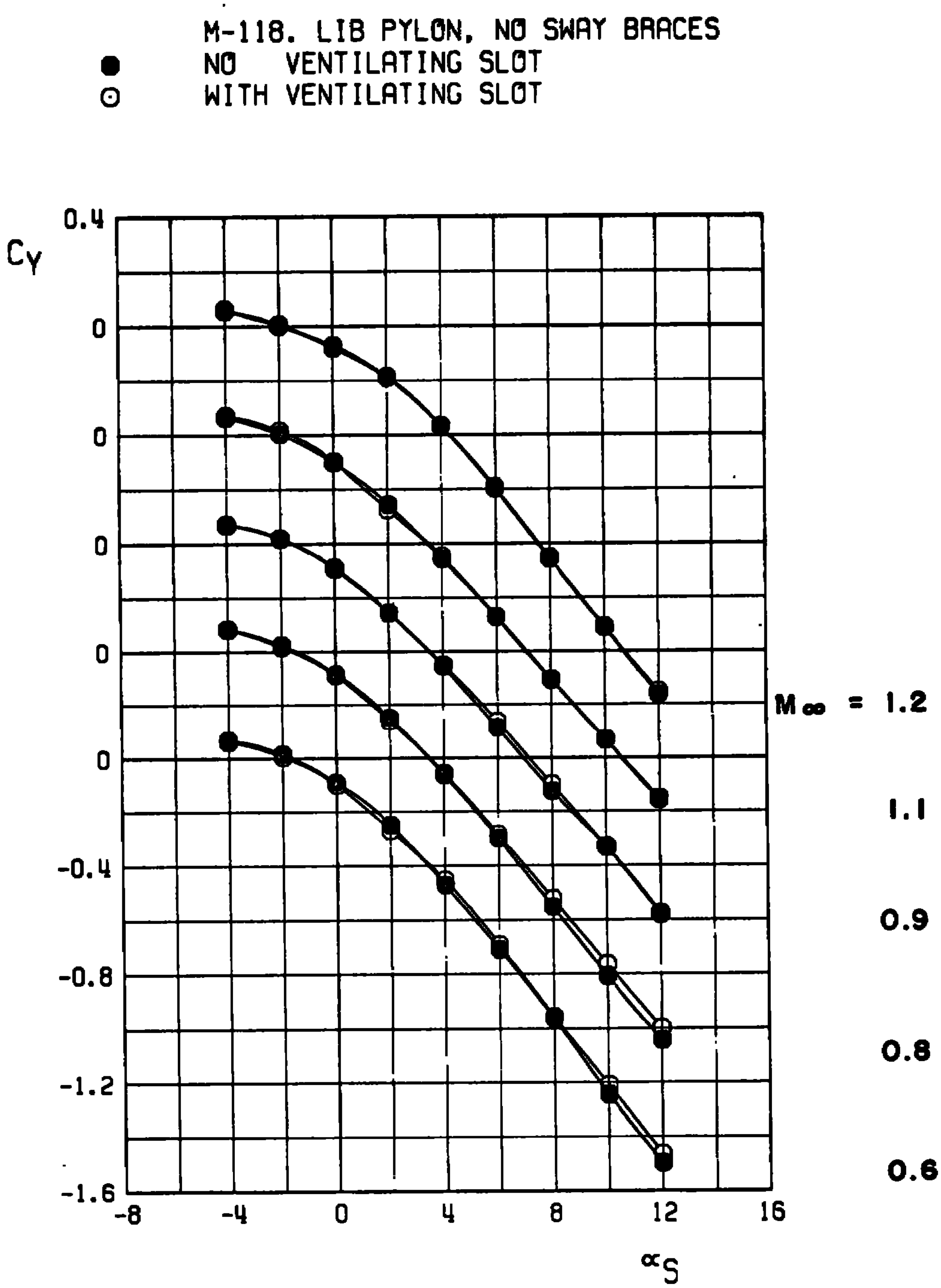

c. Side-force coefficient
Figure 14. Continued.

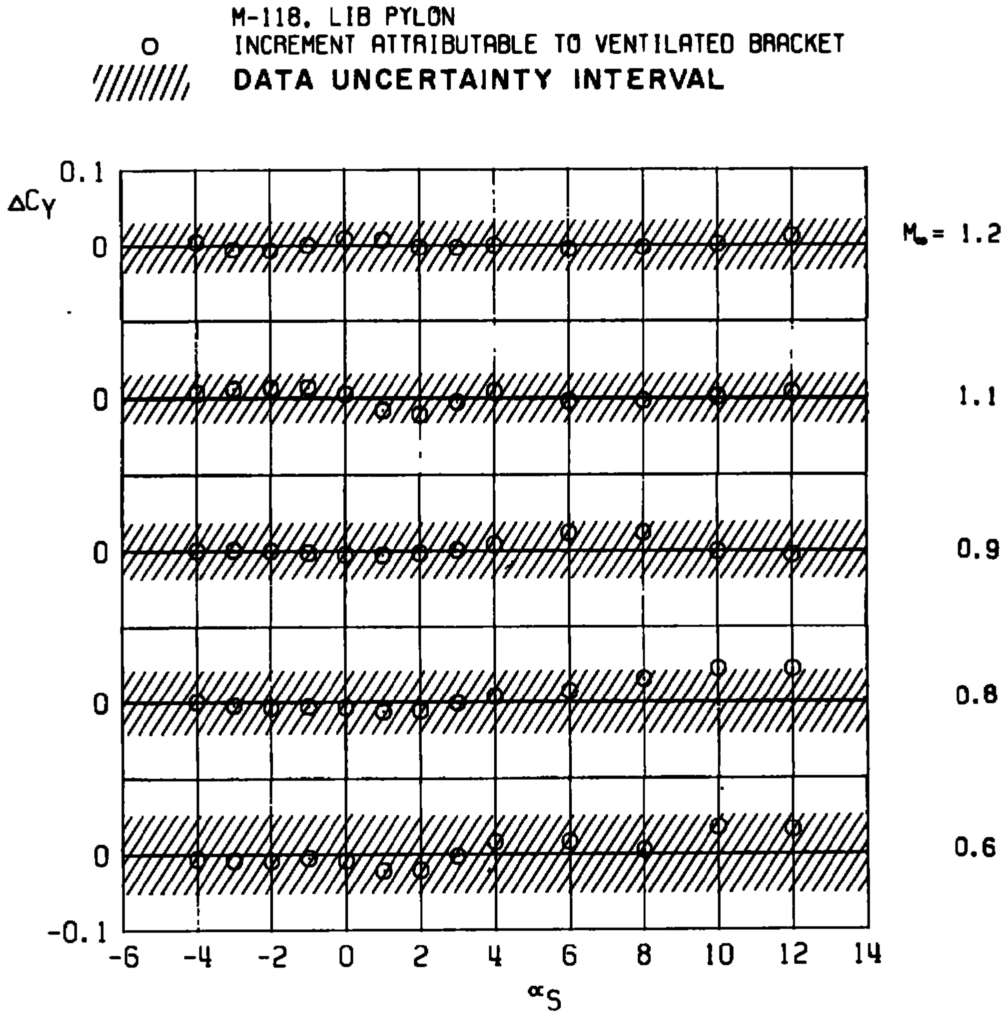

d. Increment in side-force coefficient
Figure 14. Continued.

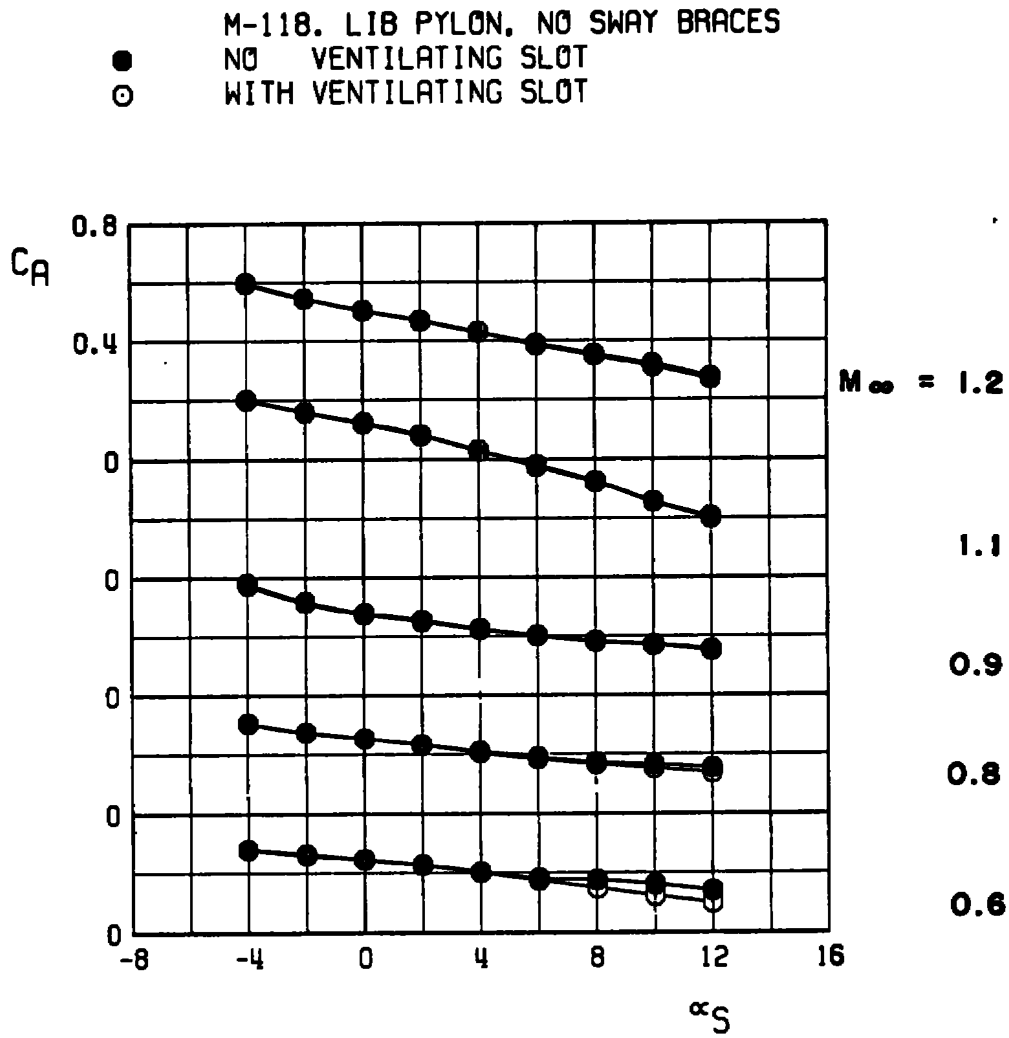

e. Axial-force coefficient
Figure 14. Continued.

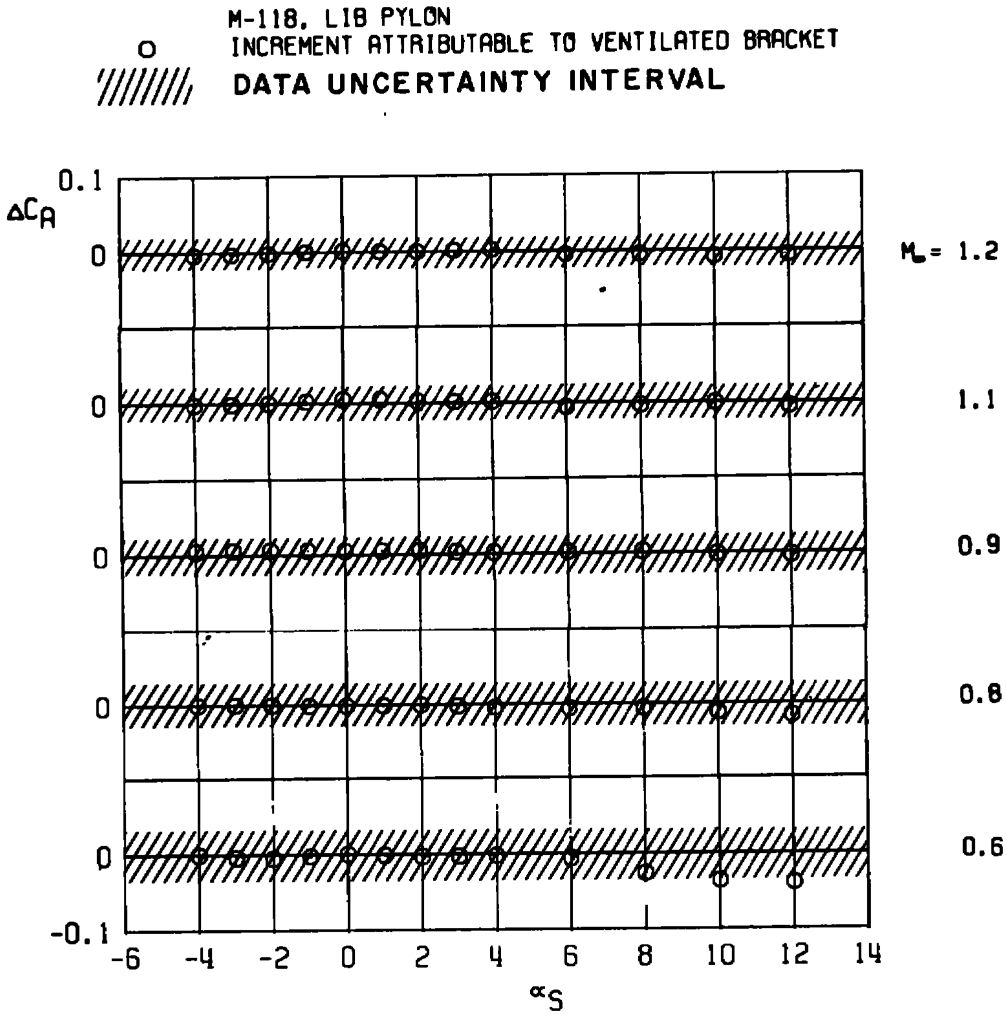

f. Increment in axial-force coefficient
Figure 14. Continued.

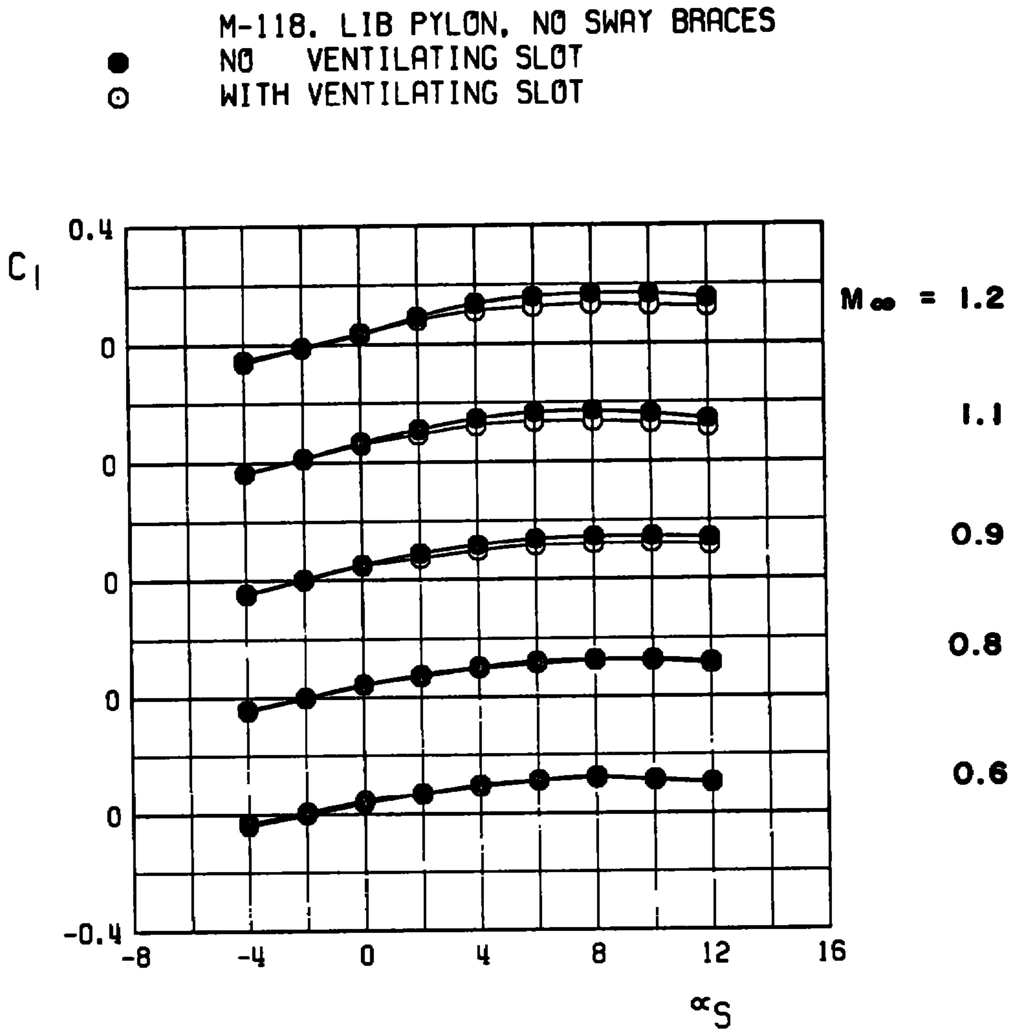

g. Rolling-moment coefficient
Figure 14. Continued.

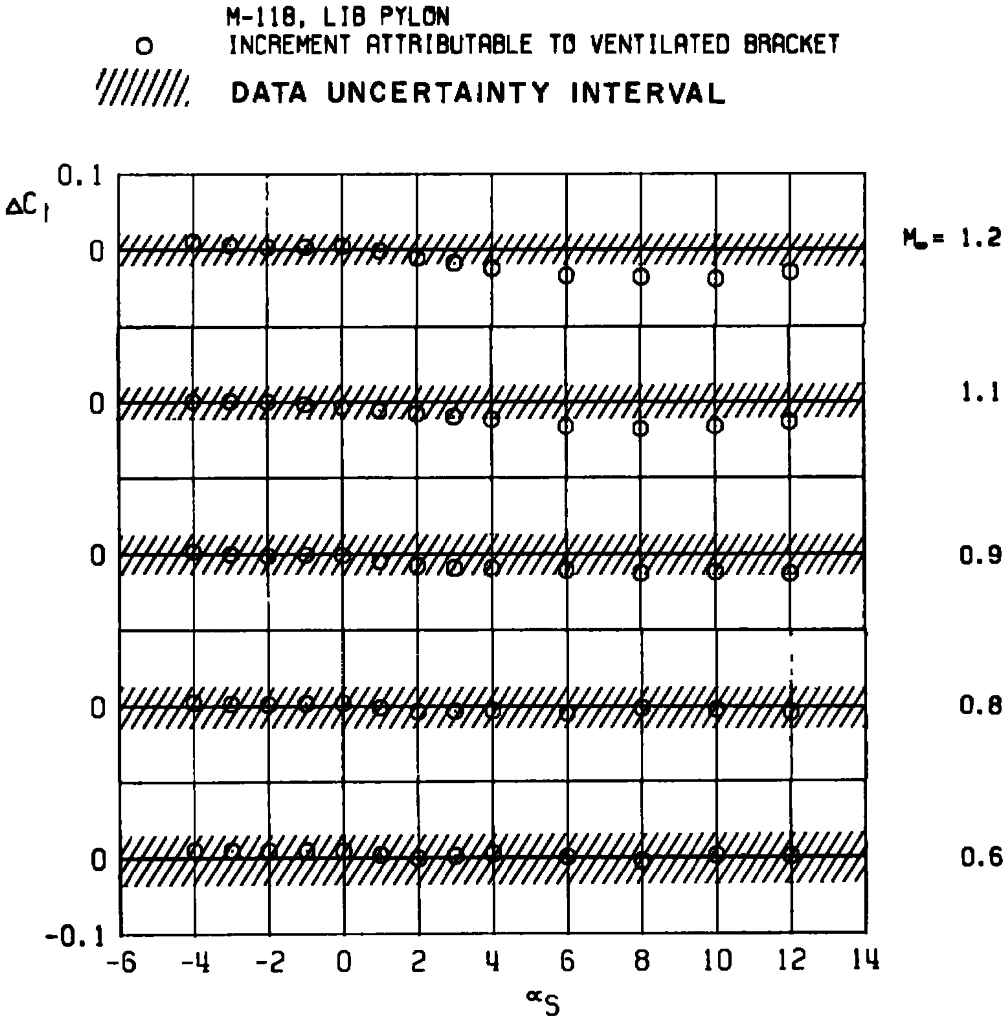

h. Increment in rolling-moment coefficient
Figure 14. Continued.

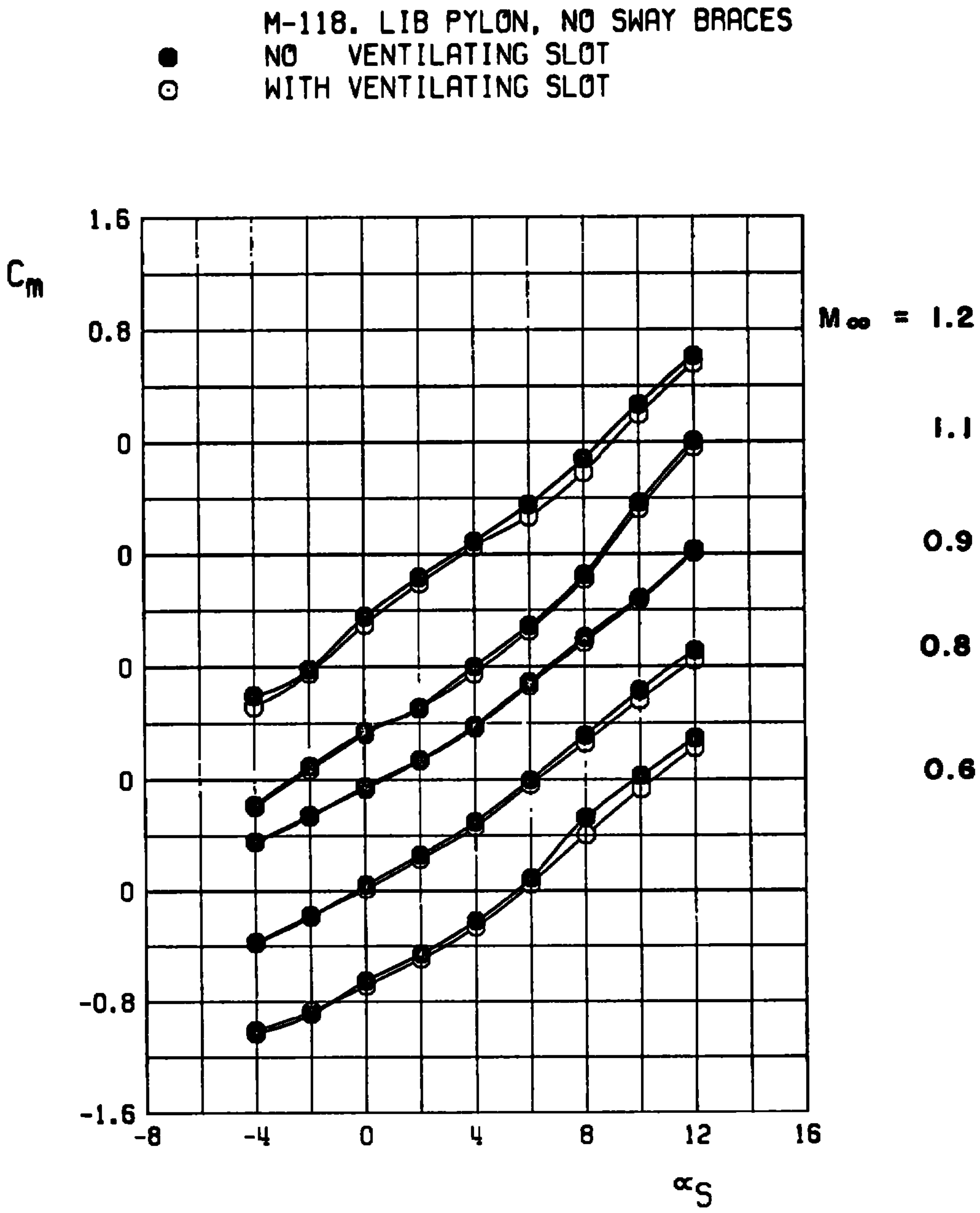

i. Pitching-moment coefficient
Figure 14. Continued.

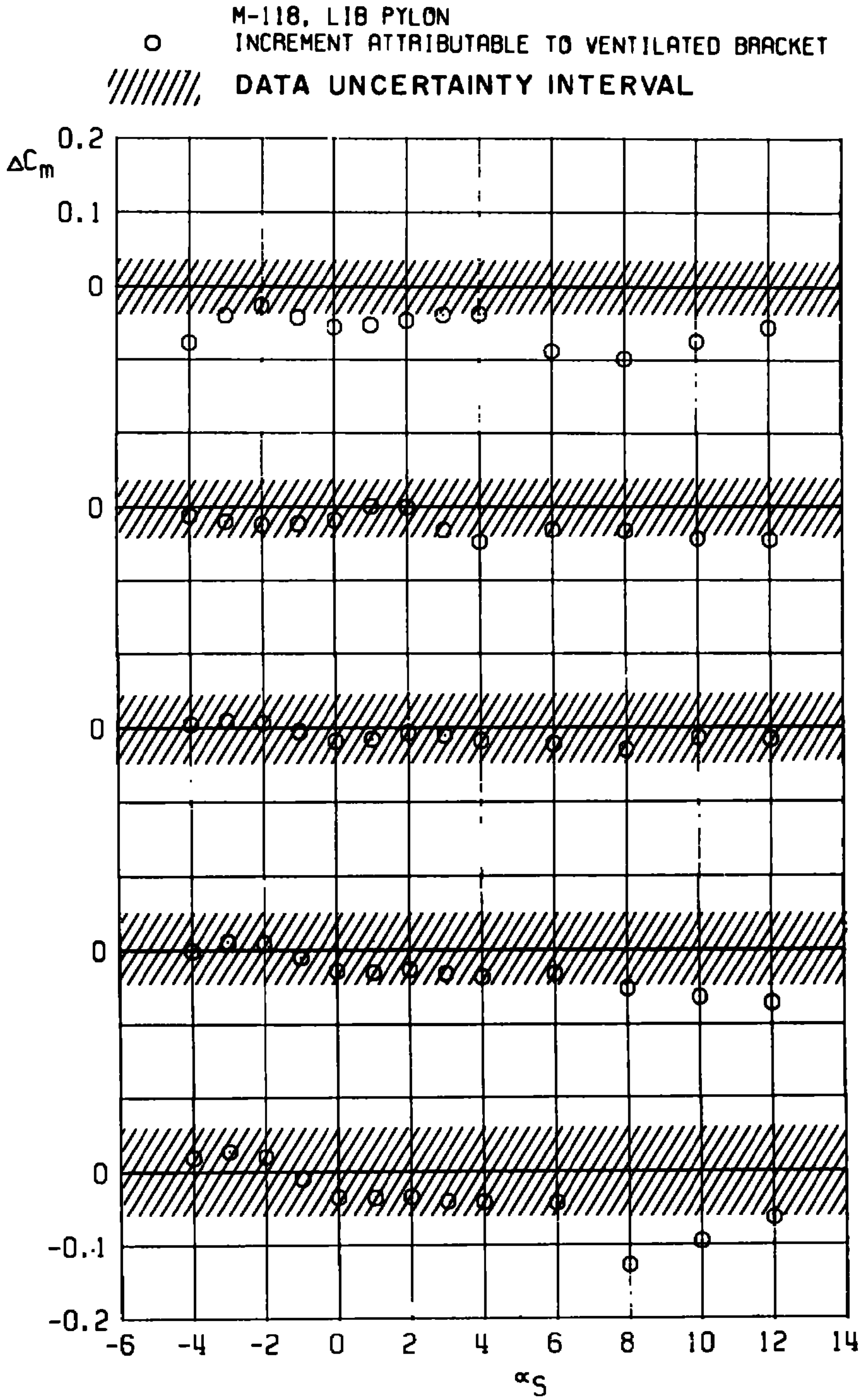

j. Increment in pitching-moment coefficient
Figure 14. Continued.

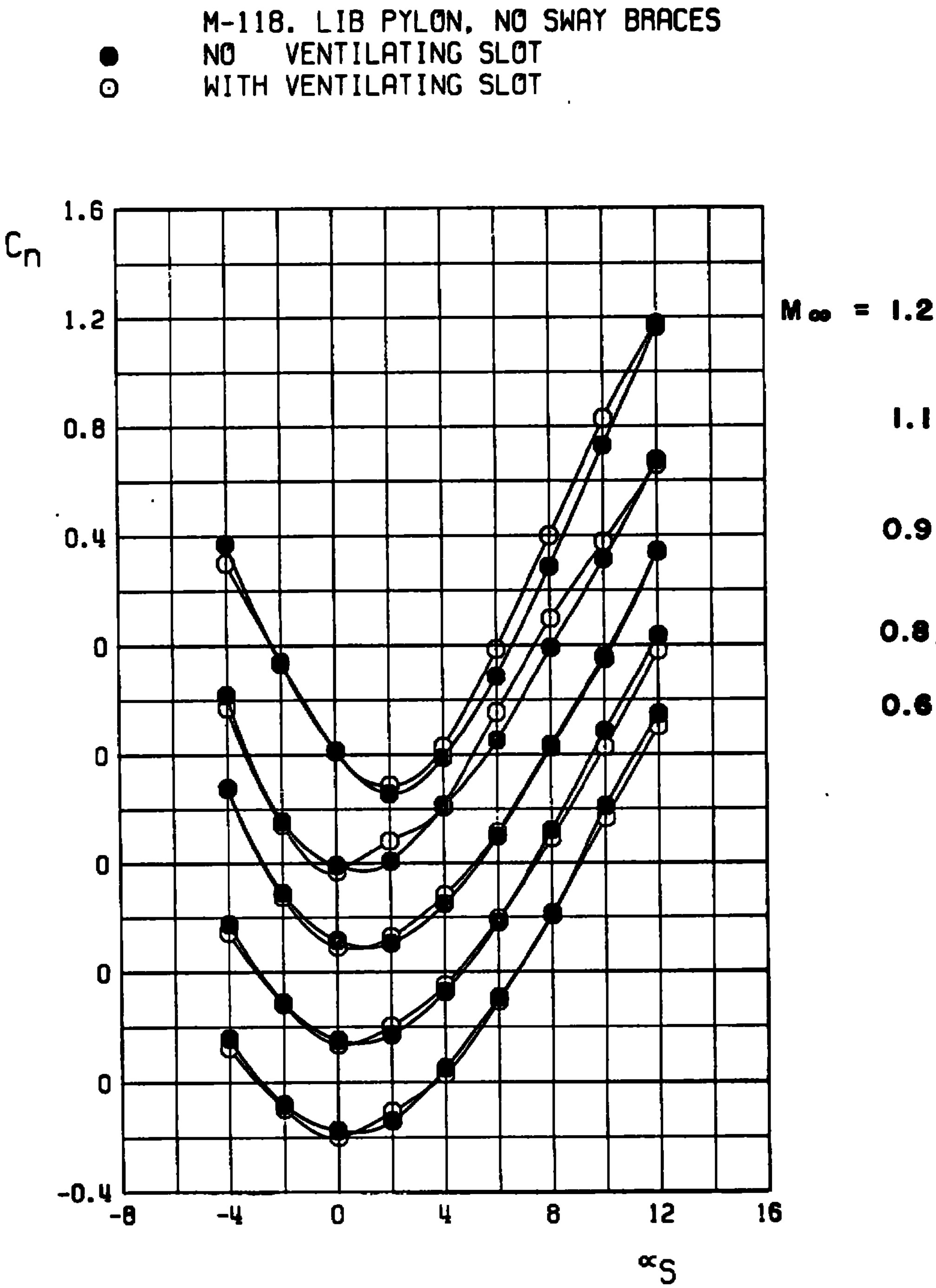

k. Yawing-moment coefficient
Figure 14. Continued.

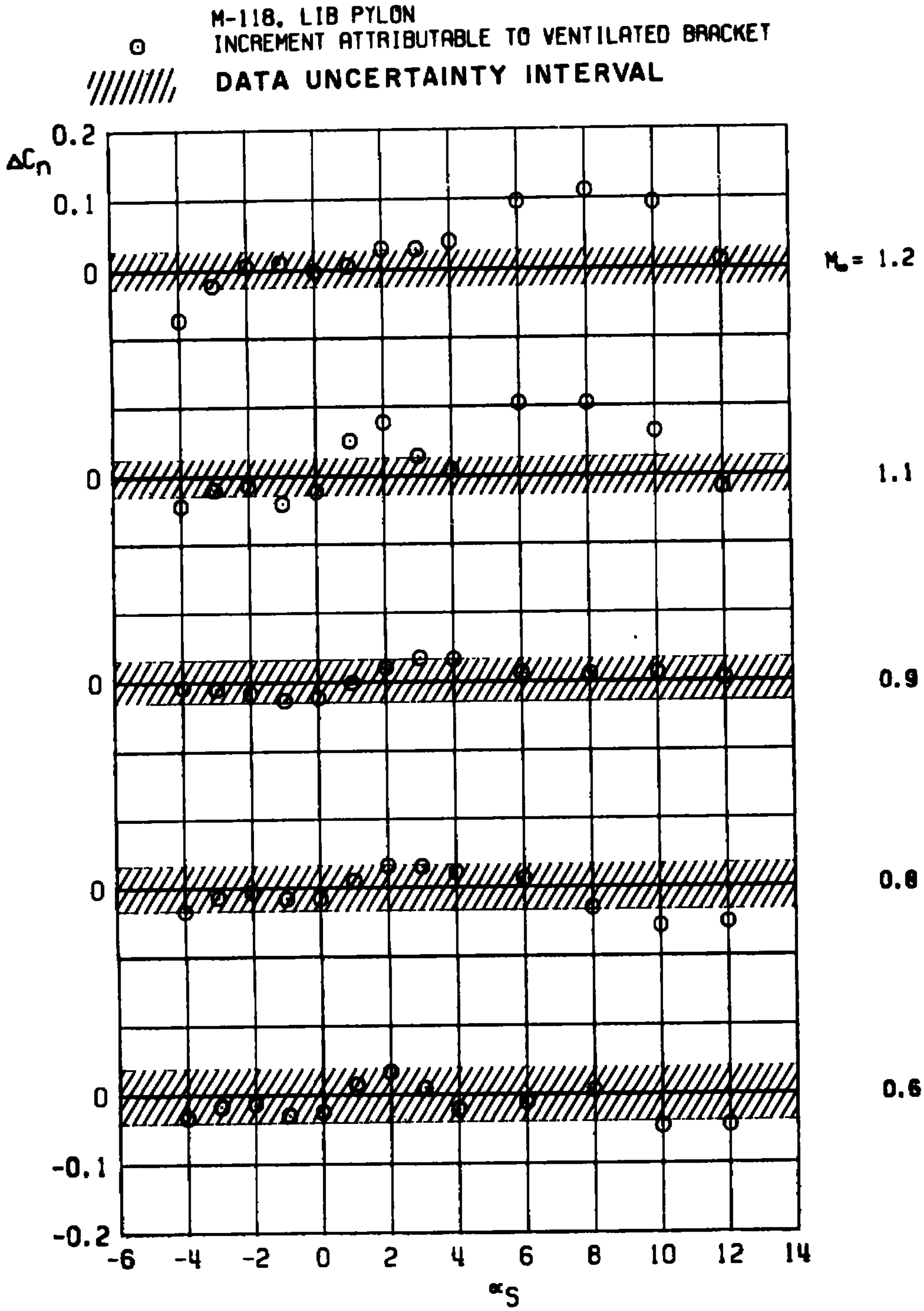

I. Increment in yawing-moment coefficient
Figure 14. Concluded.

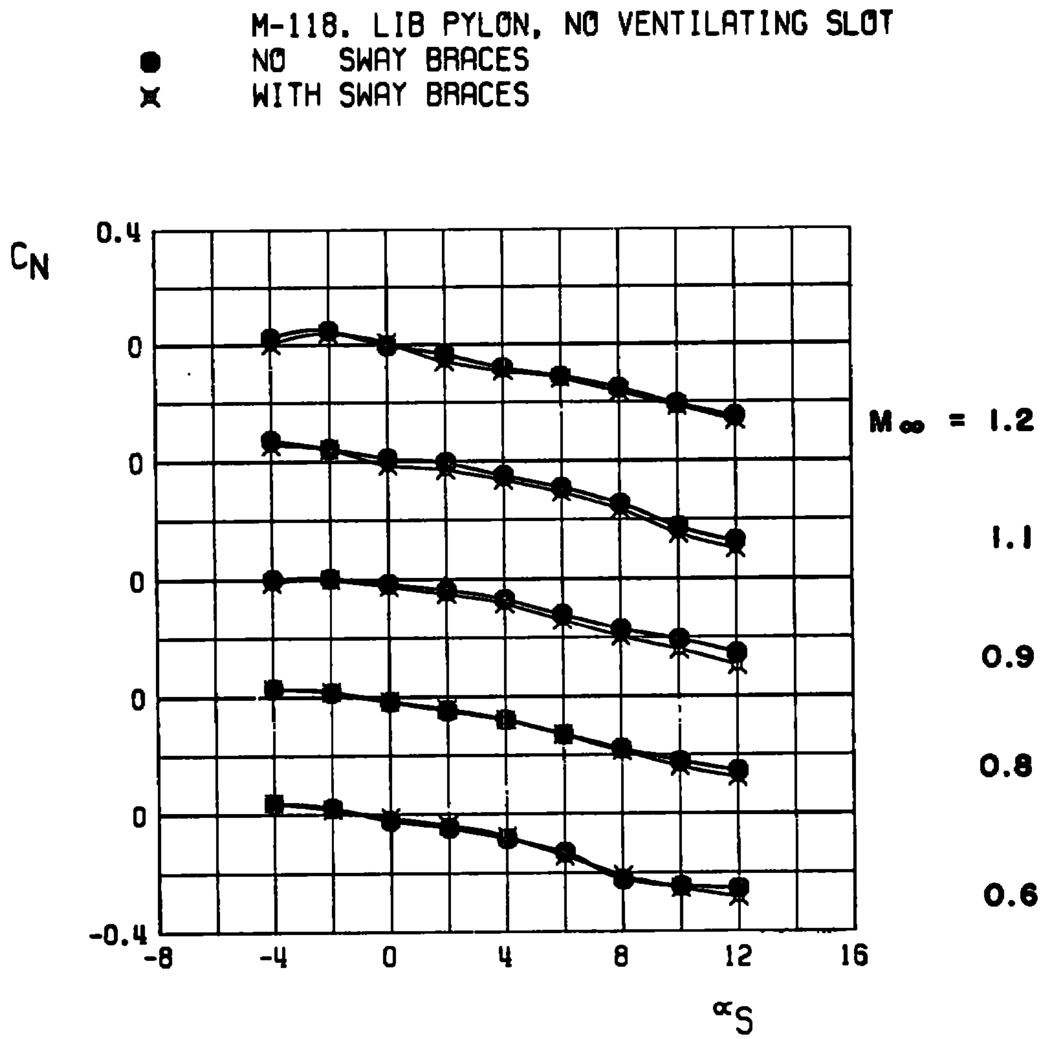

a. Normal-force coefficient

Figure 15. Isolated effect of pylon sway braces on the static aerodynamic loads acting on a stable pylon-mounted store.

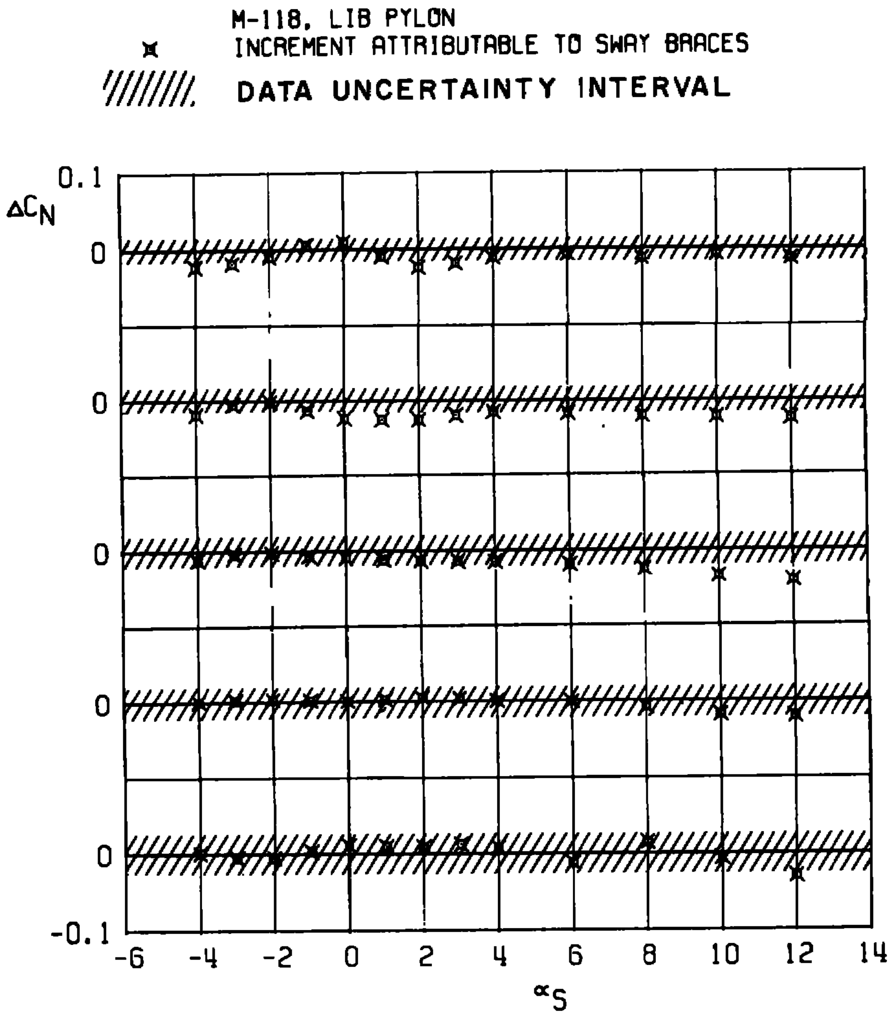

b. Increment in normal-force coefficient
Figure 15. Continued.

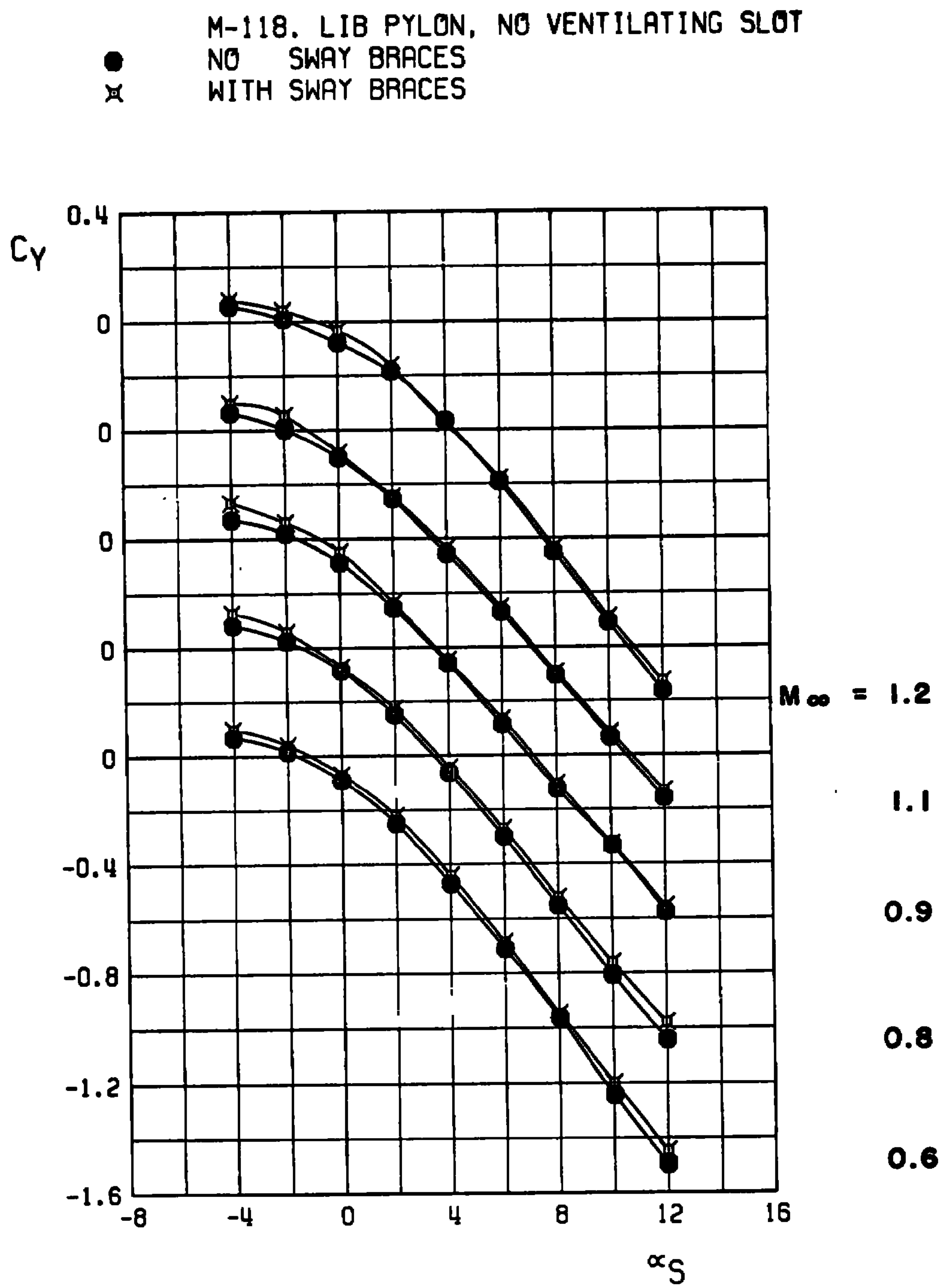

c. Side-force coefficient
Figure 15. Continued.

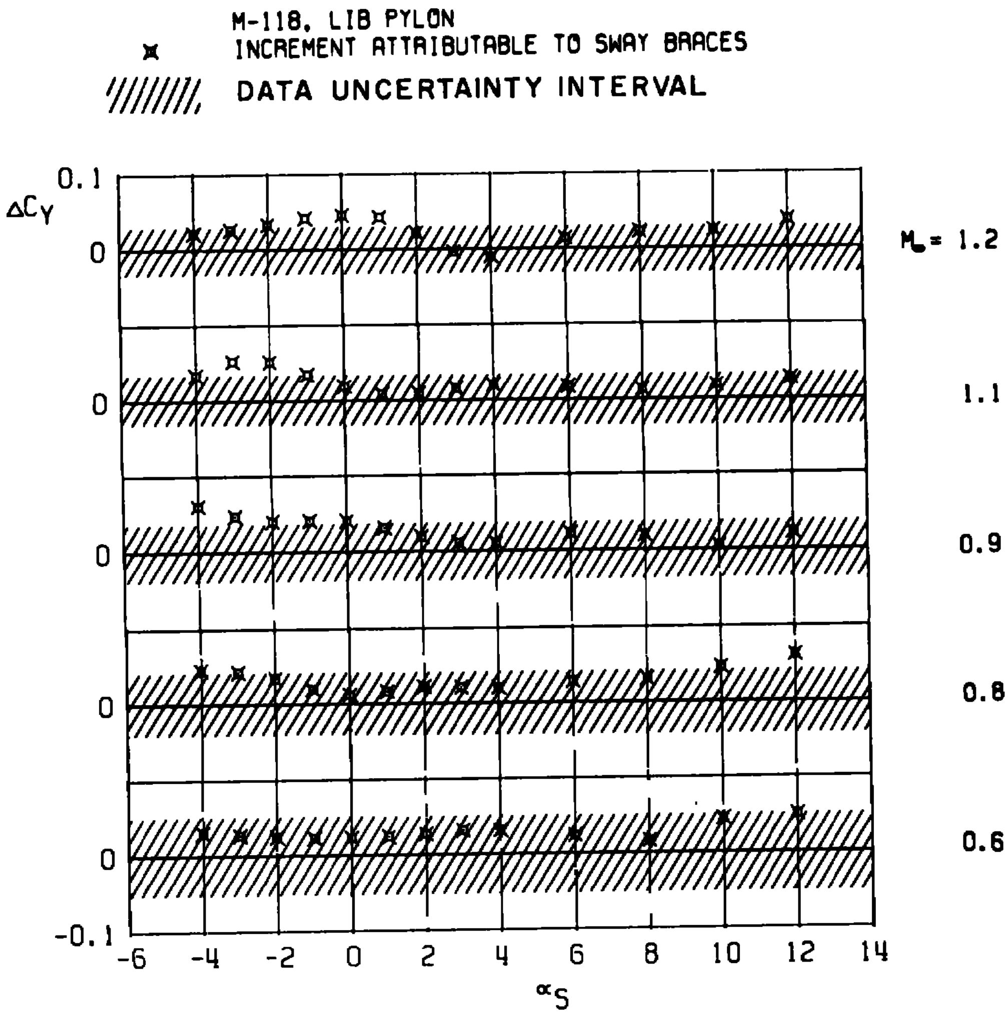

d. Increment in side-force coefficient
Figure 15. Continued.

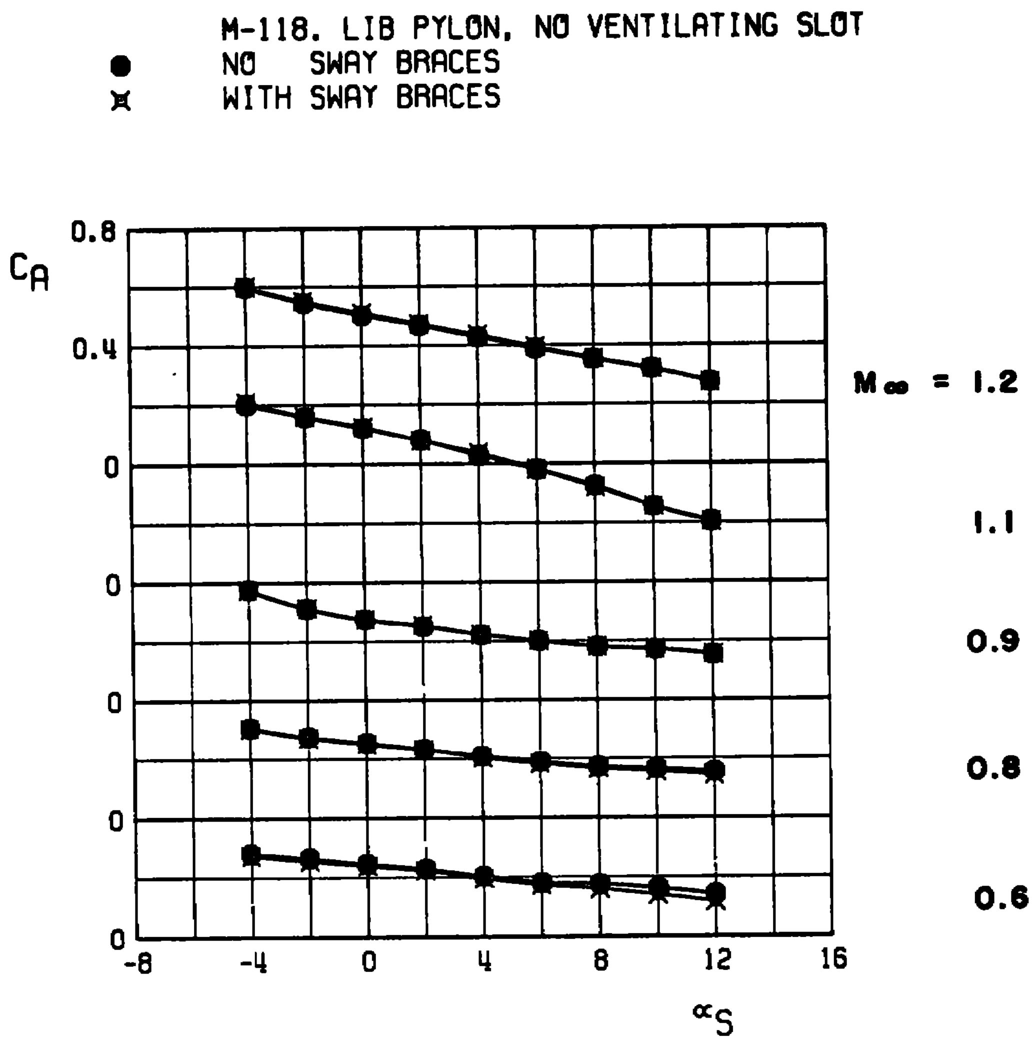

e. Axial-force coefficient
Figure 15. Continued.

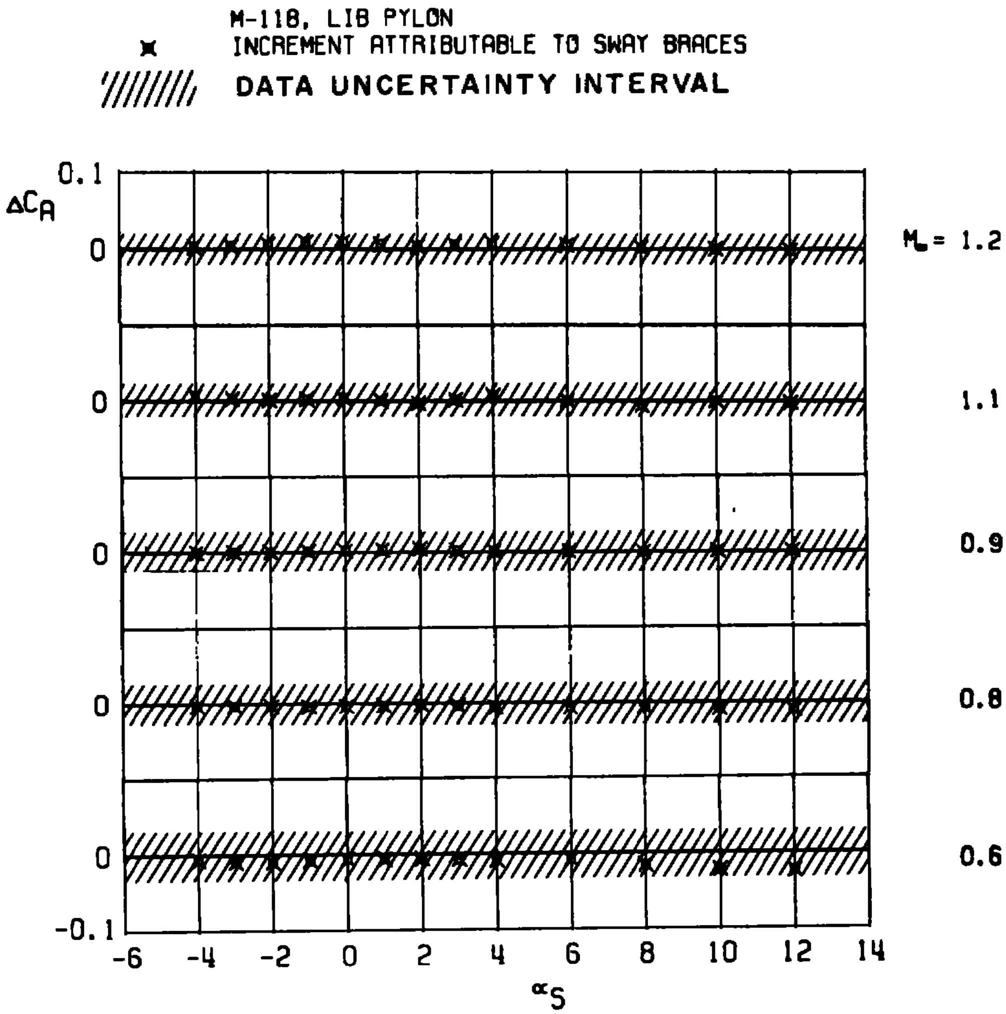

f. Increment in axial-force coefficient
Figure 15. Continued.

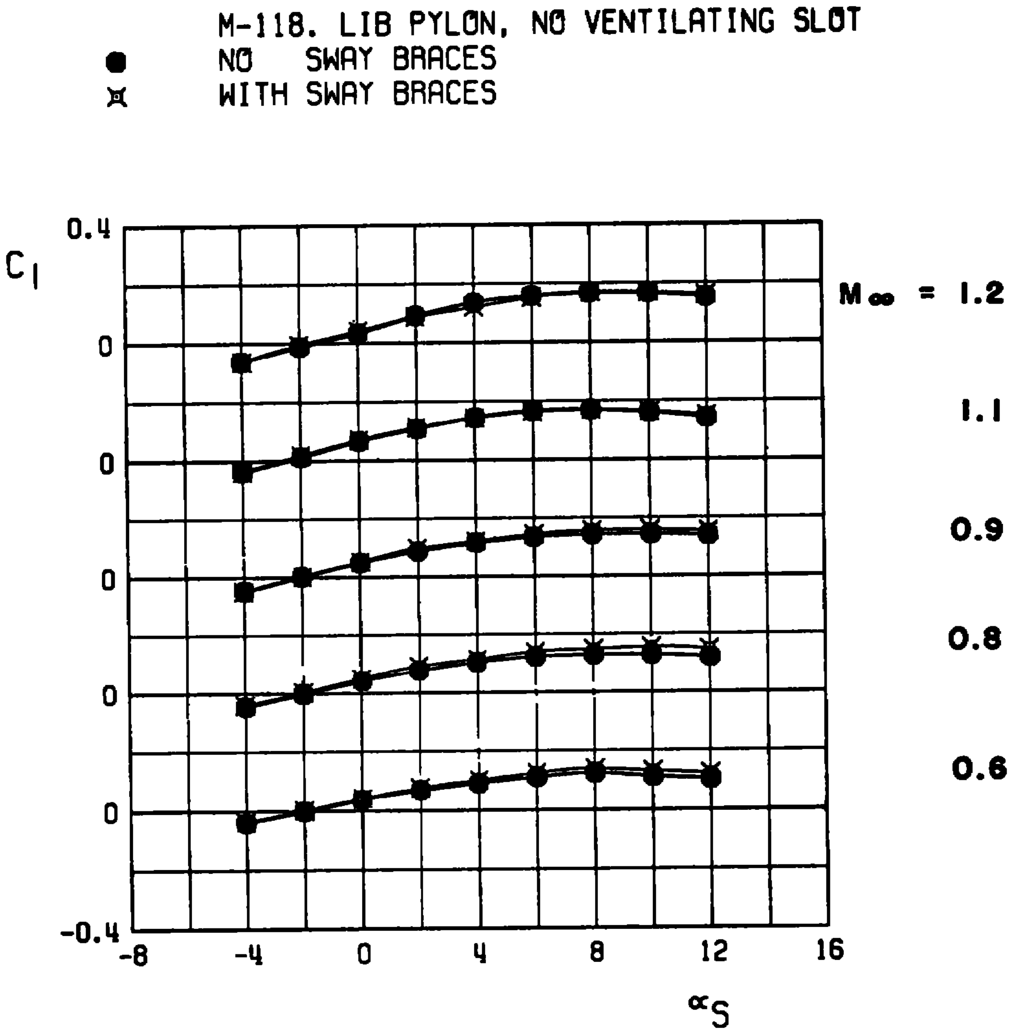

g. Rolling-moment coefficient
Figure 15. Continued.

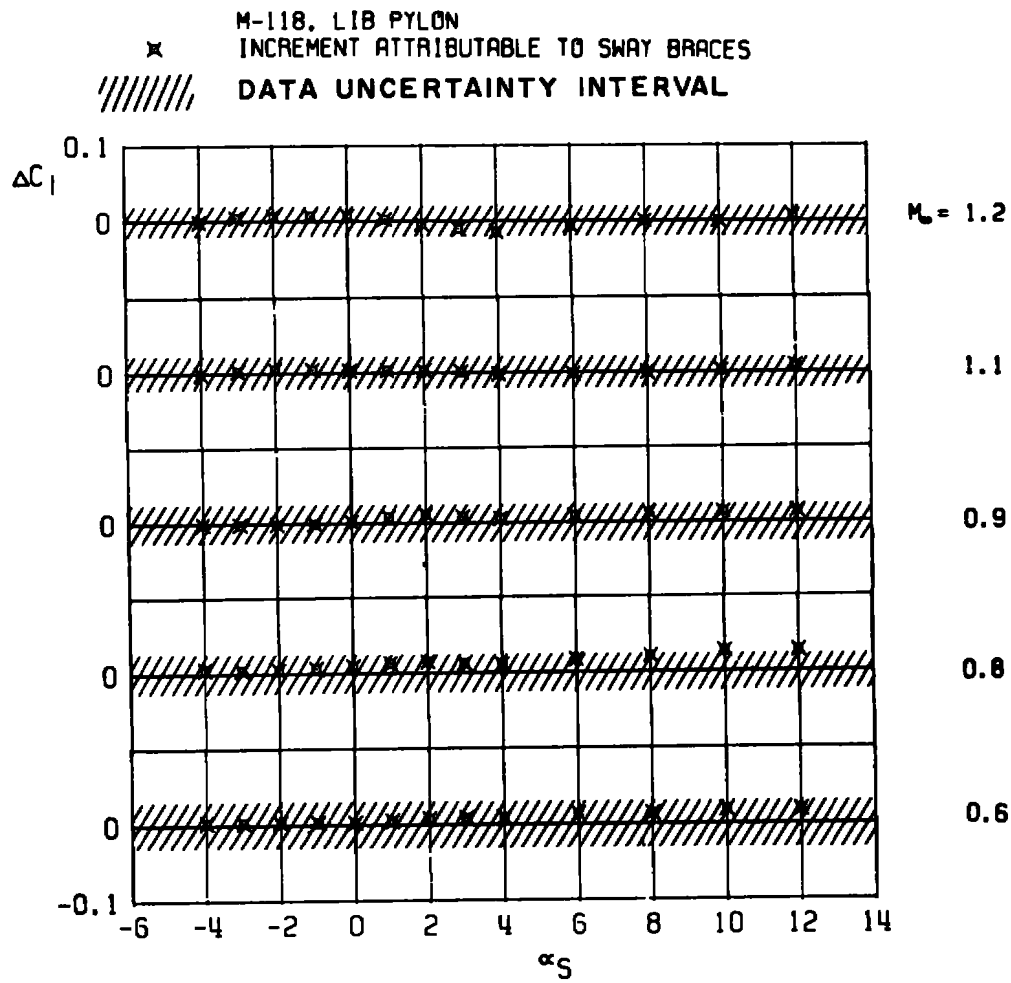

h. Increment in rolling-moment coefficient
Figure 15. Continued.

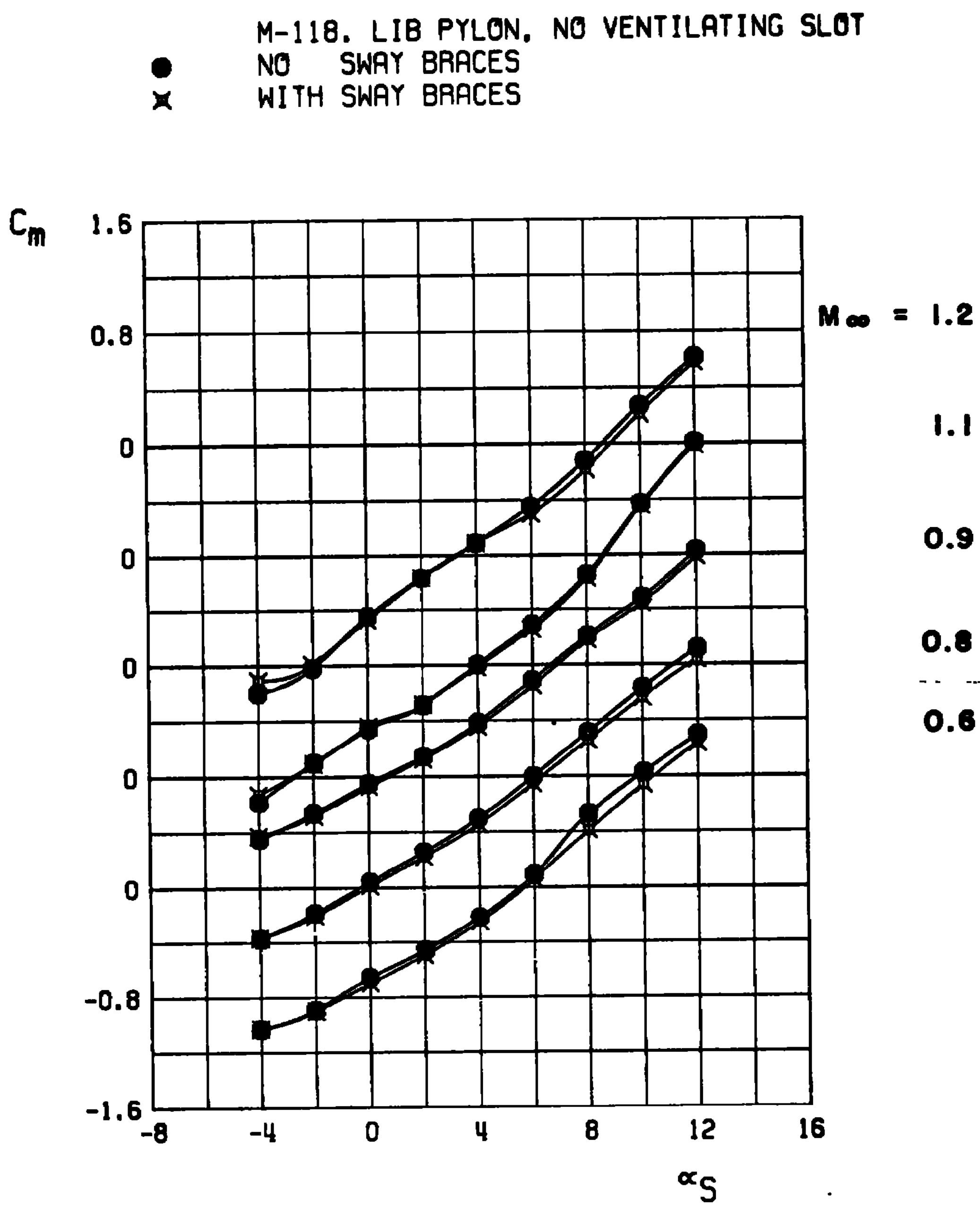

i. Pitching-moment coefficient
Figure 15. Continued.

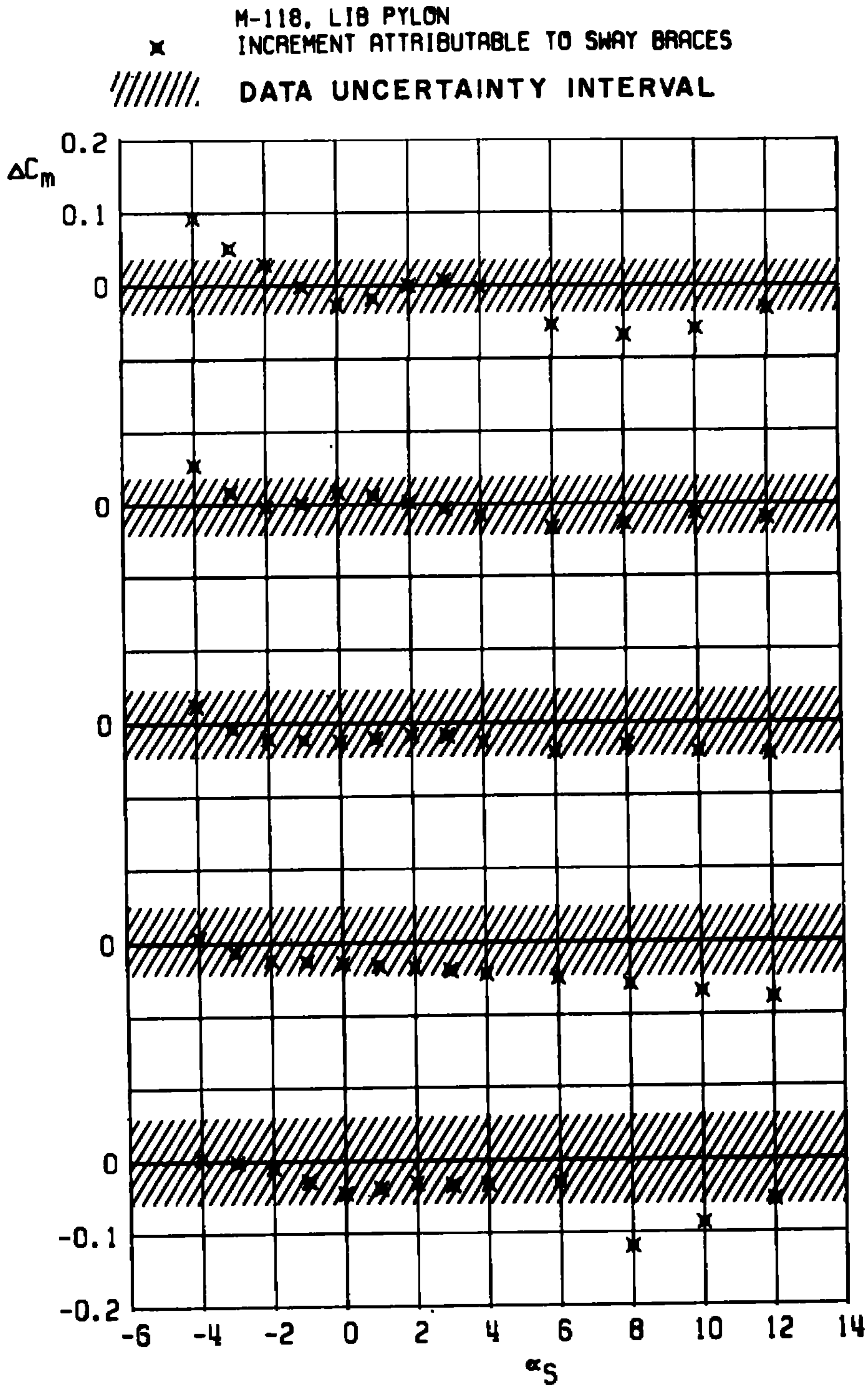

j. Increment in pitching-moment coefficient
Figure 15. Continued.

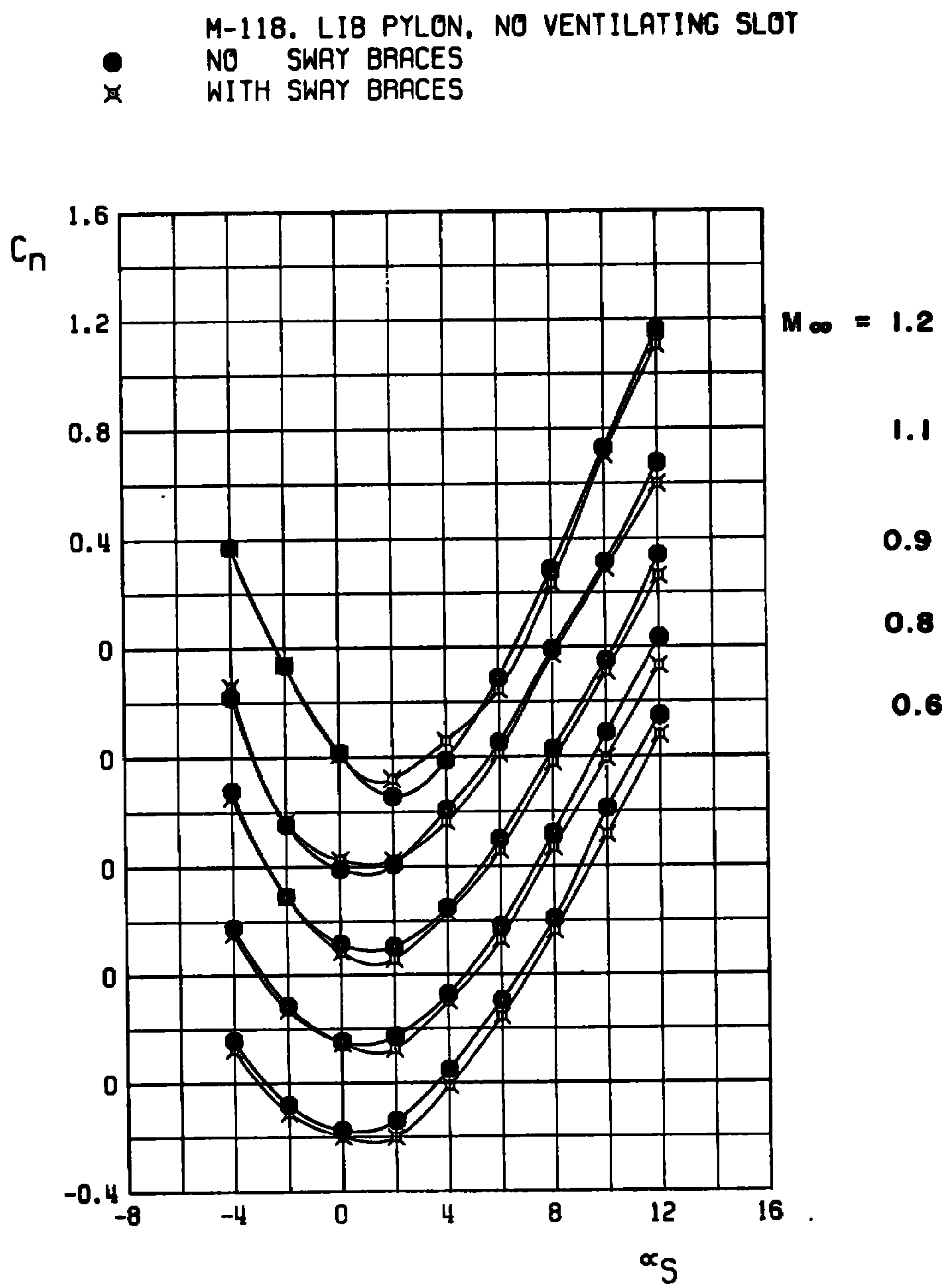

k. Yawing-moment coefficient
Figure 15. Continued.

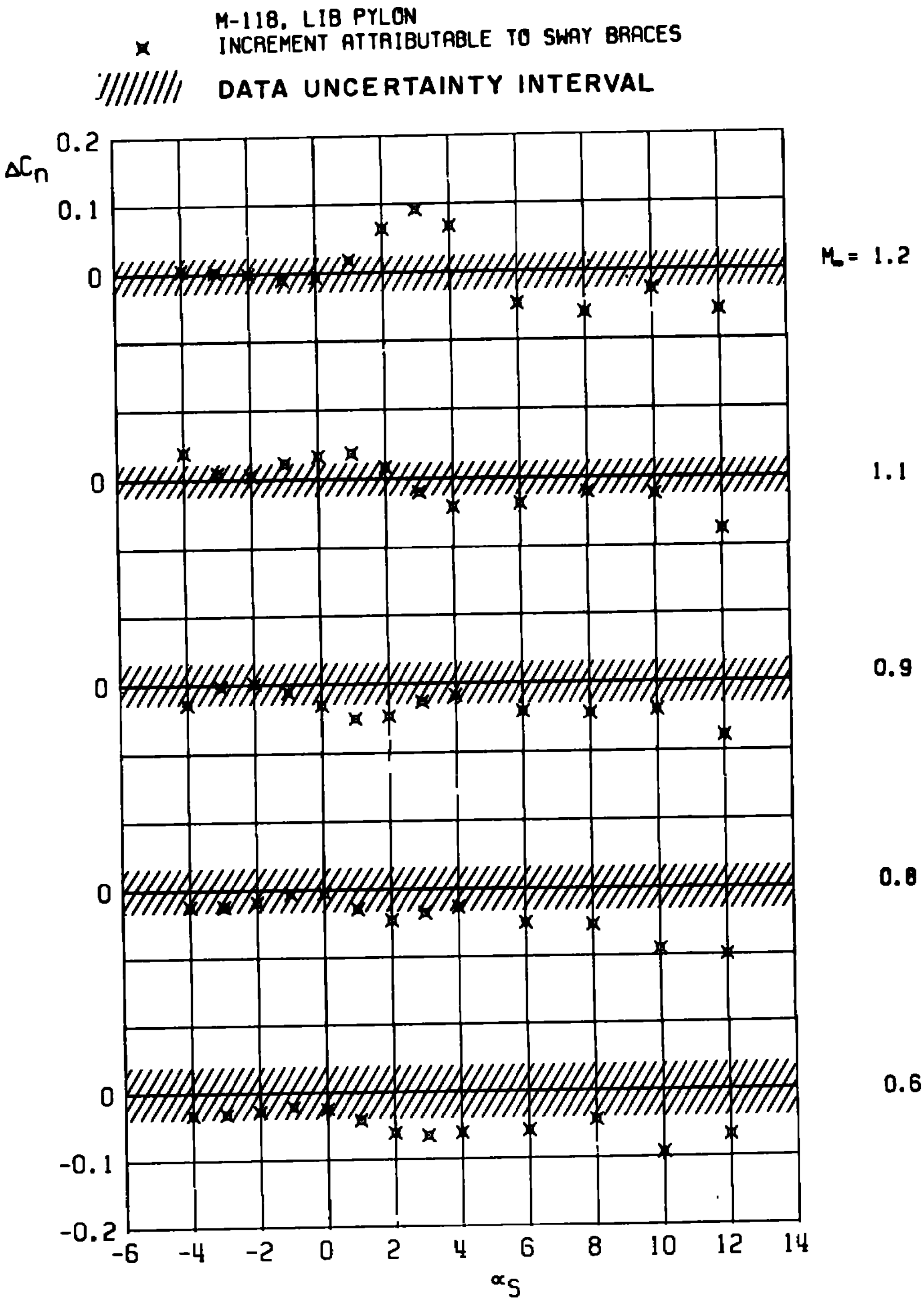

I. Increment in yawing-moment coefficient
Figure 15. Concluded.

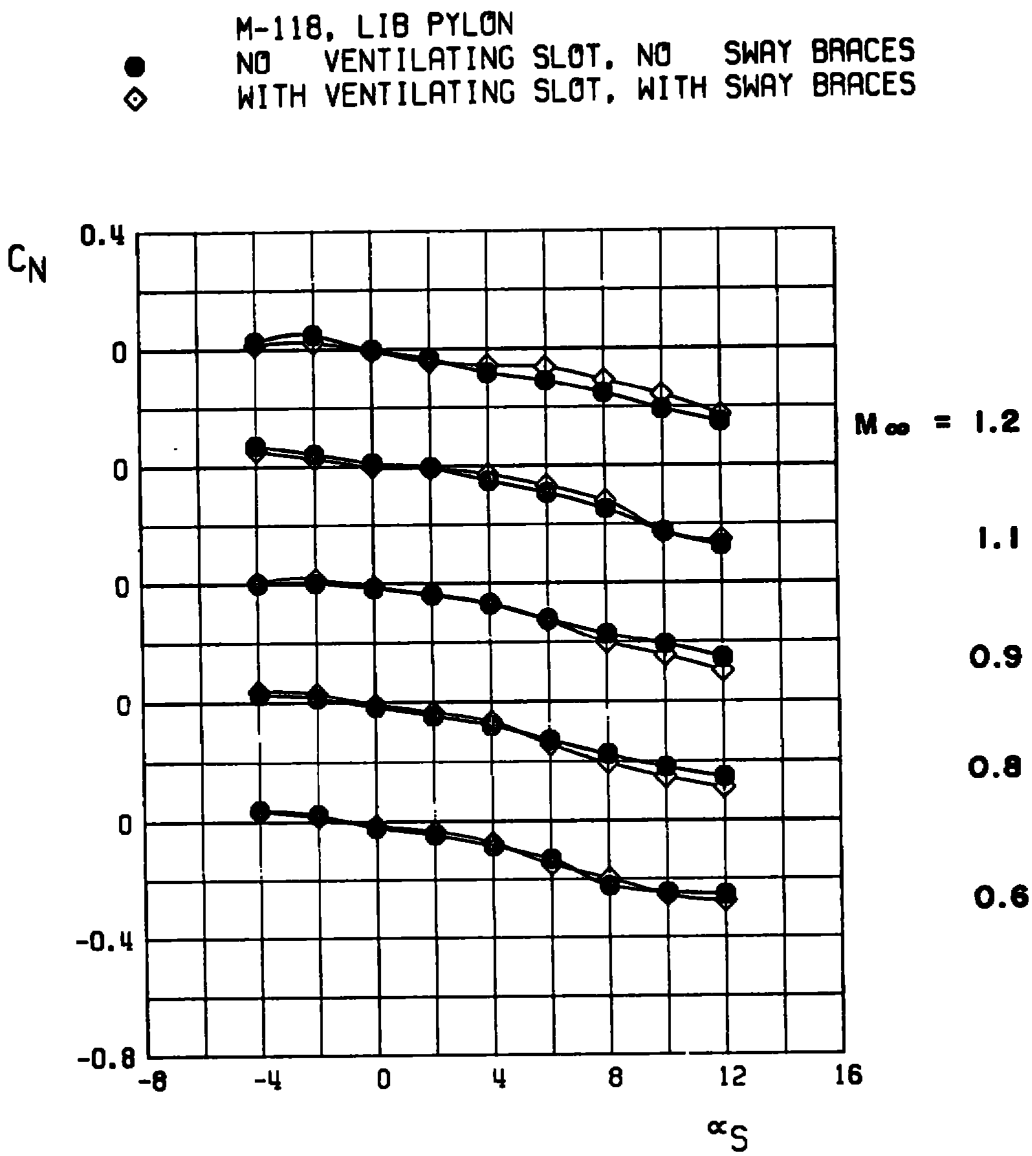

a. Normal-force coefficient

Figure 16. Combined effects of both a ventilated supporting bracket and pylon sway braces on the static aerodynamic loads acting on a stable pylon-mounted store.

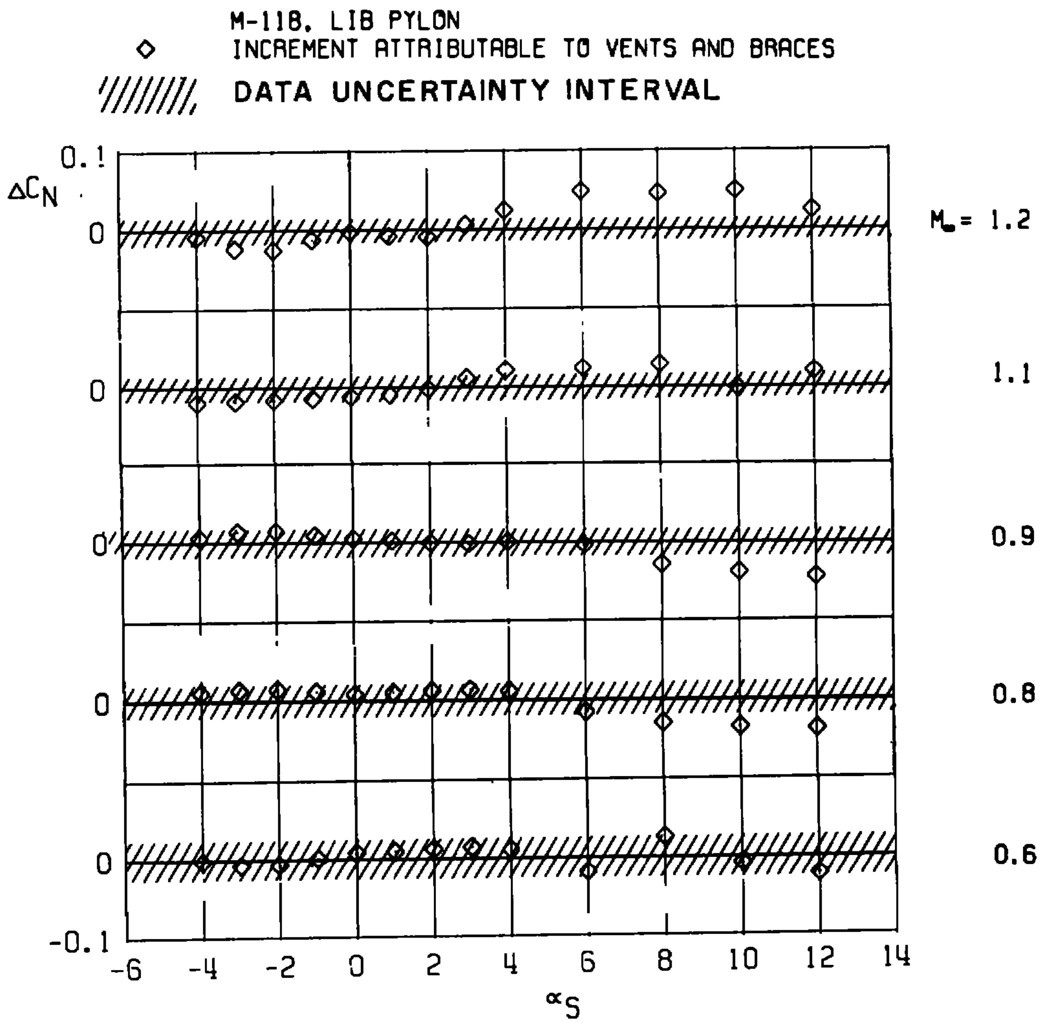

b. Increment in normal-force coefficient
Figure 16. Continued.

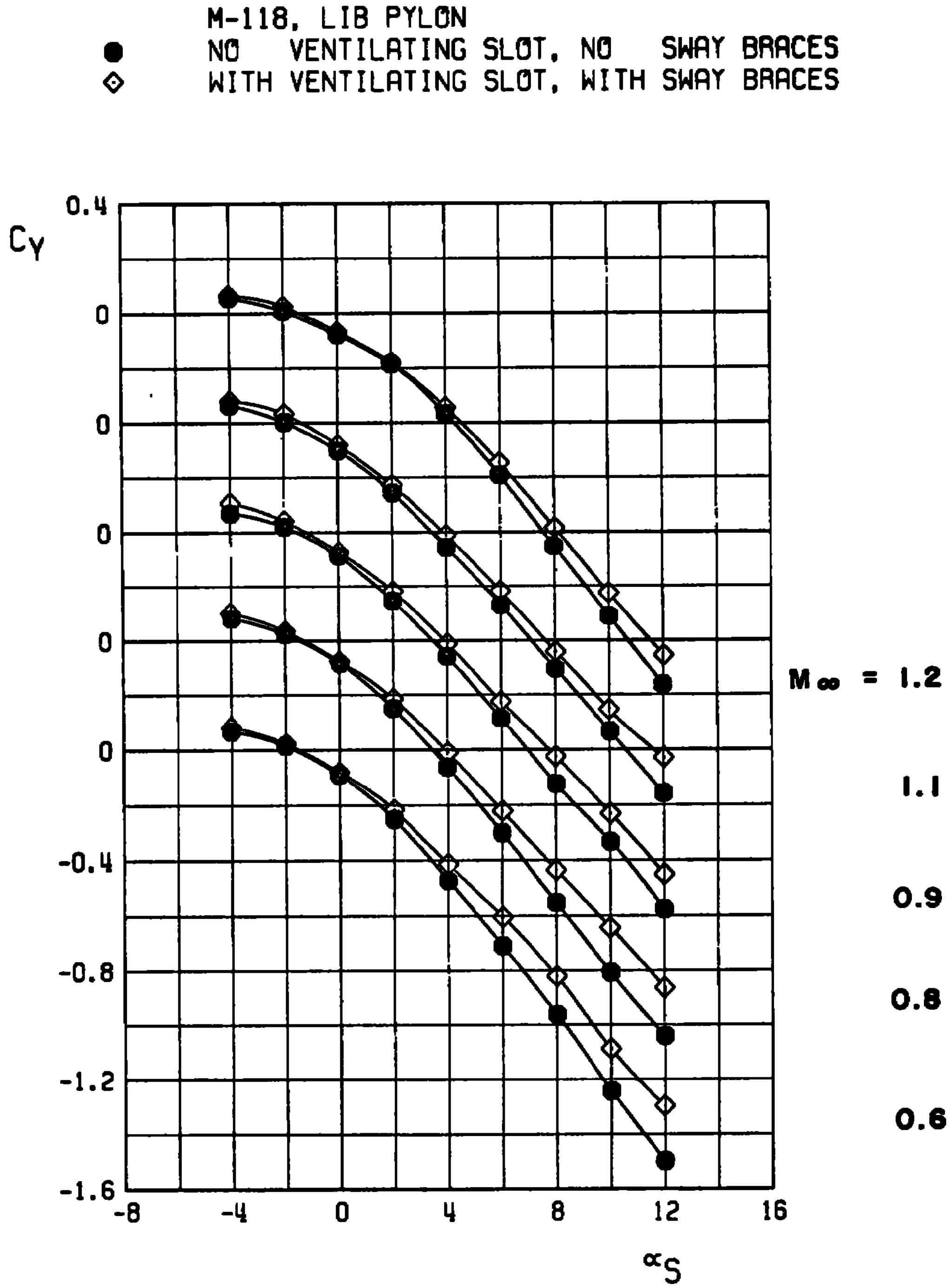

c. Side-force coefficient
Figure 16. Continued.

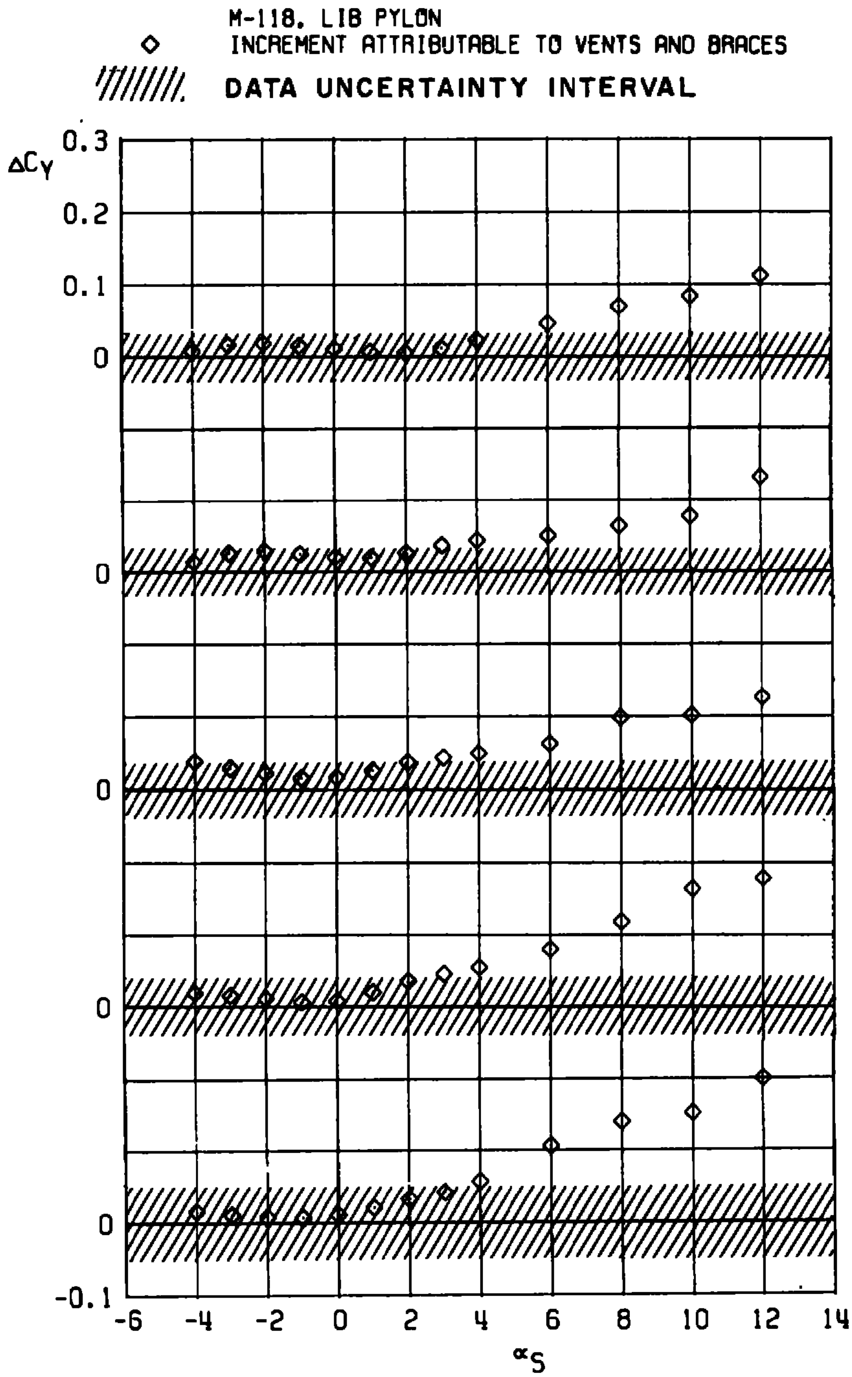

d. Increment in side-force coefficient
Figure 16. Continued.

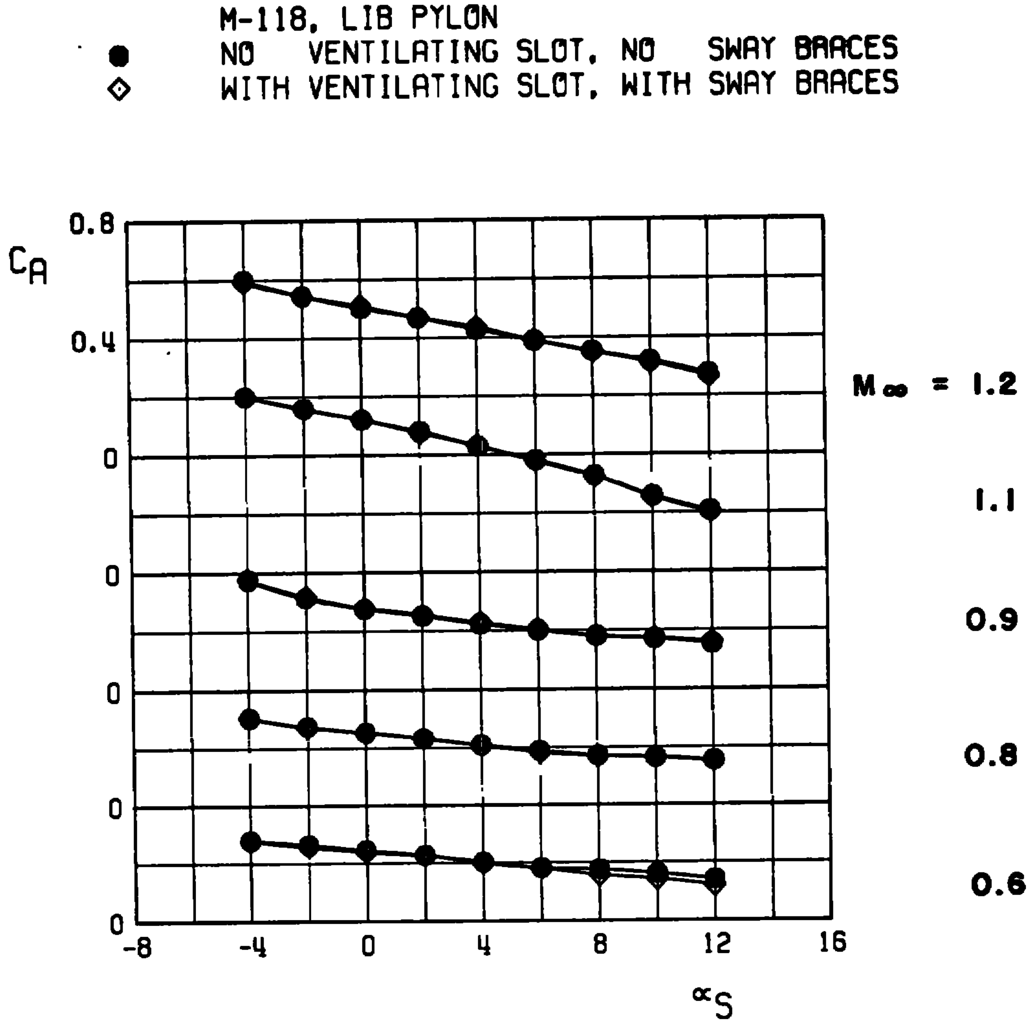

e. Axial-force coefficient
Figure 16. Continued.

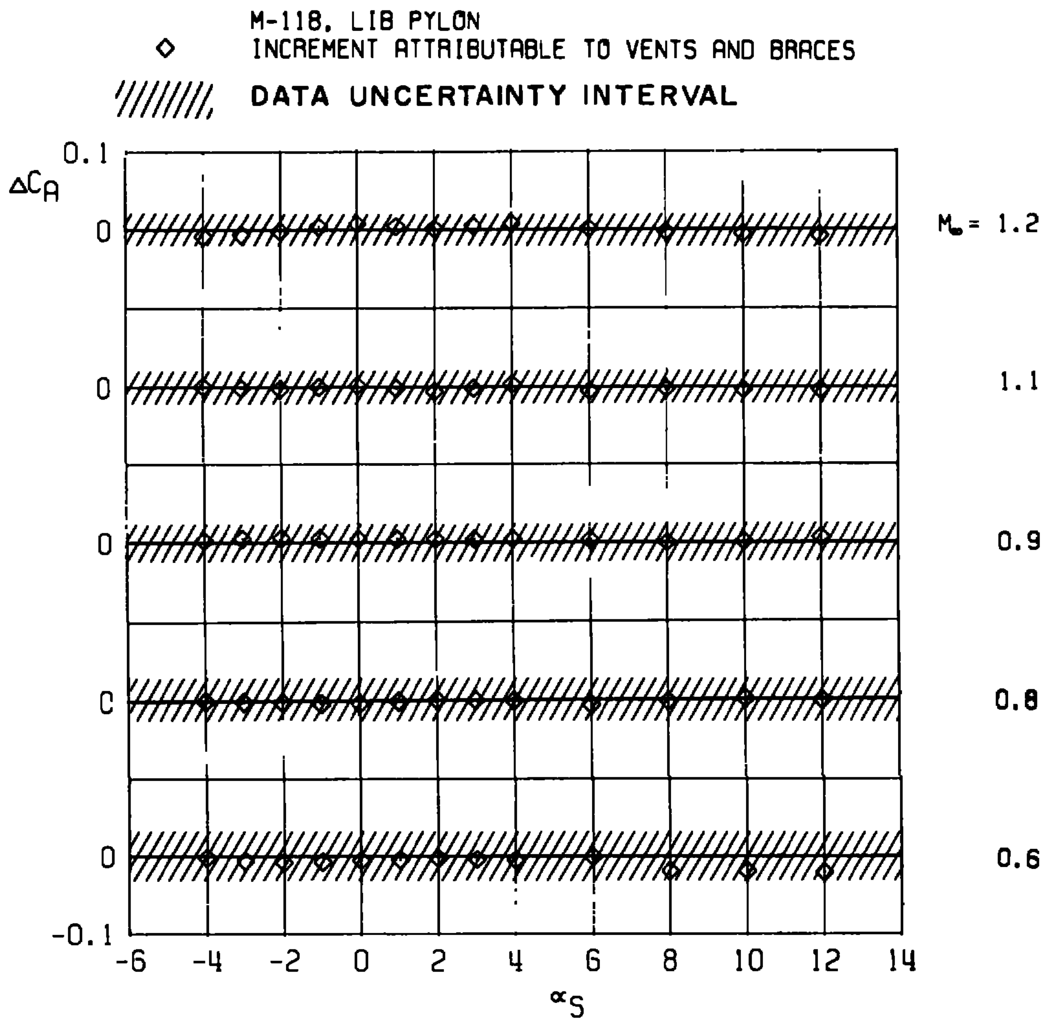

f. Increment in axial-force coefficient
Figure 16. Continued.

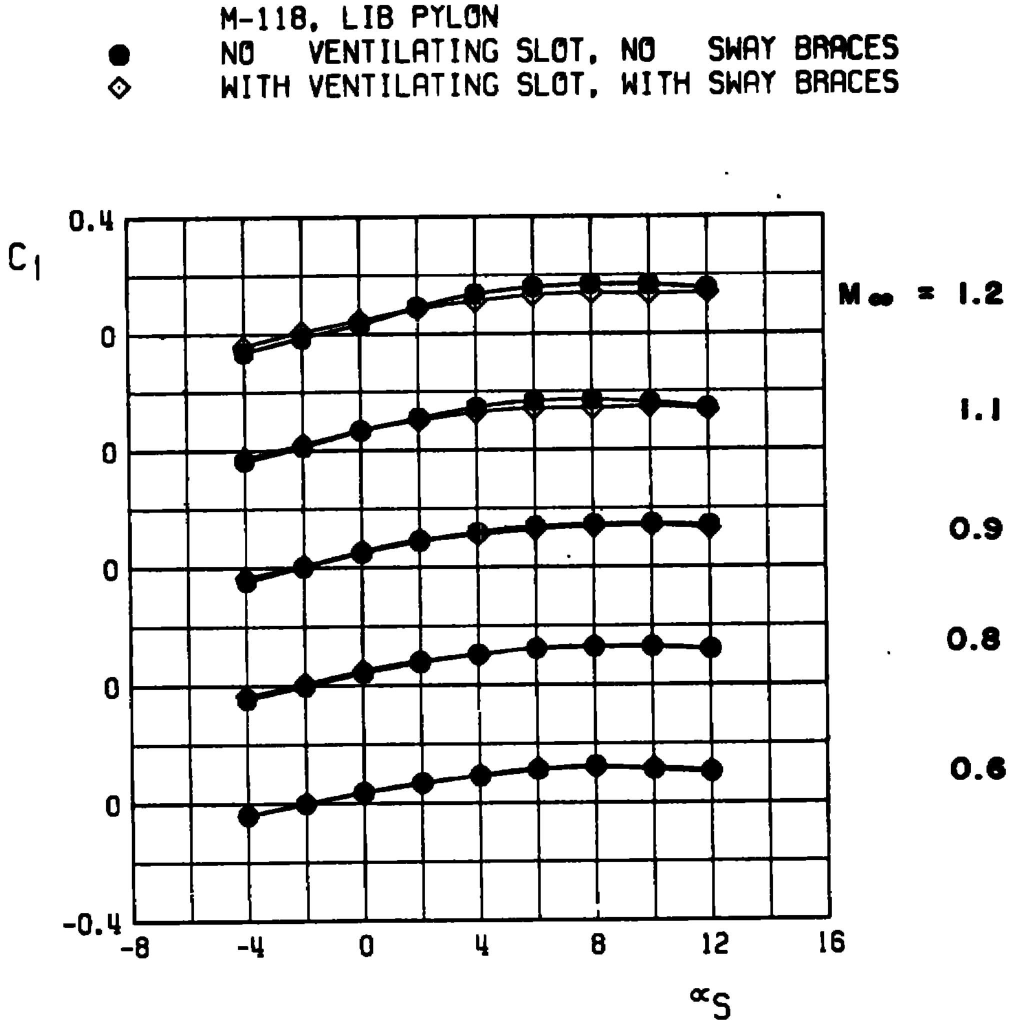

g. Rolling-moment coefficient
Figure 16. Continued.

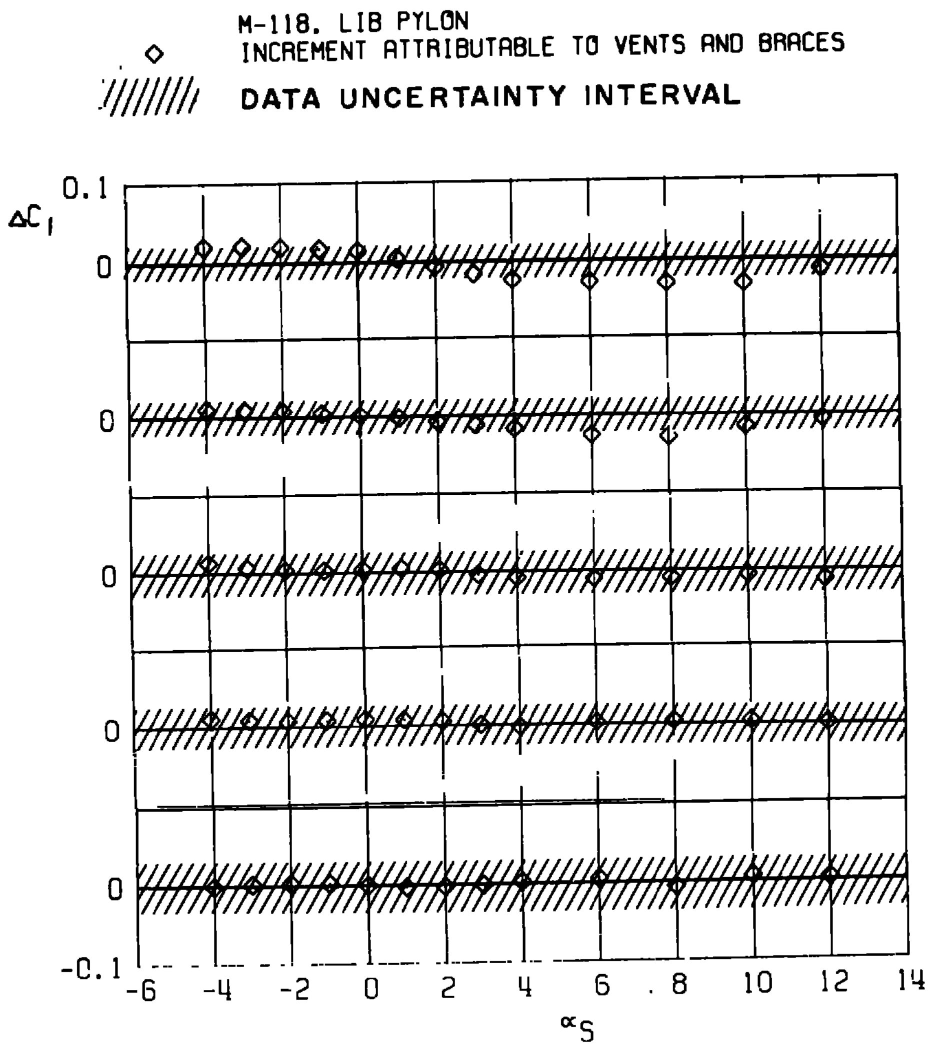

h. Increment in rolling-moment coefficient
Figure 16. Continued.

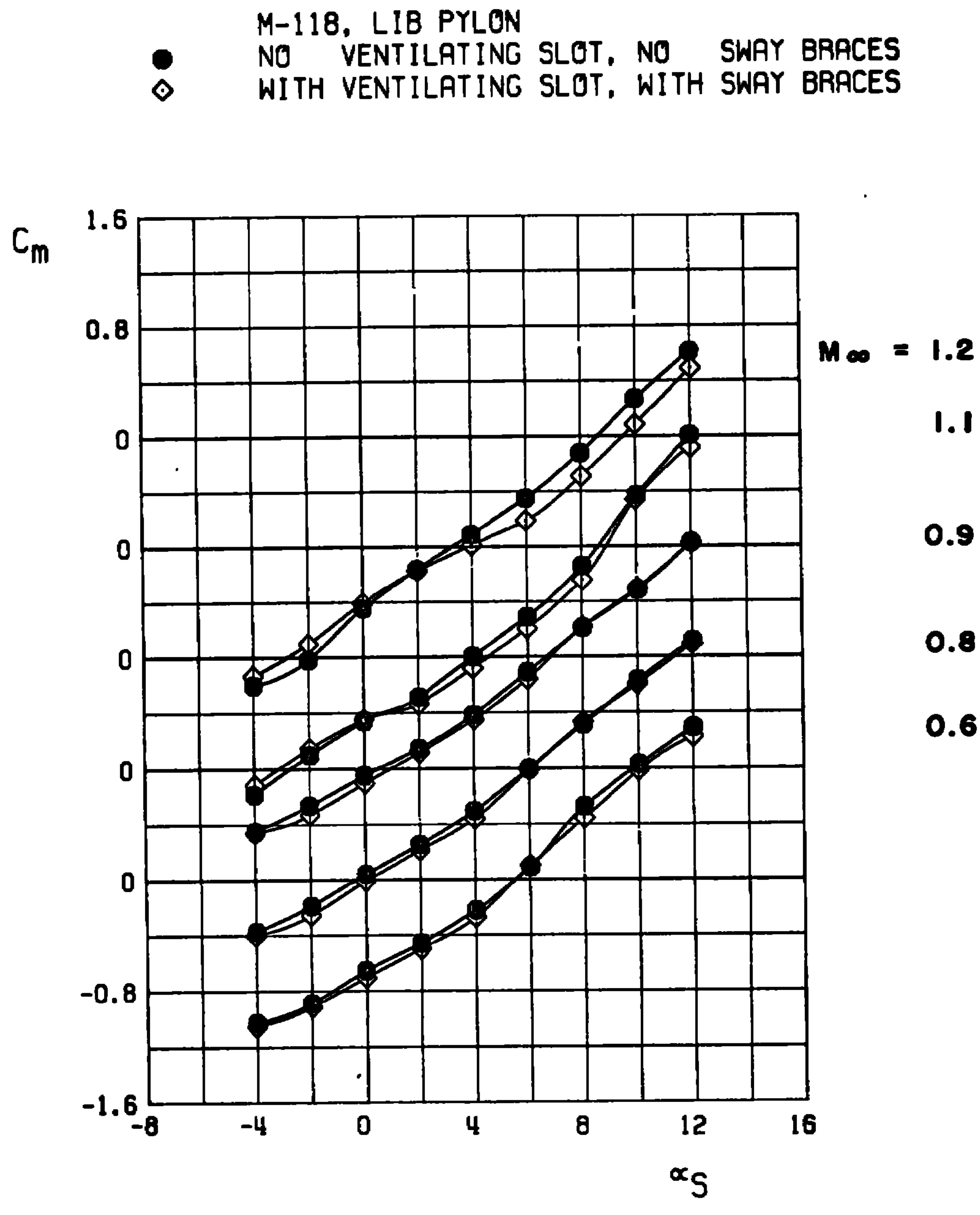

i. Pitching-moment coefficient
Figure 16. Continued.

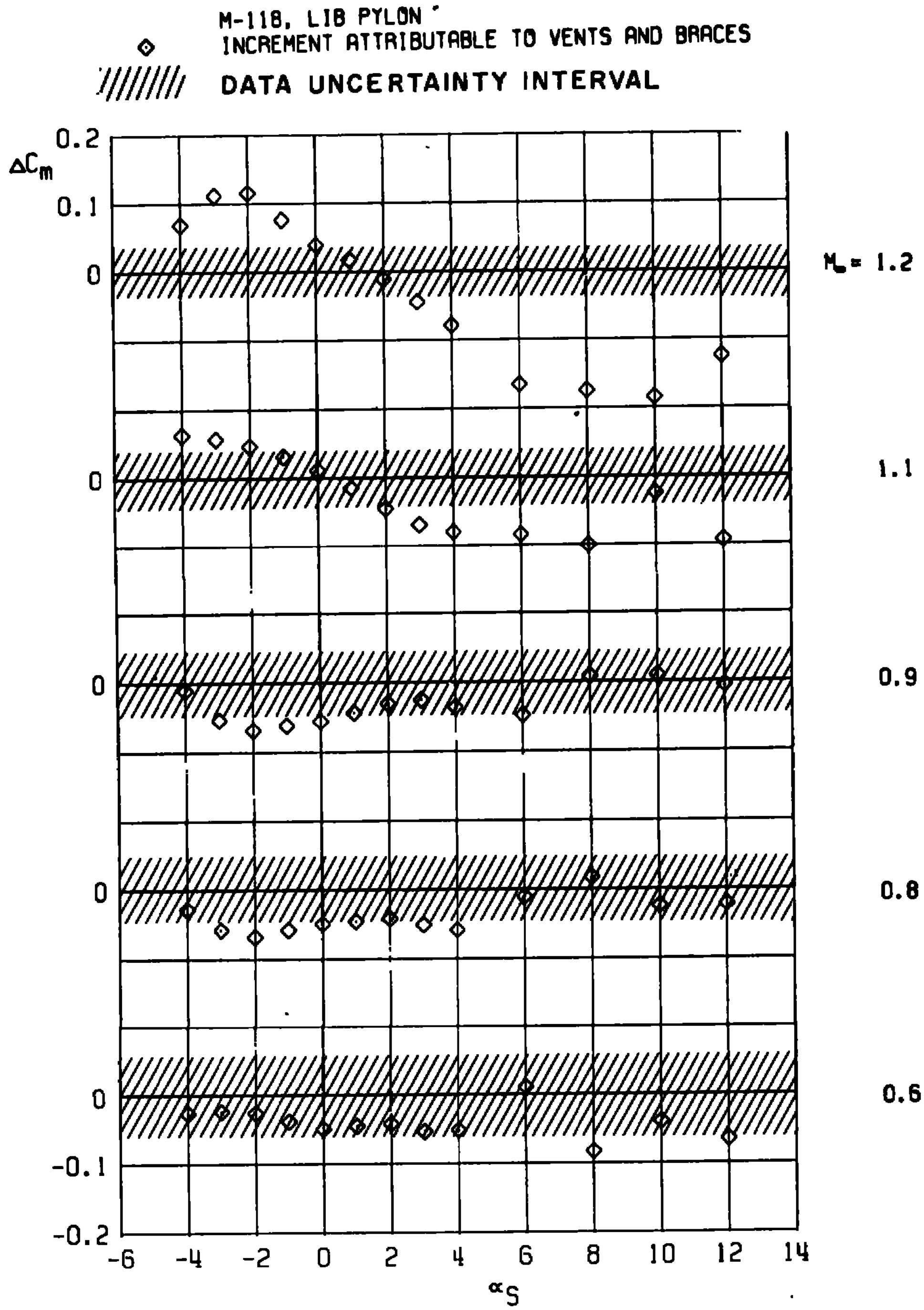

j. Increment in pitching-moment coefficient
Figure 16. Continued.

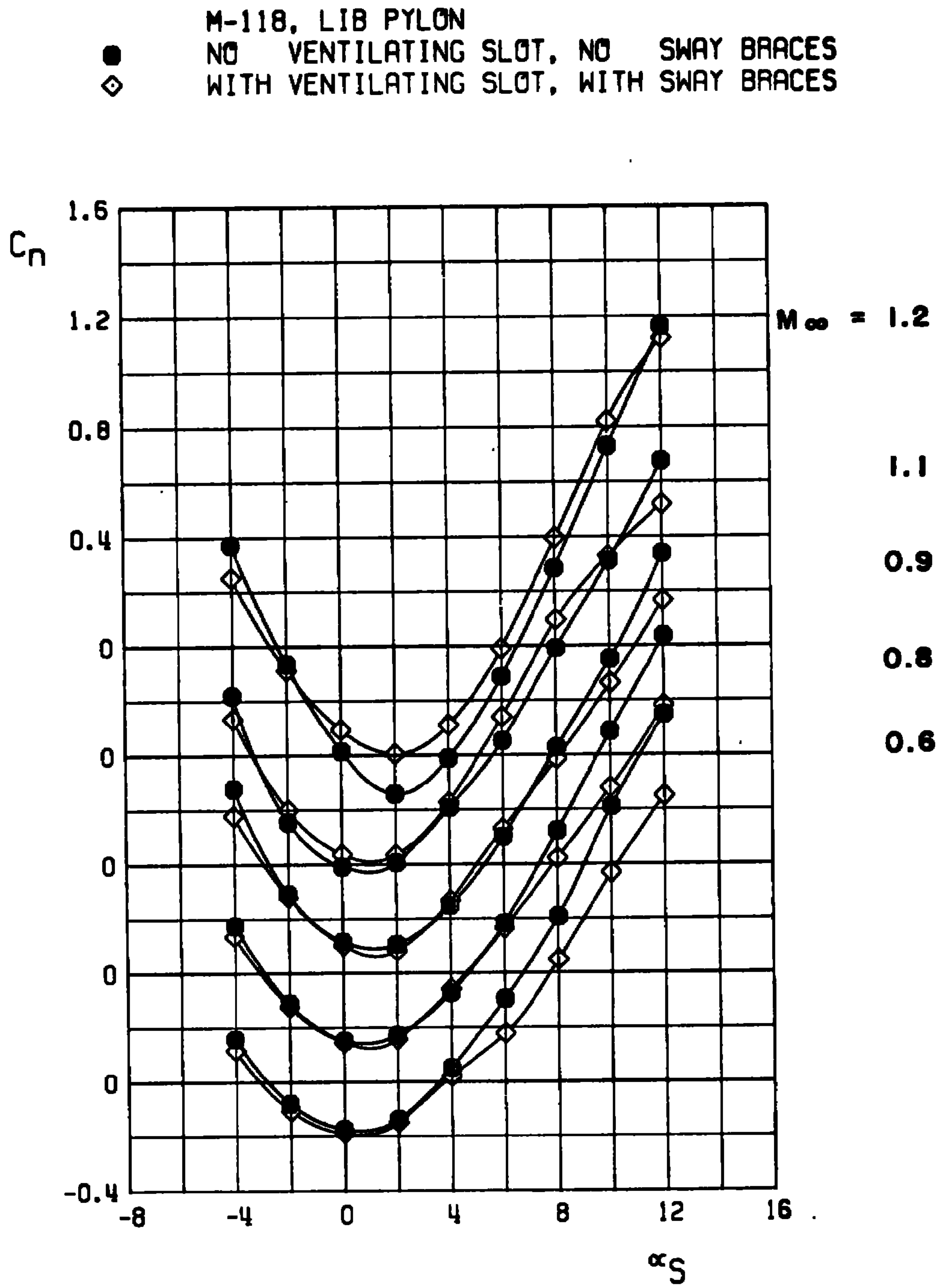

k. Yawing-moment coefficient
Figure 16. Continued.

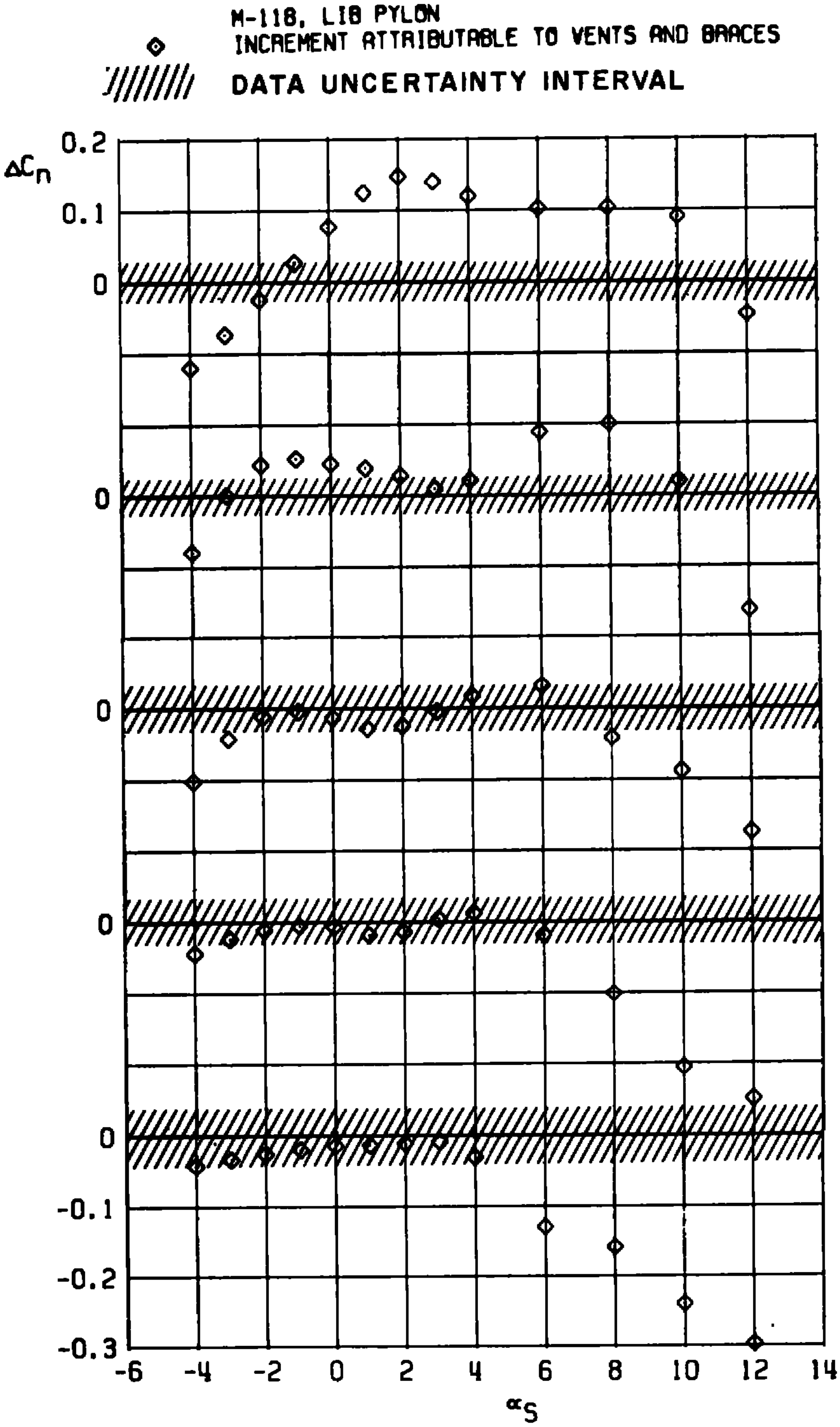

I. Increment in yawing-moment coefficient
Figure 16. Concluded.

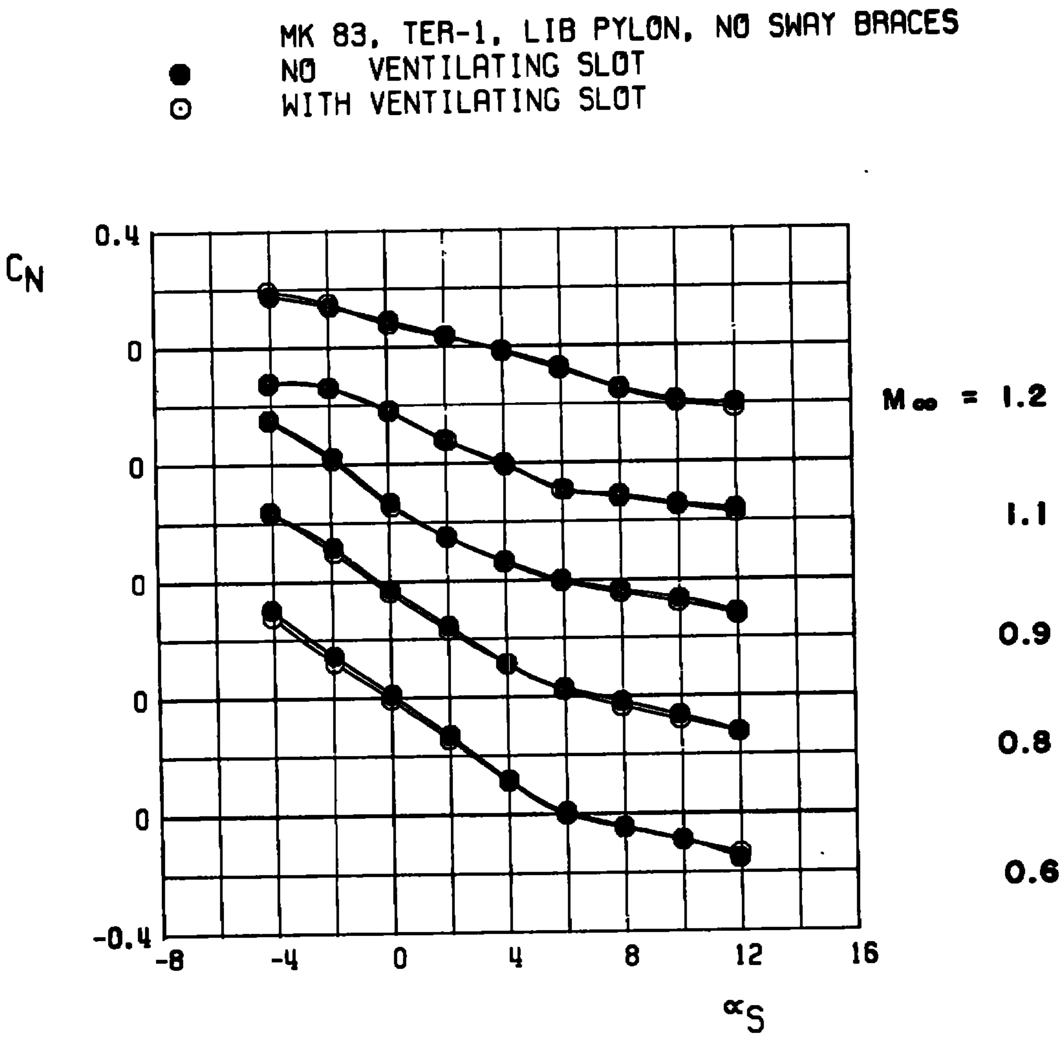

a. Normal-force coefficient

Figure 17. Isolated effect of a ventilated supporting bracket and triple ejector rack model on the static aerodynamic loads acting on a stable, triple ejector rack-mounted store.

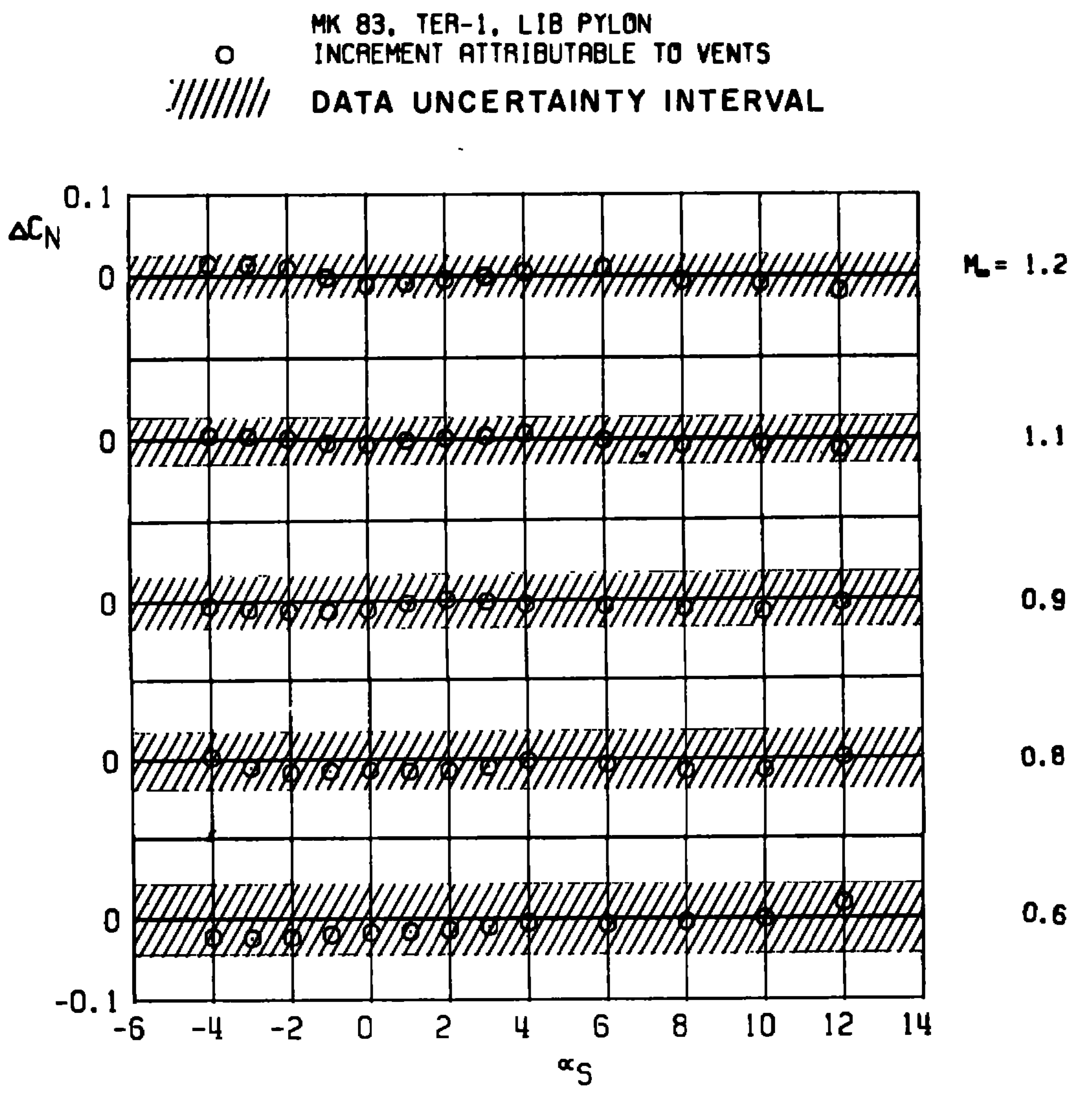

b. Increment in normal-force coefficient
Figure 17. Continued.

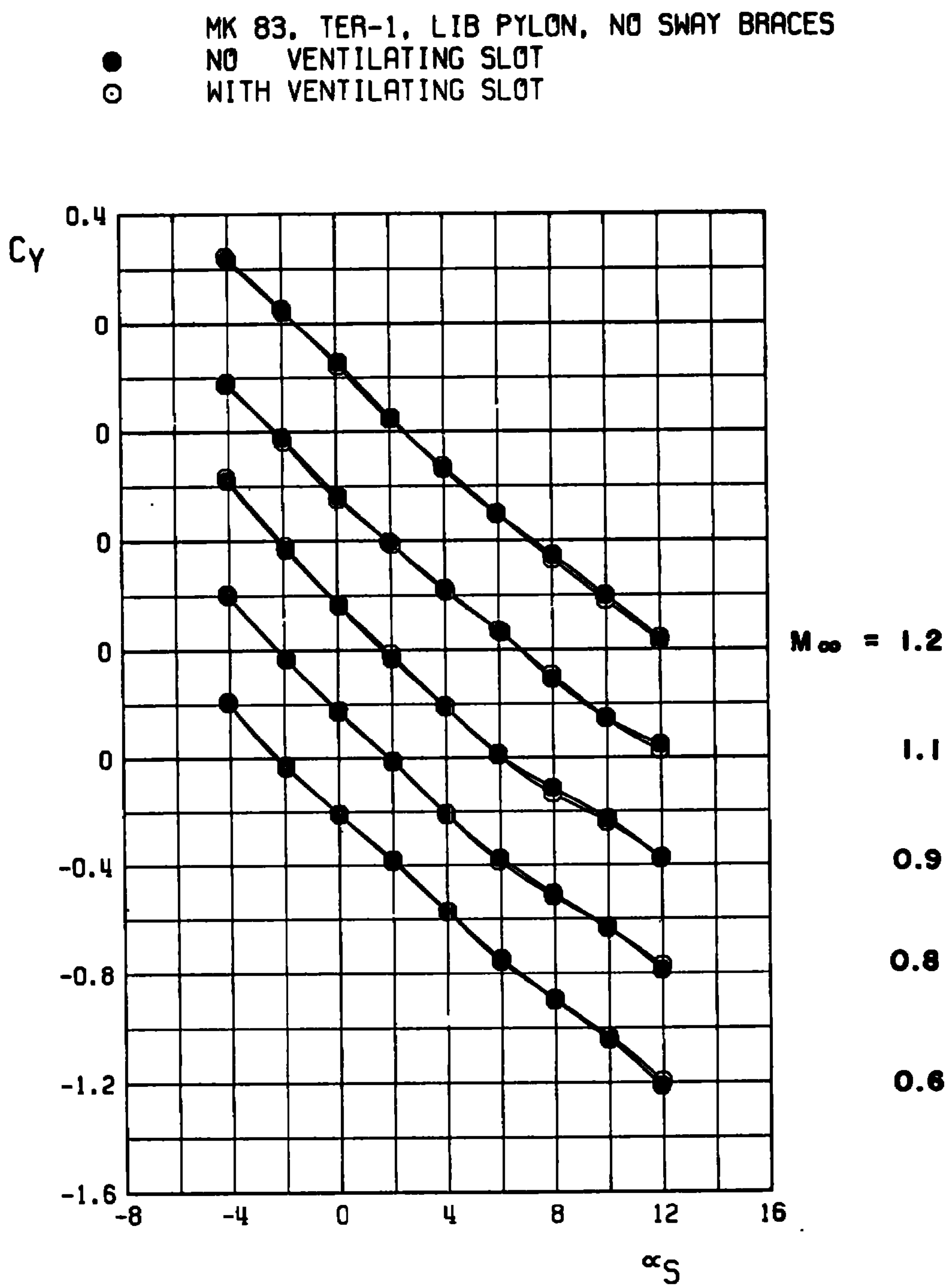

c. Side-force coefficient
Figure 17. Continued.

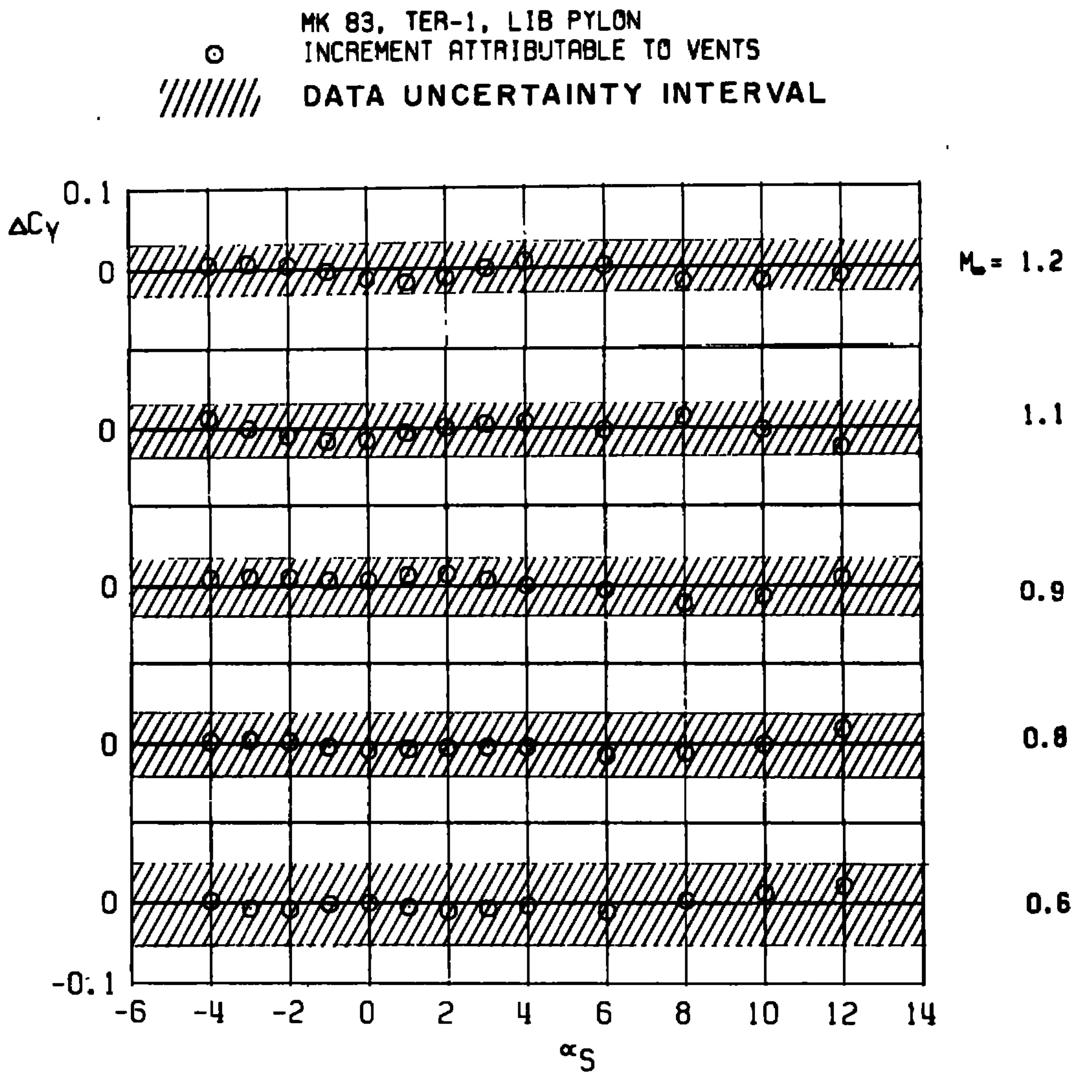

d. Increment in side-force coefficient
Figure 17. Continued.

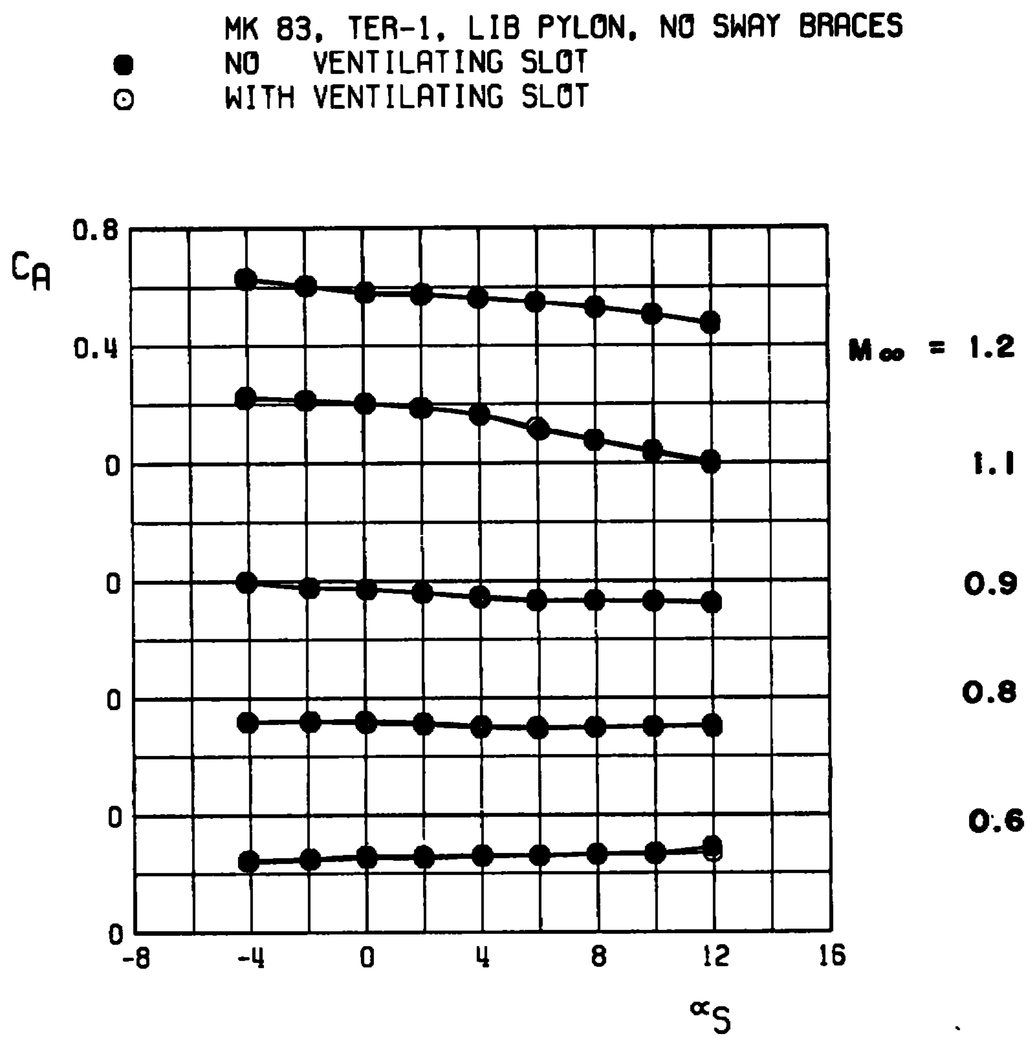

e. Axial-force coefficient
Figure 17. Continued.

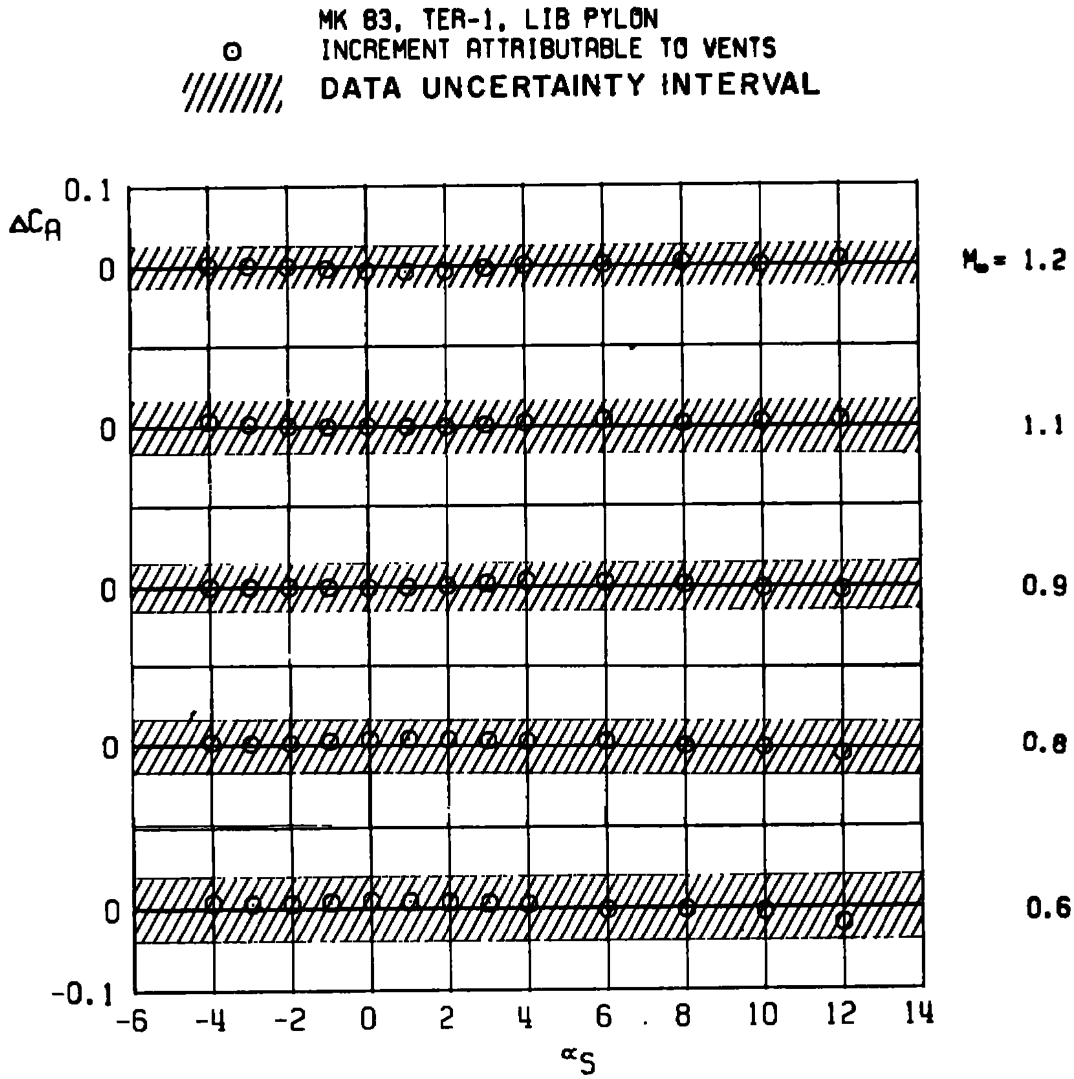

f. Increment in axial-force coefficient
Figure 17. Continued.

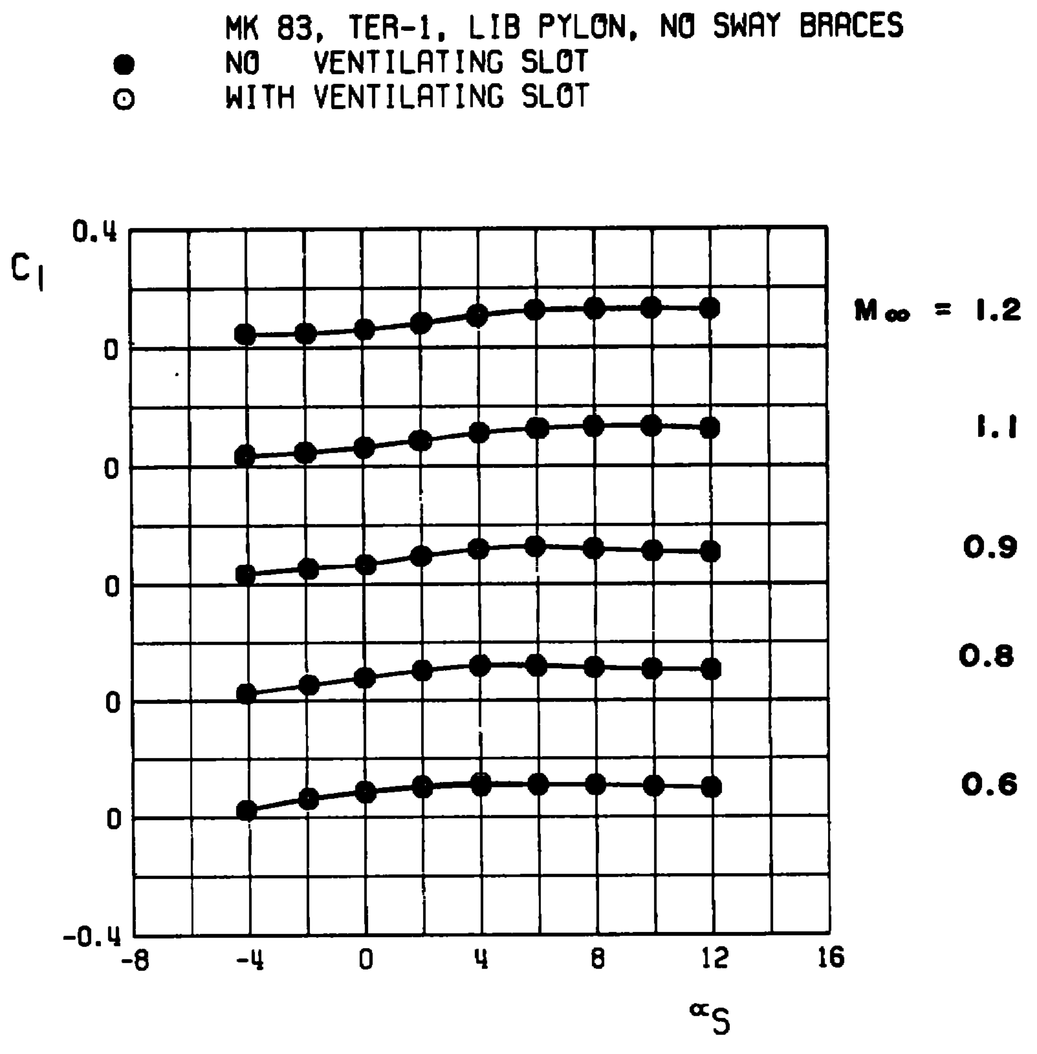

g. Rolling-moment coefficient
Figure 17. Continued.

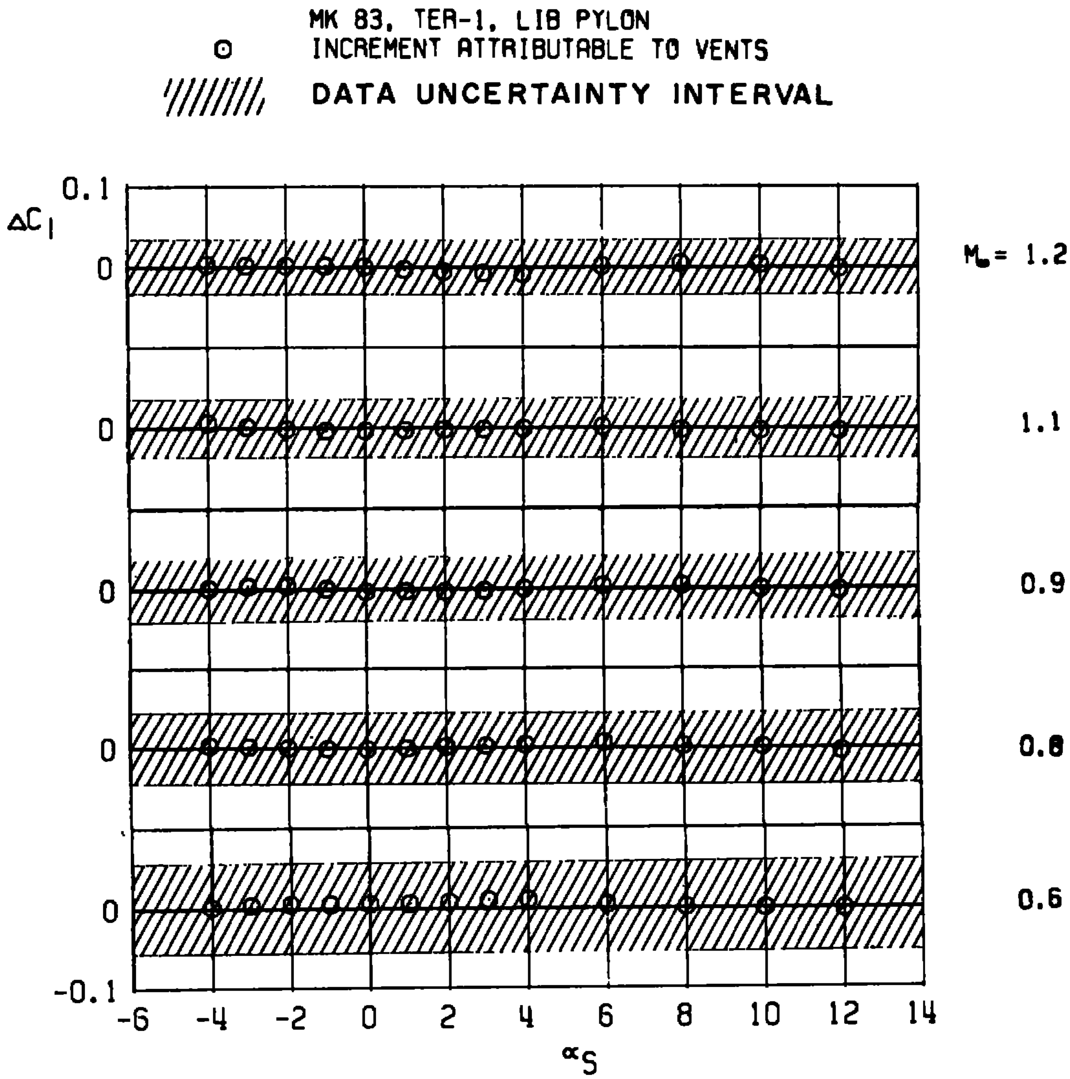

h. Increment in rolling-moment coefficient.
Figure 17. Continued.

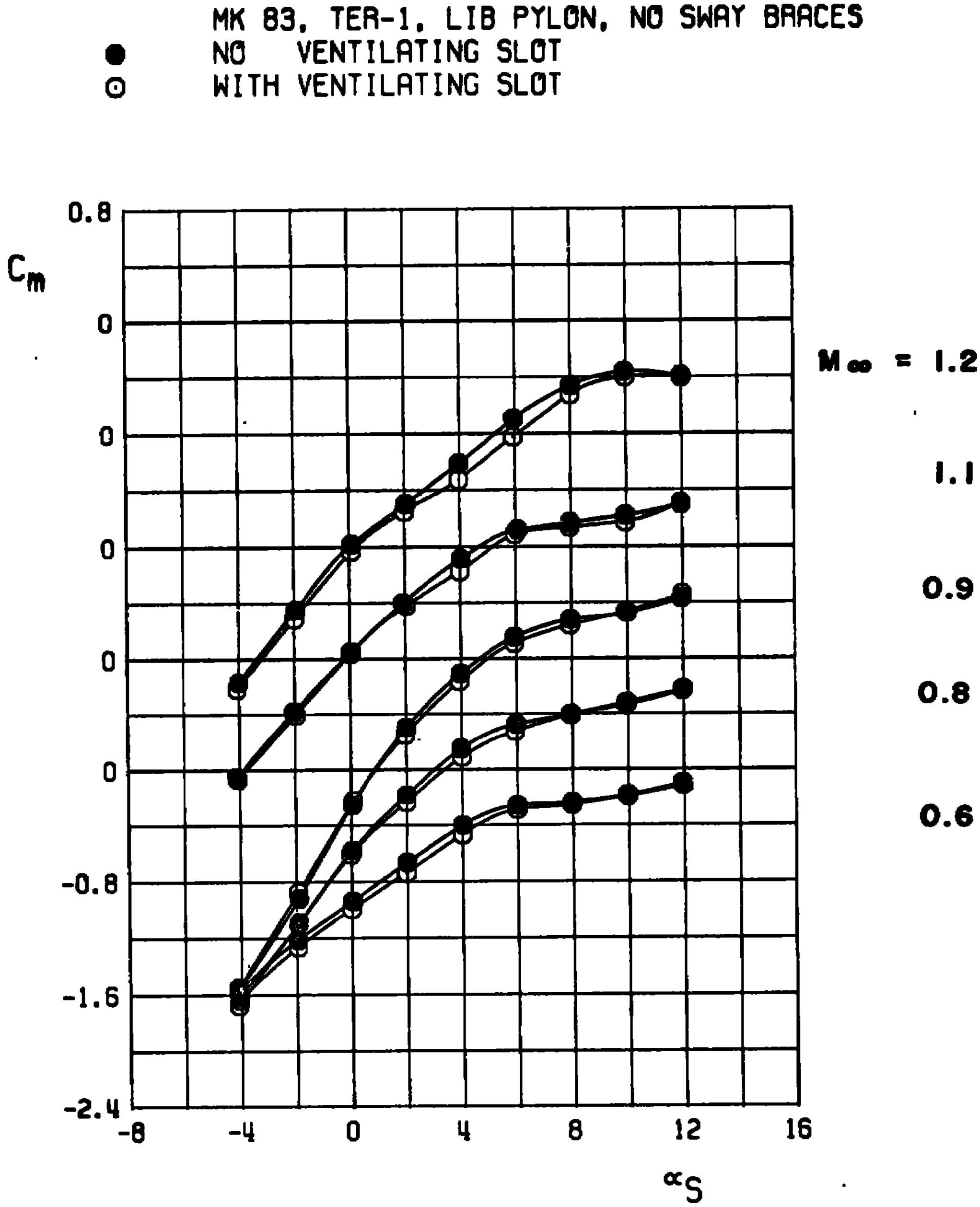

i. Pitching-moment coefficient
Figure 17. Continued.

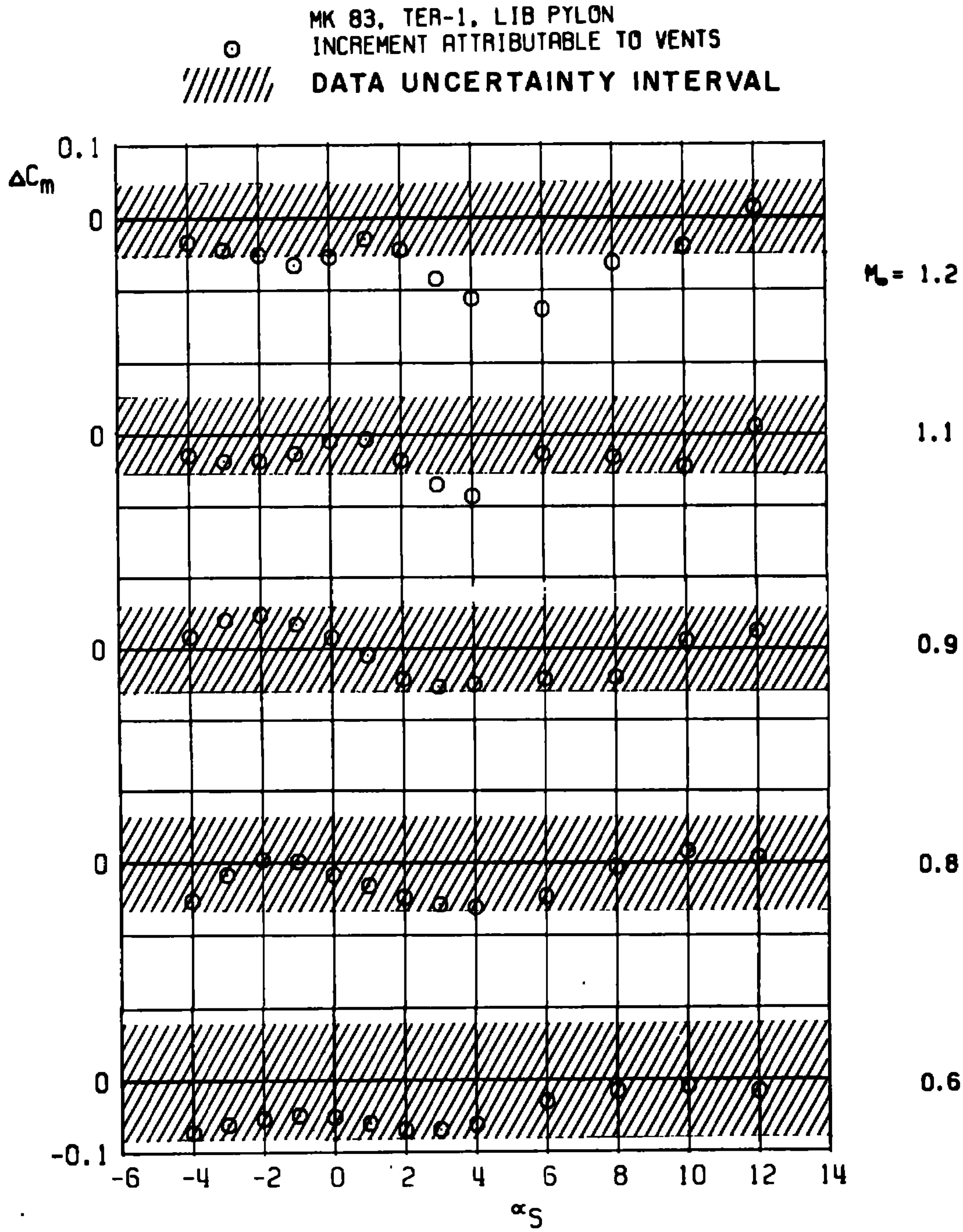

j. Increment in pitching-moment coefficient
Figure 17. Continued.

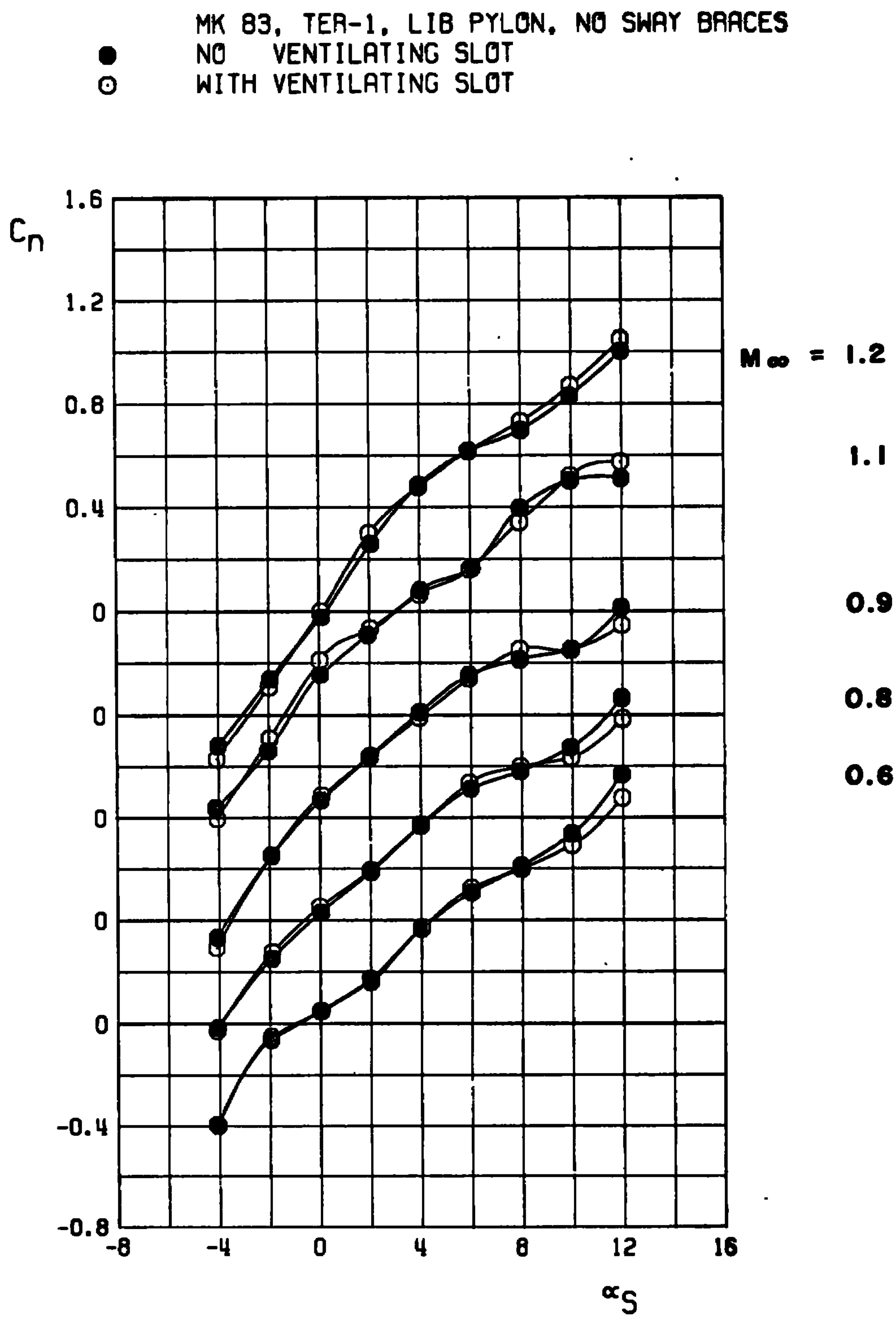

k. Yawing-moment coefficient
Figure 17. Continued.

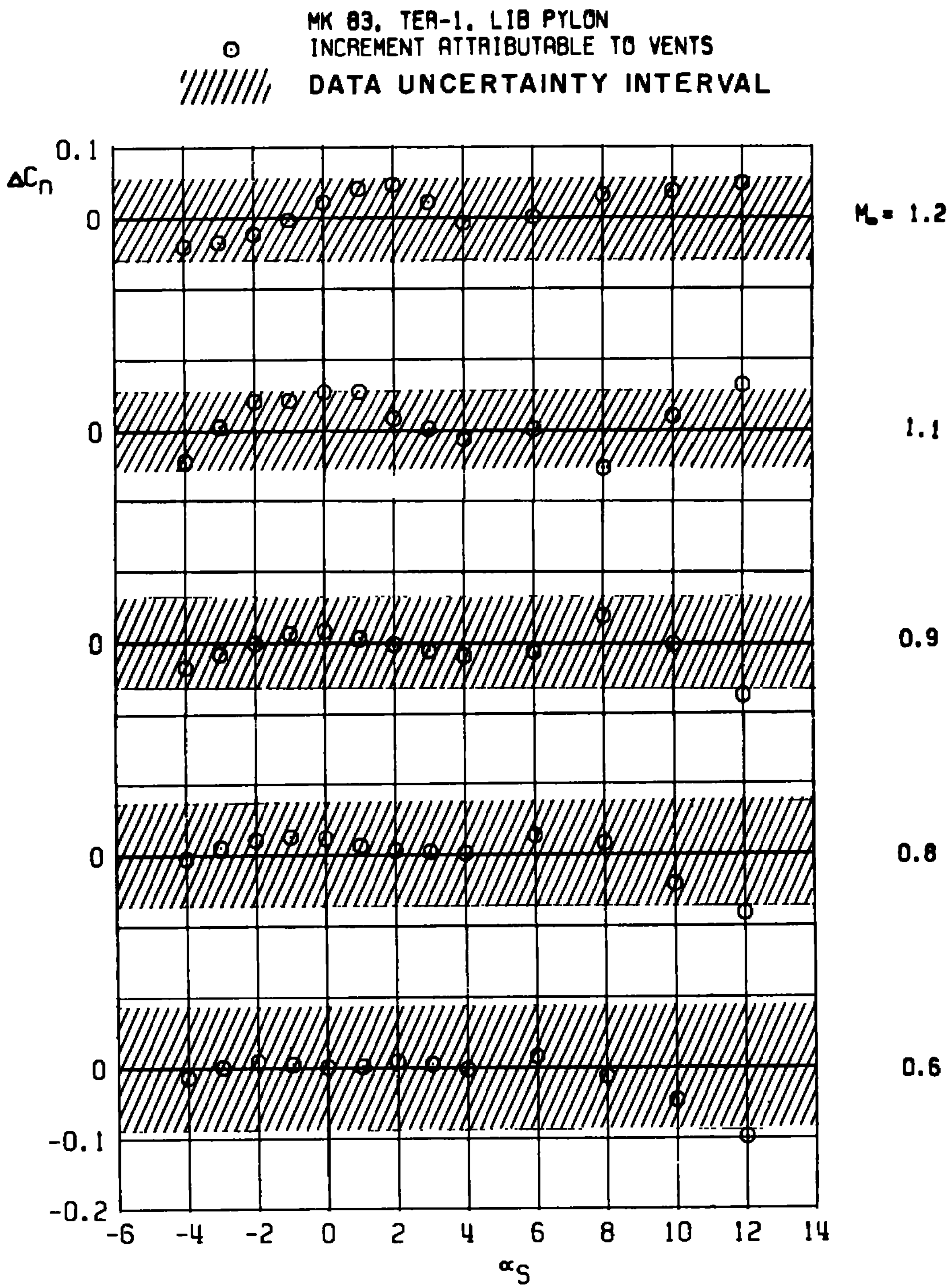

I. Increment in yawing-moment coefficient
Figure 17. Concluded.

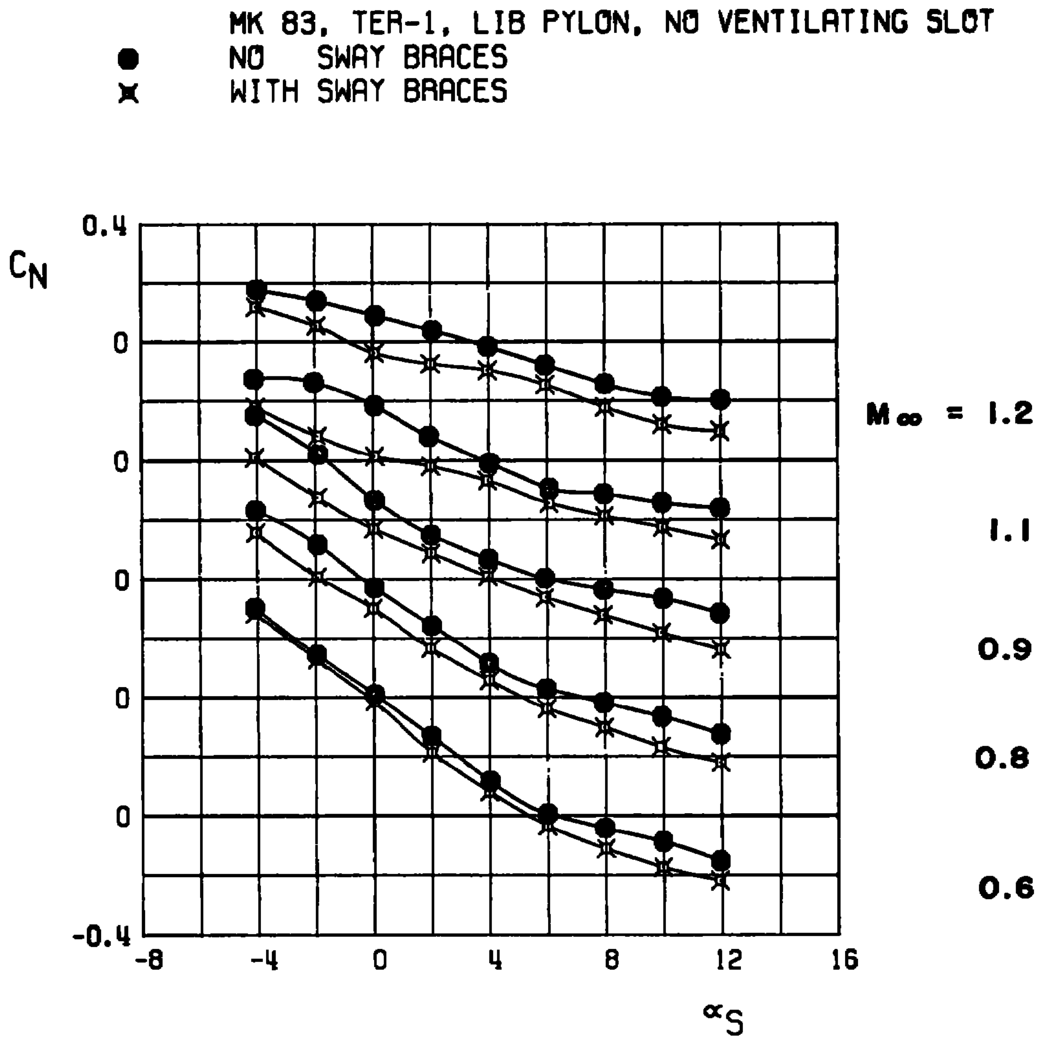

a. Normal-force coefficient

Figure 18. Isolated effect of triple ejector rack sway braces on the static aerodynamic loads acting on a stable triple ejector rack-mounted store.

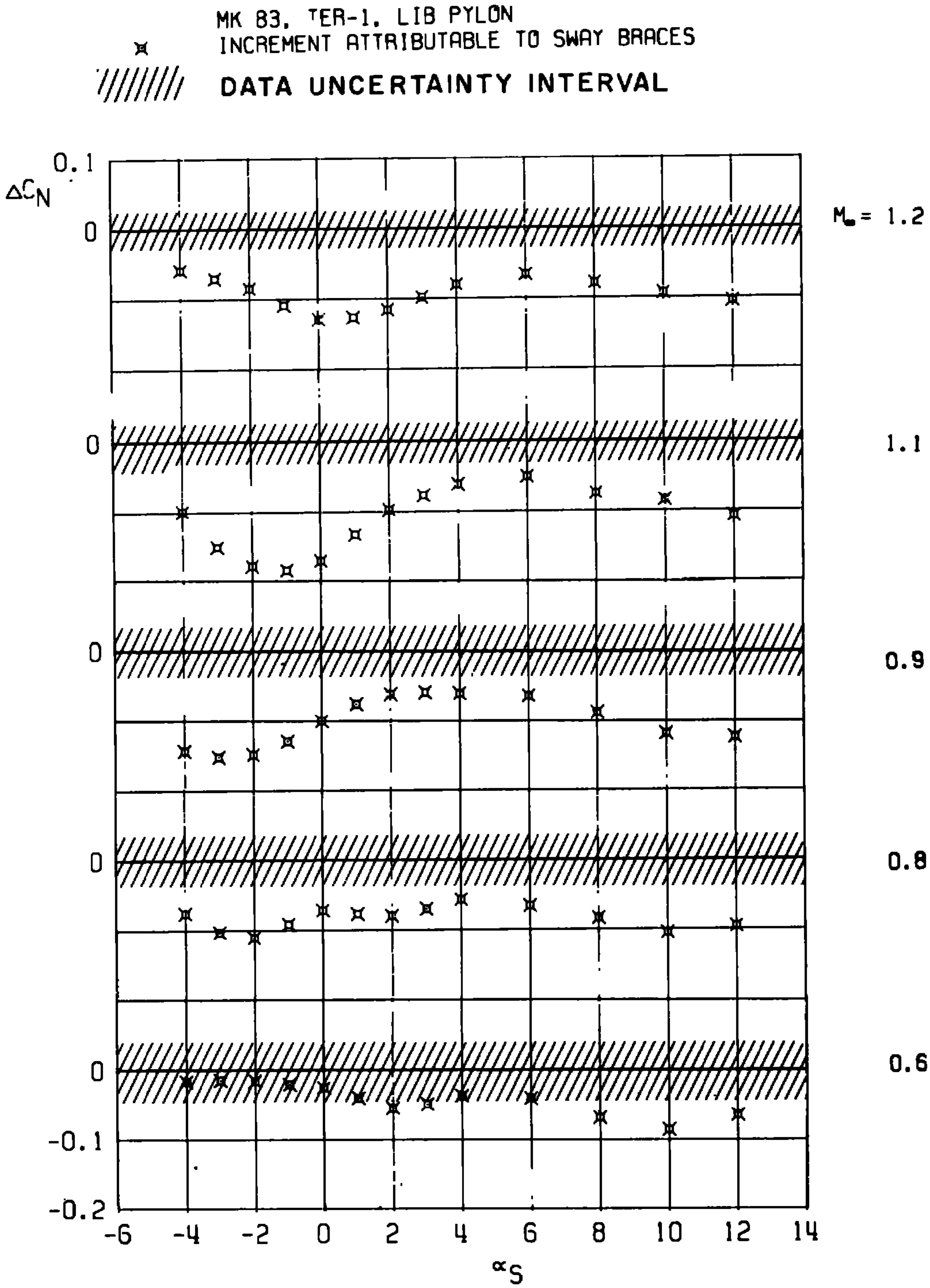

b. Increment in normal-force coefficient
Figure 18. Continued.

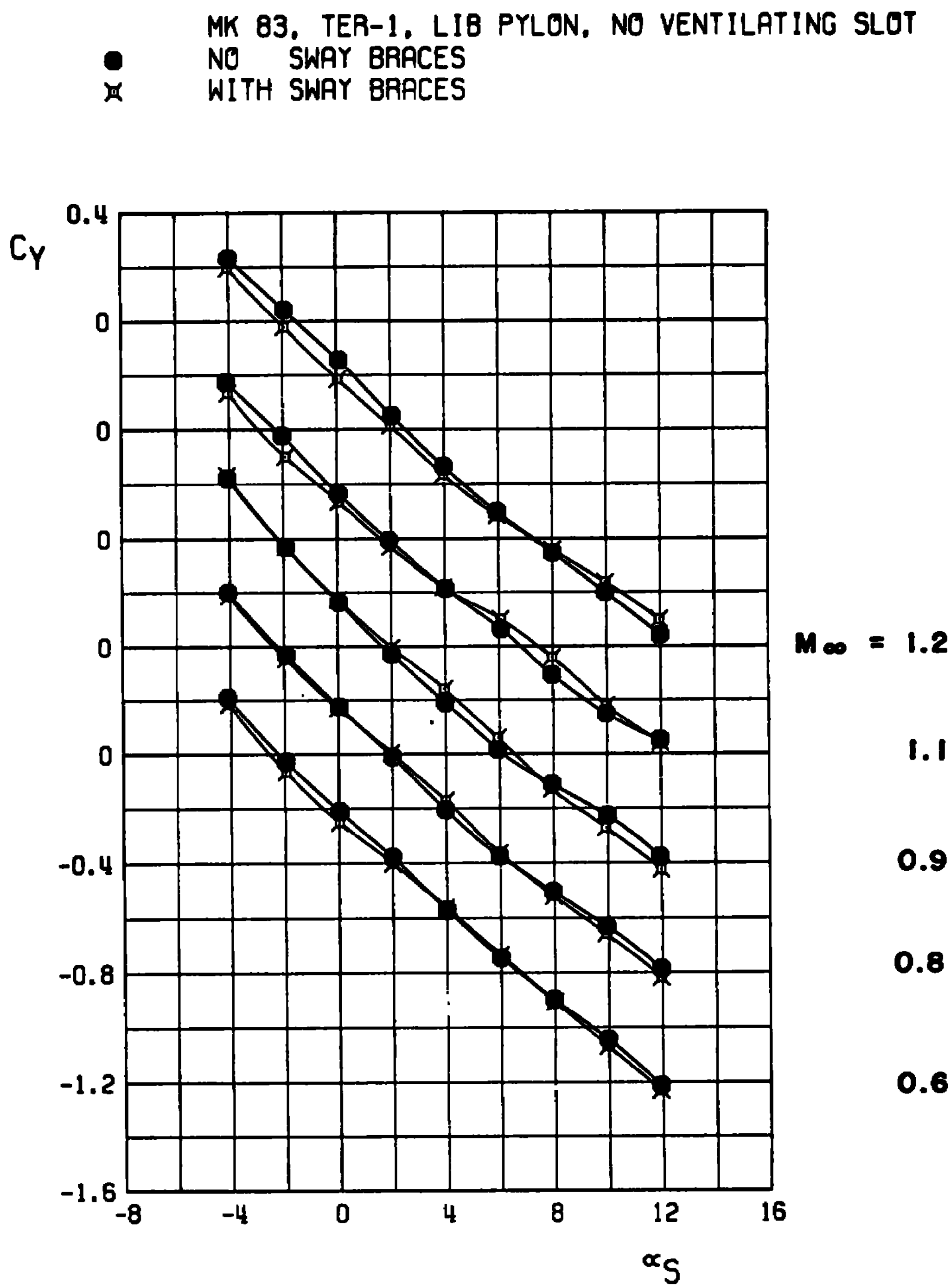

c. Side-force coefficient
Figure 18. Continued.

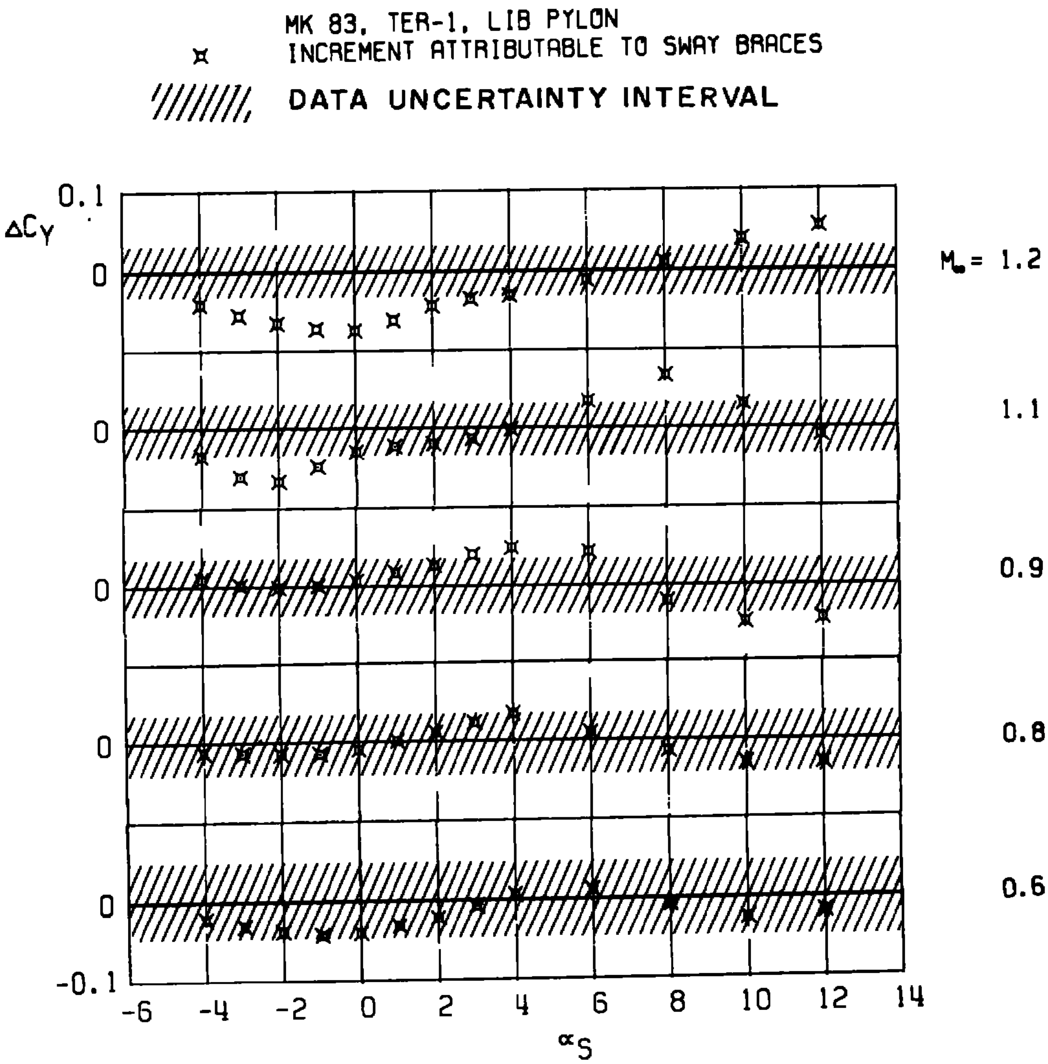

d. Increment in side-force coefficient
Figure 18. Continued.

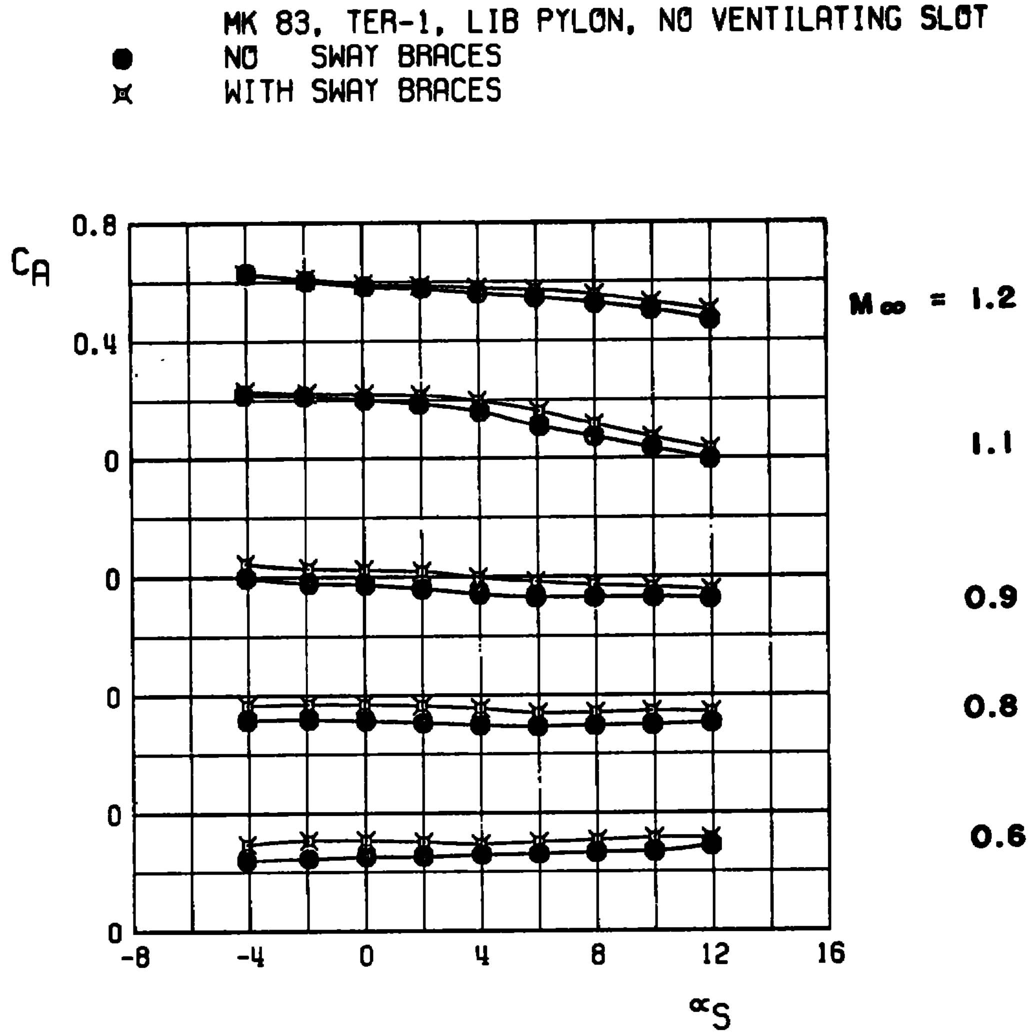

e. Axial-force coefficient
Figure 18. Continued.

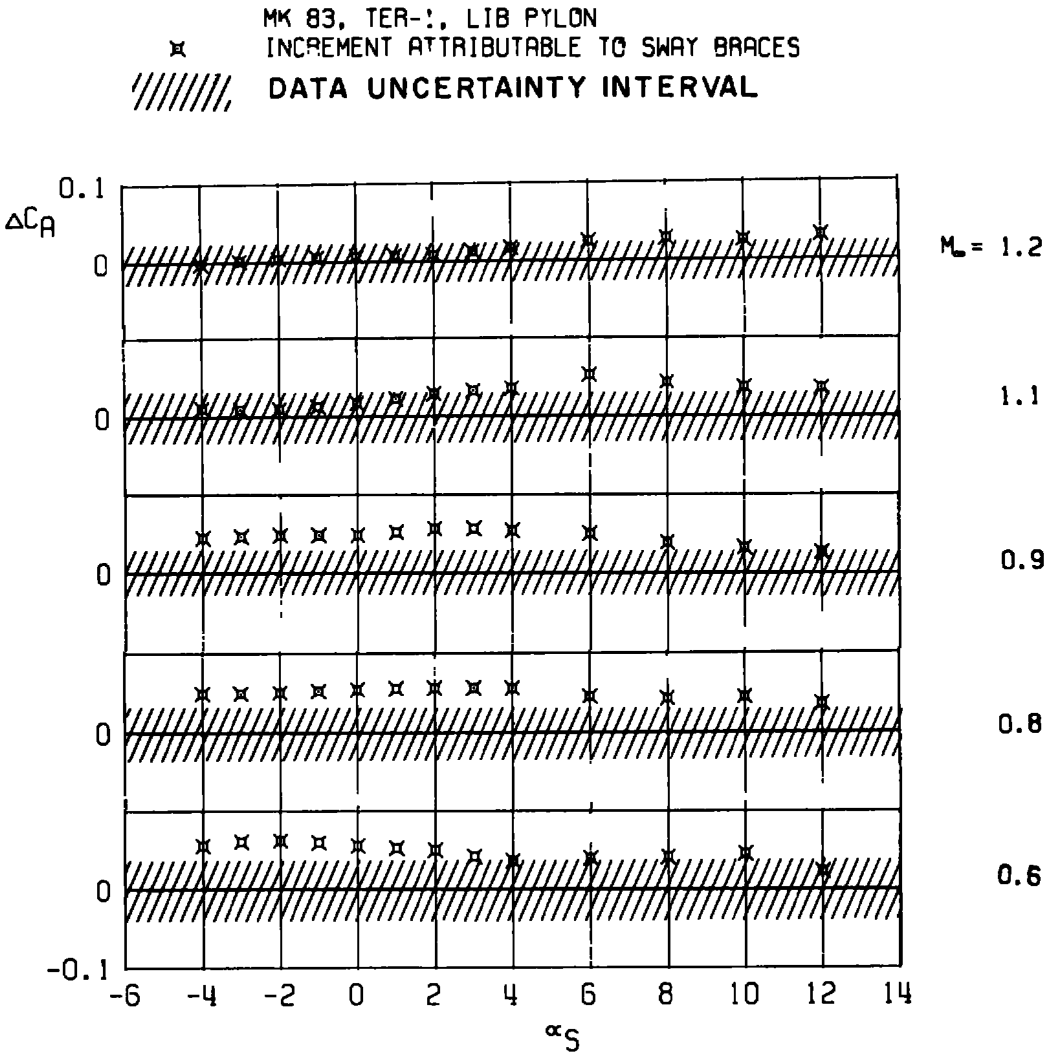

f. Increment in axial-force coefficient
Figure 18. Continued.

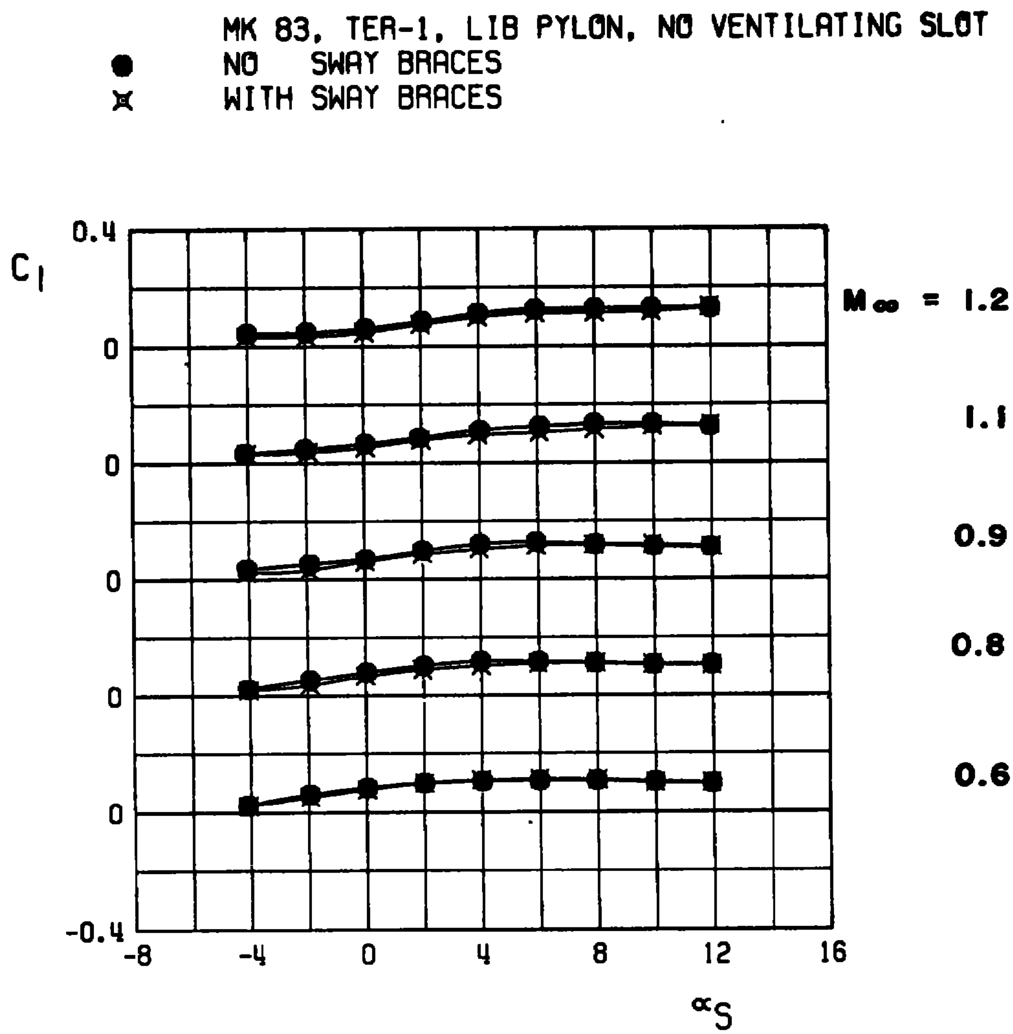

g. Rolling-moment coefficient
Figure 18. Continued.

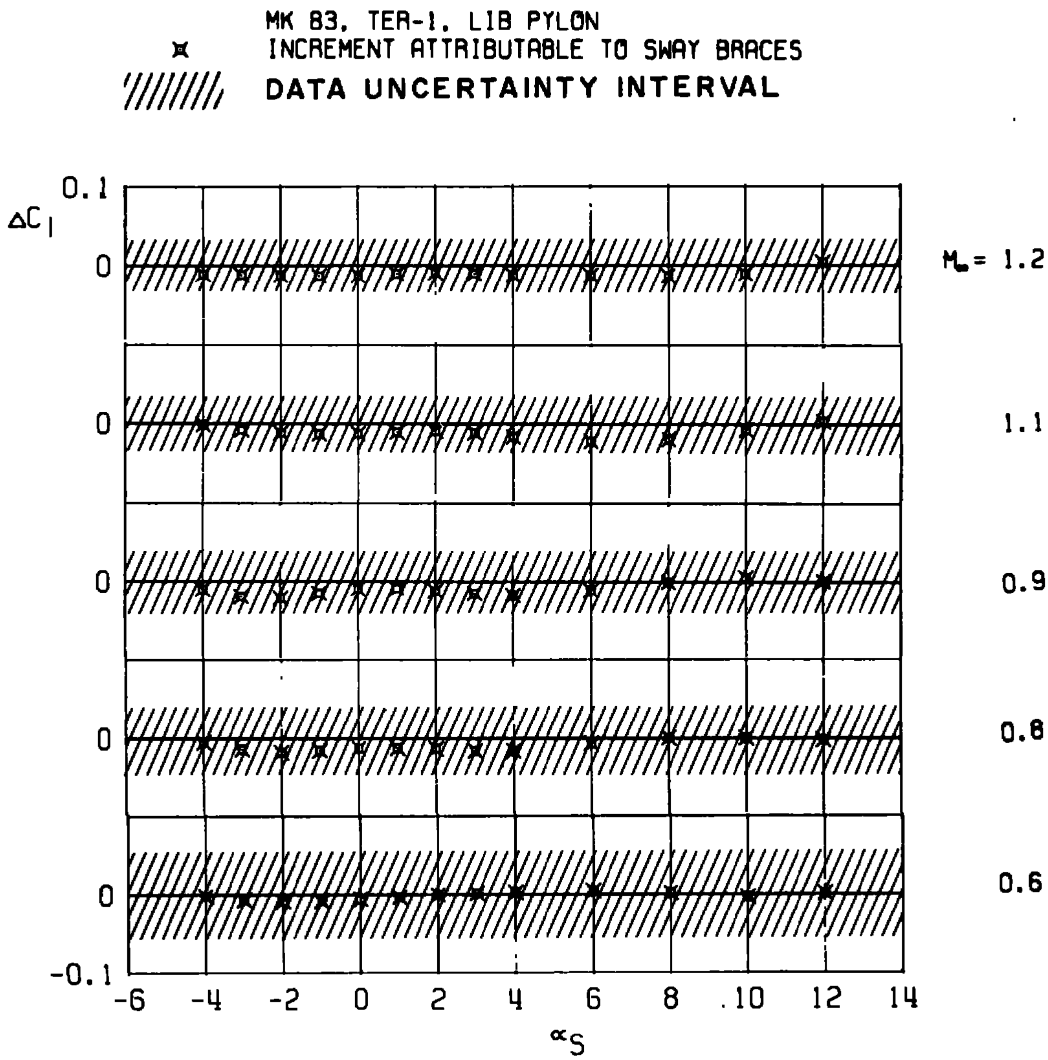

h. Increment in rolling-moment coefficient
Figure 18. Continued.

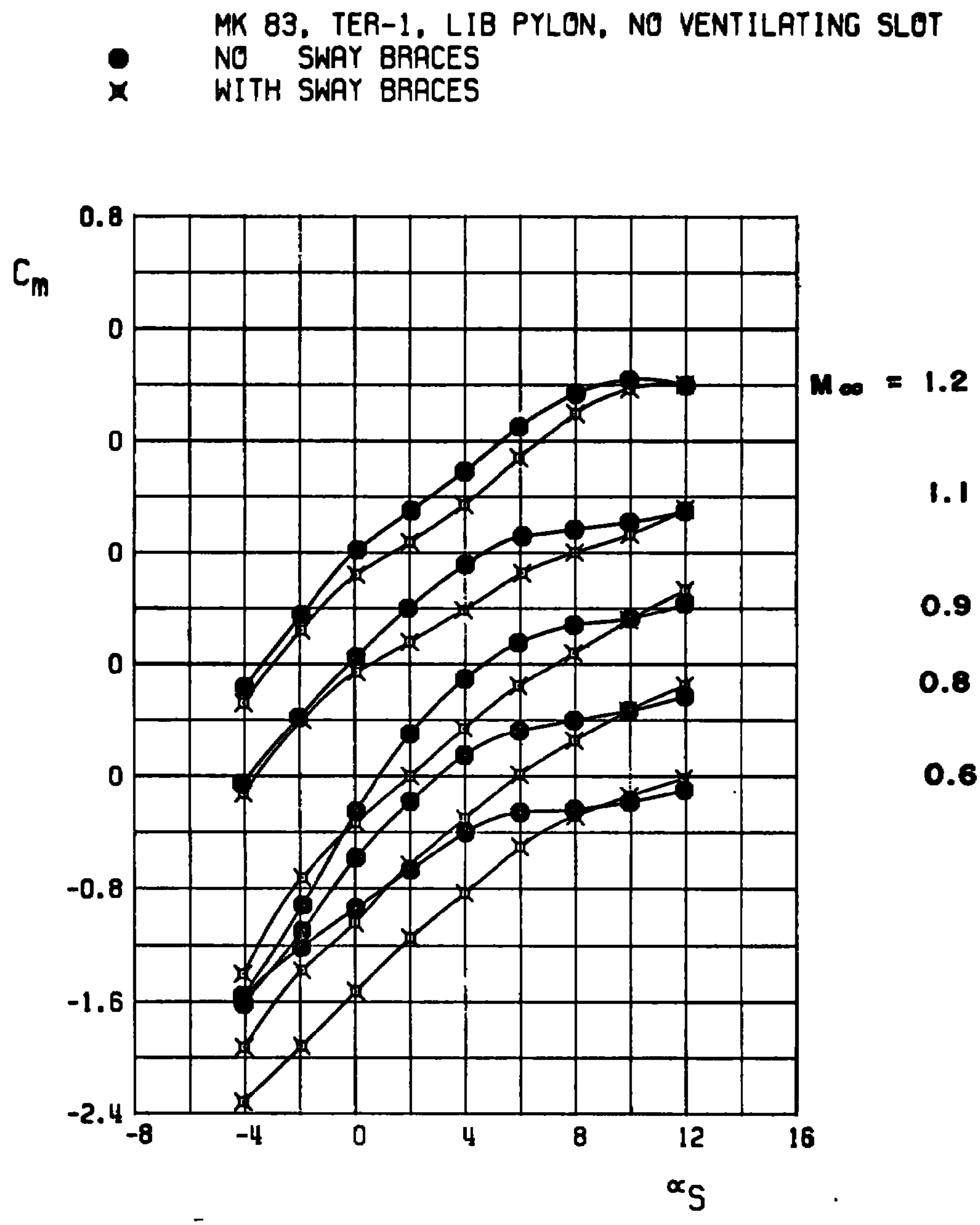

i. Pitching-moment coefficient
Figure 18. Continued.

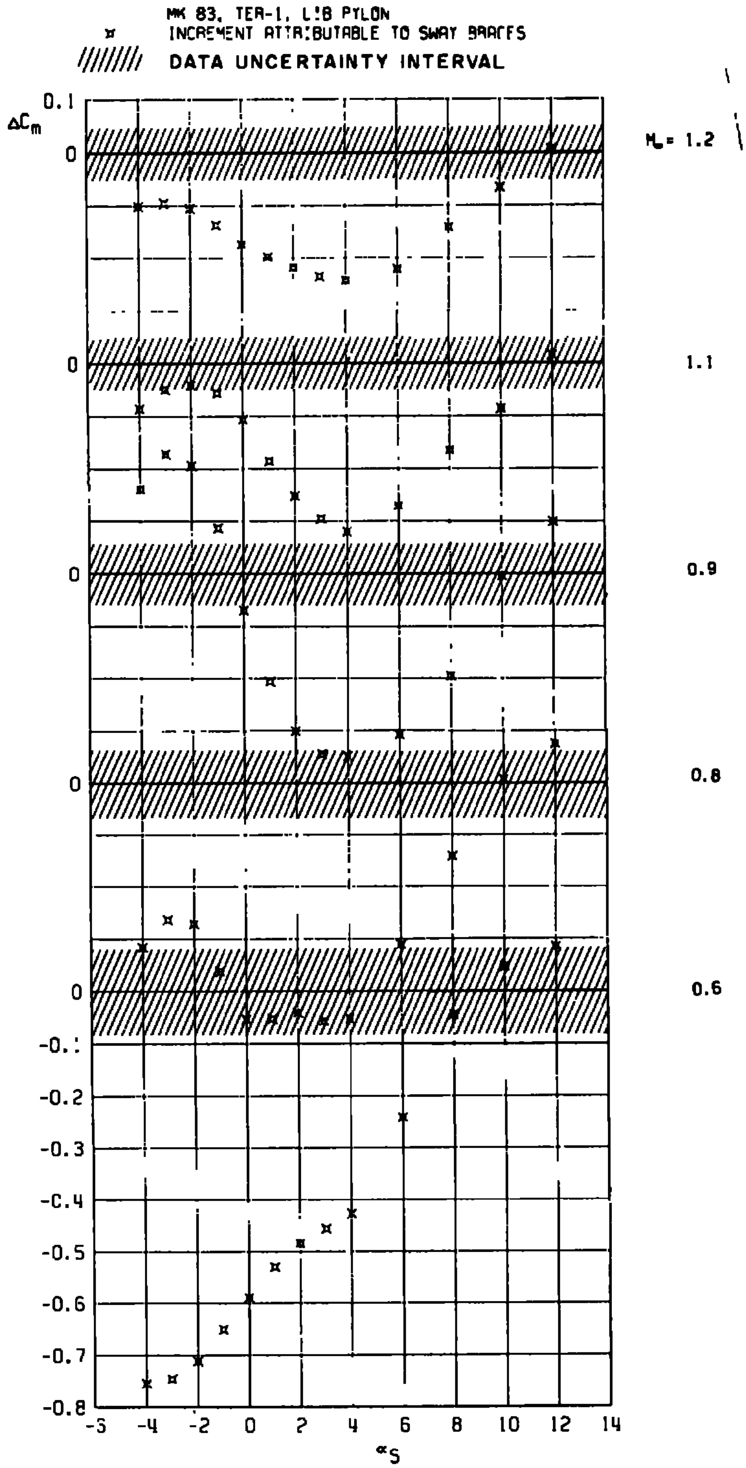

j. Increment in pitching-moment coefficient
Figure 18. Continued.

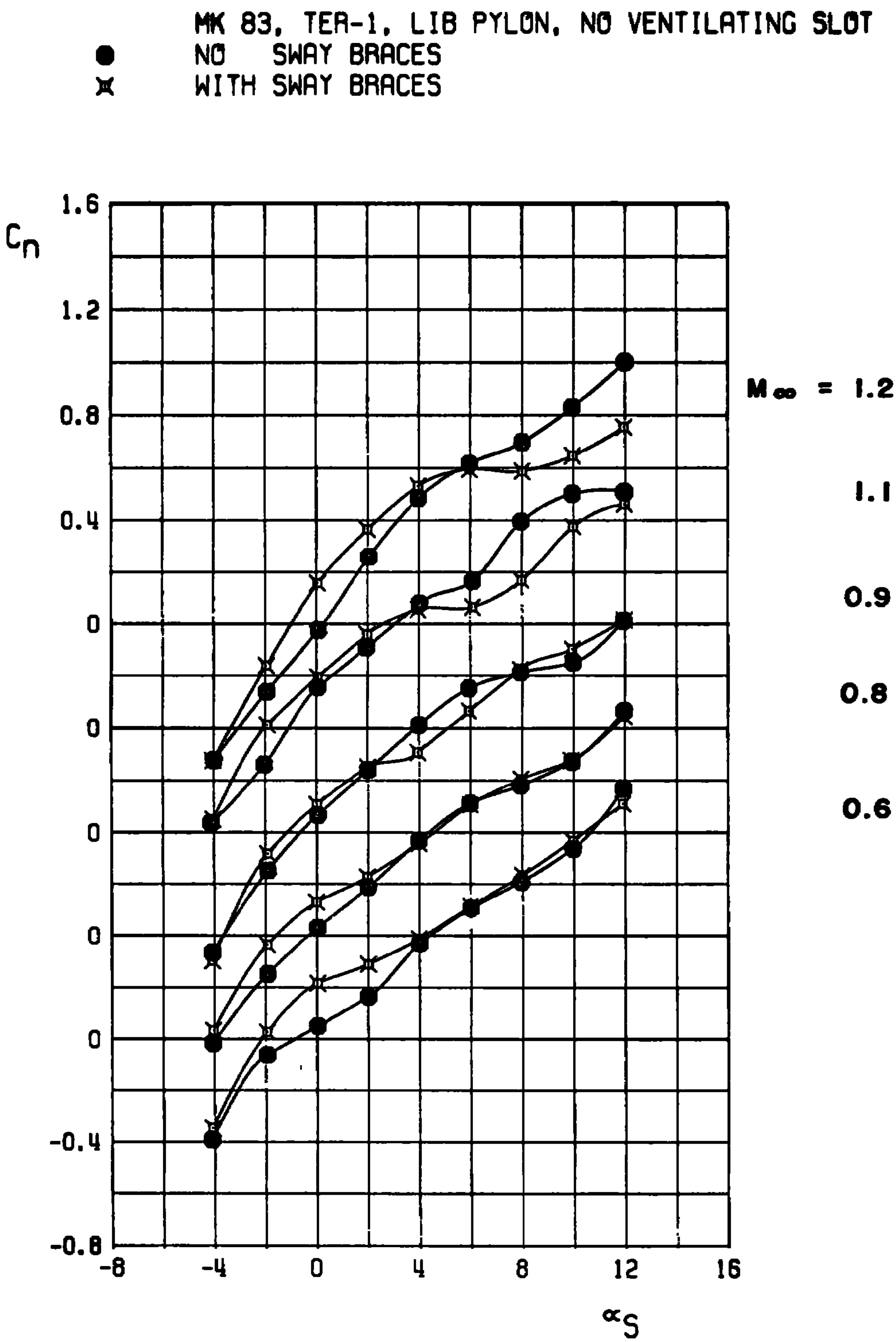

k. Yawing-moment coefficient
Figure 18. Continued.

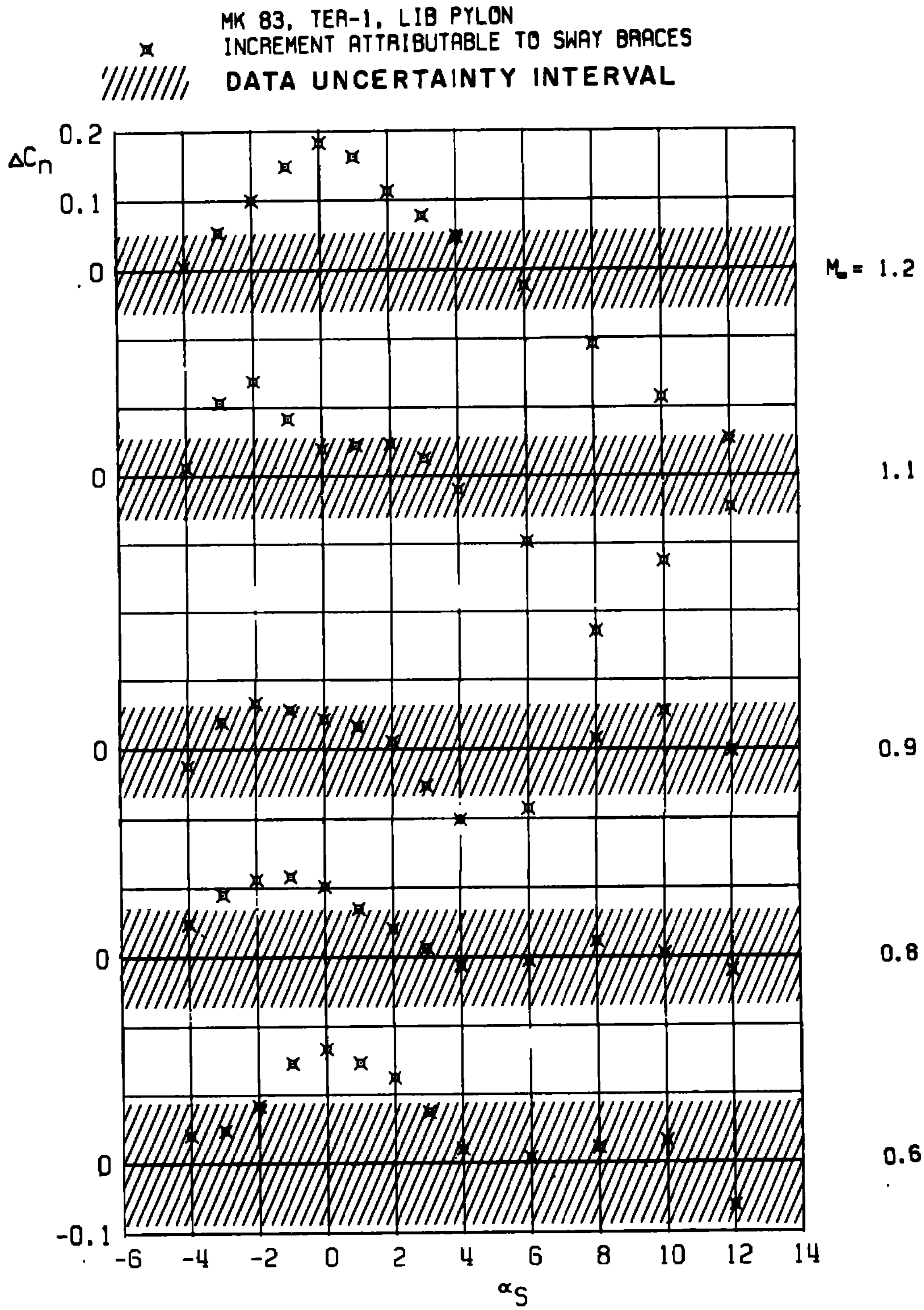

l. Increment in yawing-moment coefficient
Figure 18. Concluded.

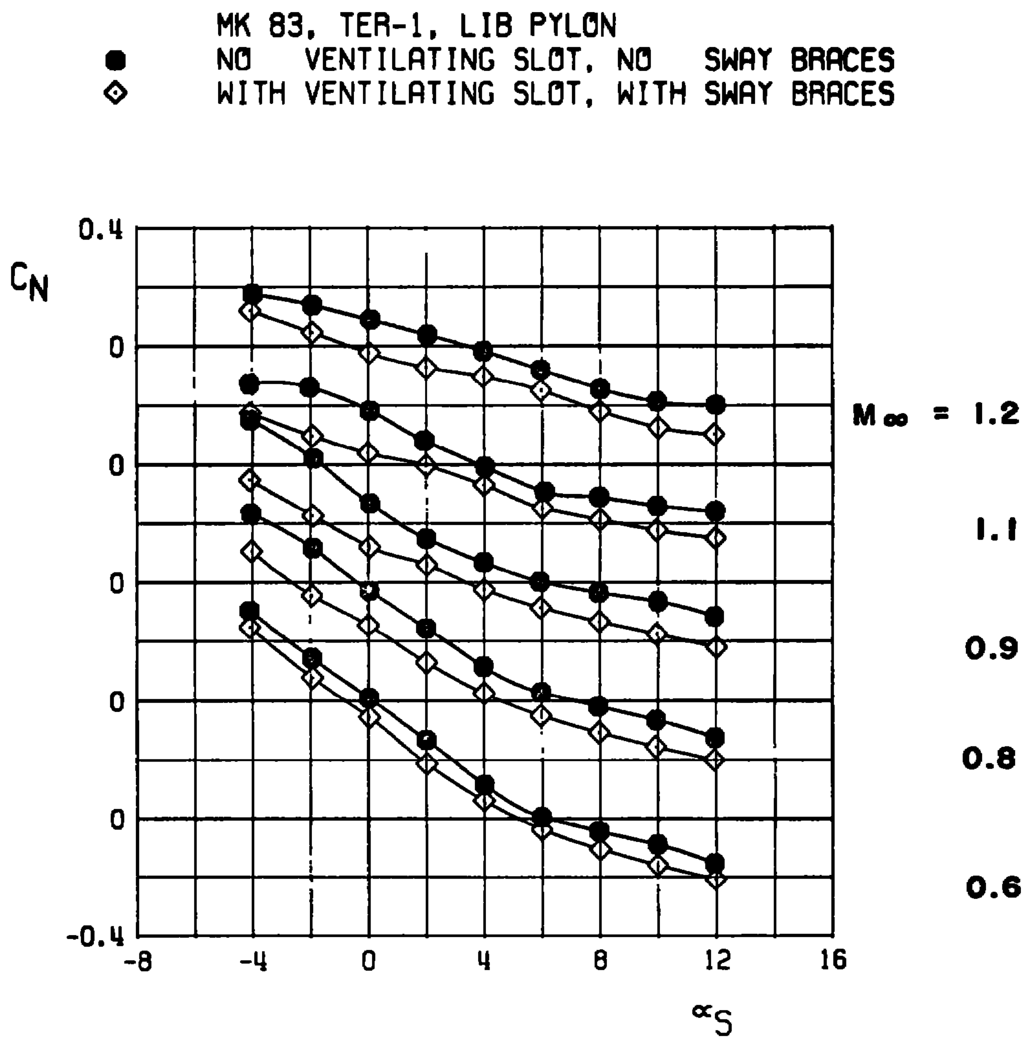

a. Normal-force coefficient

Figure 19. Combined effects of both a ventilated supporting bracket and triple ejector rack and triple ejector rack sway braces on the static aerodynamic loads acting on a stable triple ejector rack-mounted store.

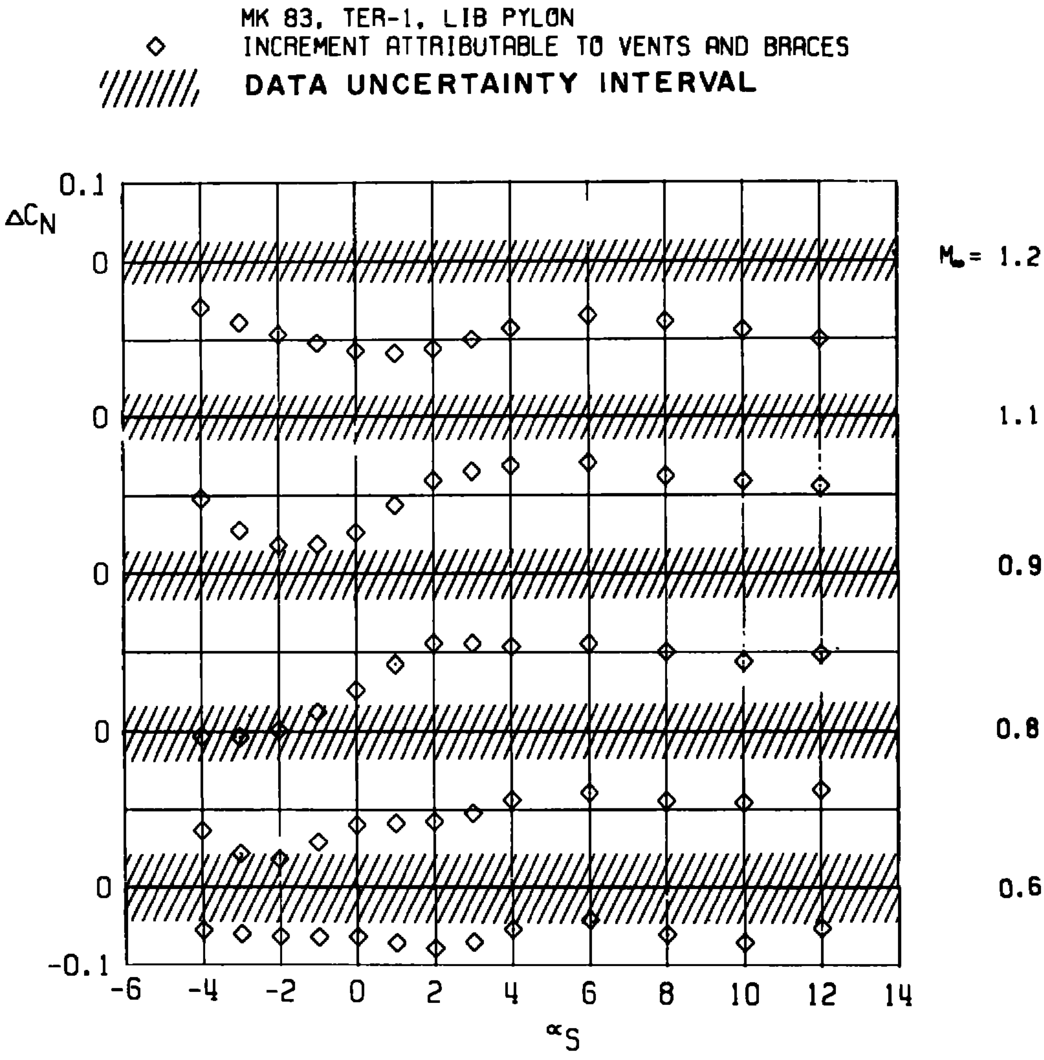

b. Increment in normal-force coefficient
Figure 19. Continued.

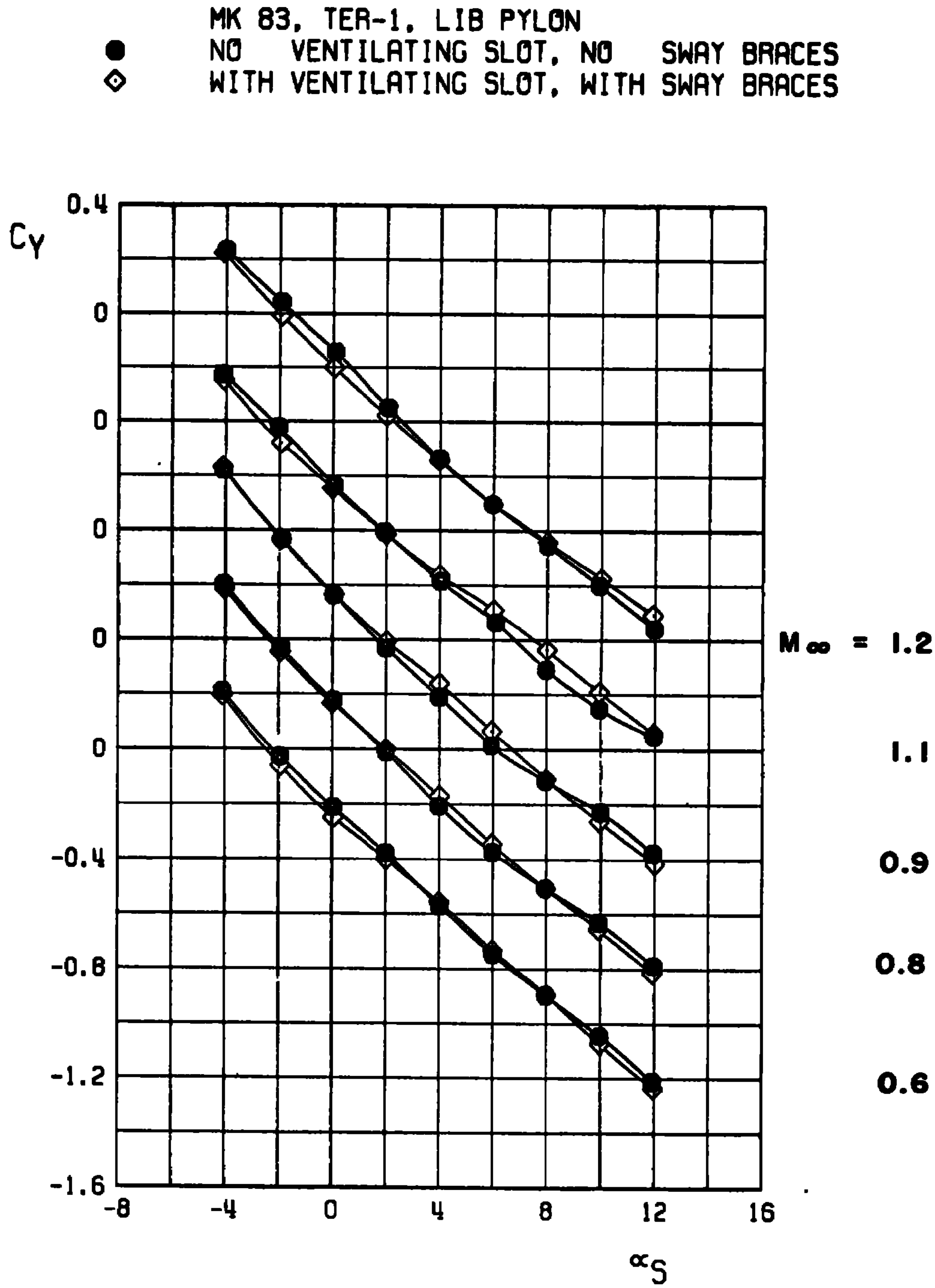

c. Side-force coefficient
Figure 19. Continued.

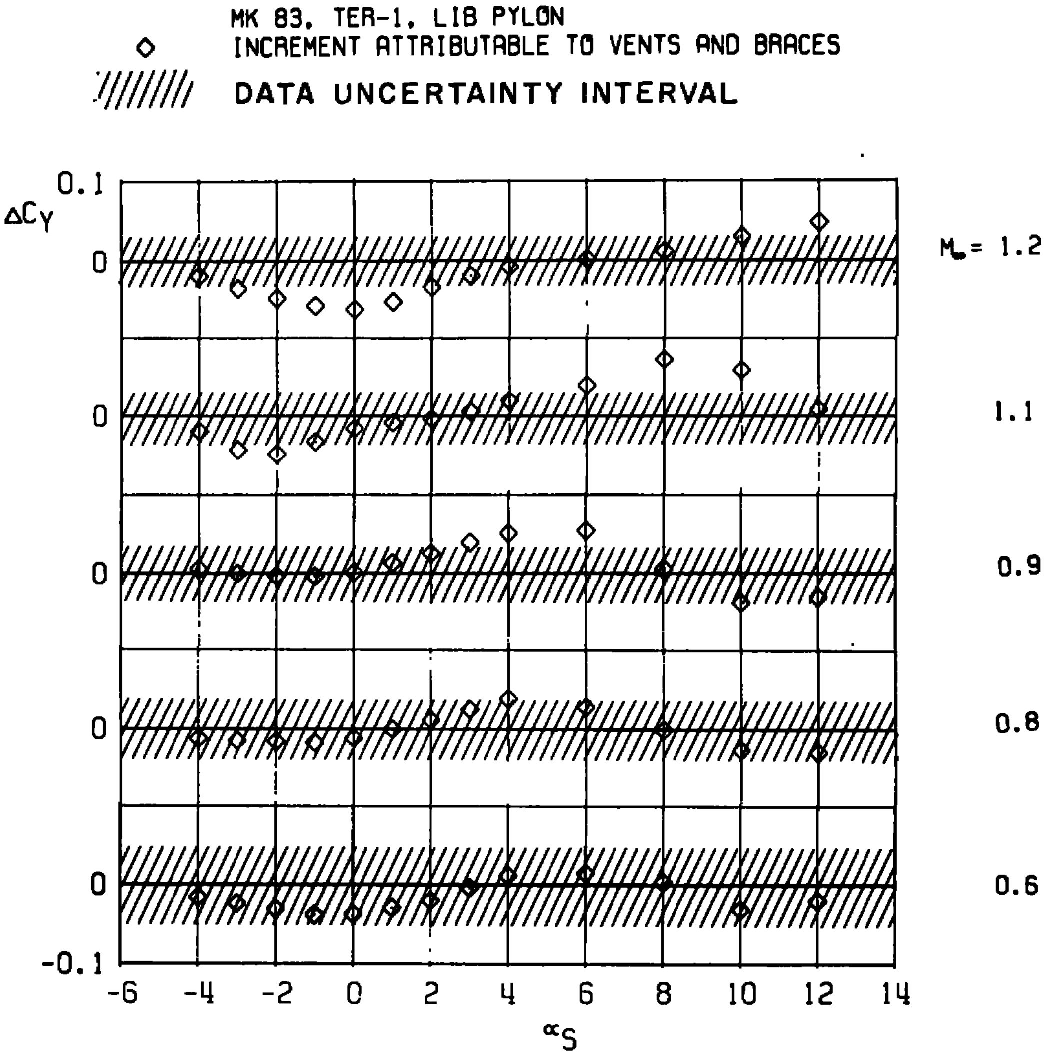

d. Increment in side-force coefficient
Figure 19. Continued.

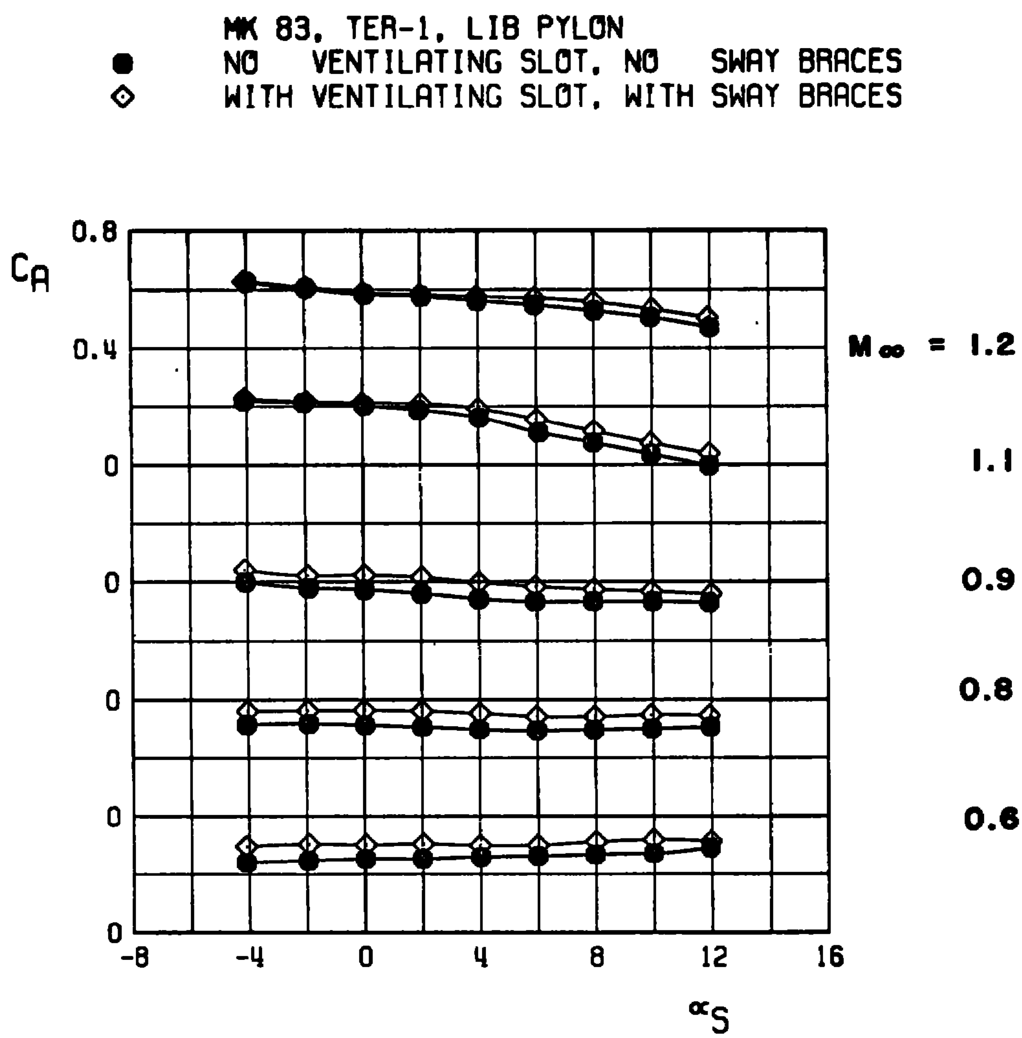

e. Axial-force coefficient
Figure 19. Continued.

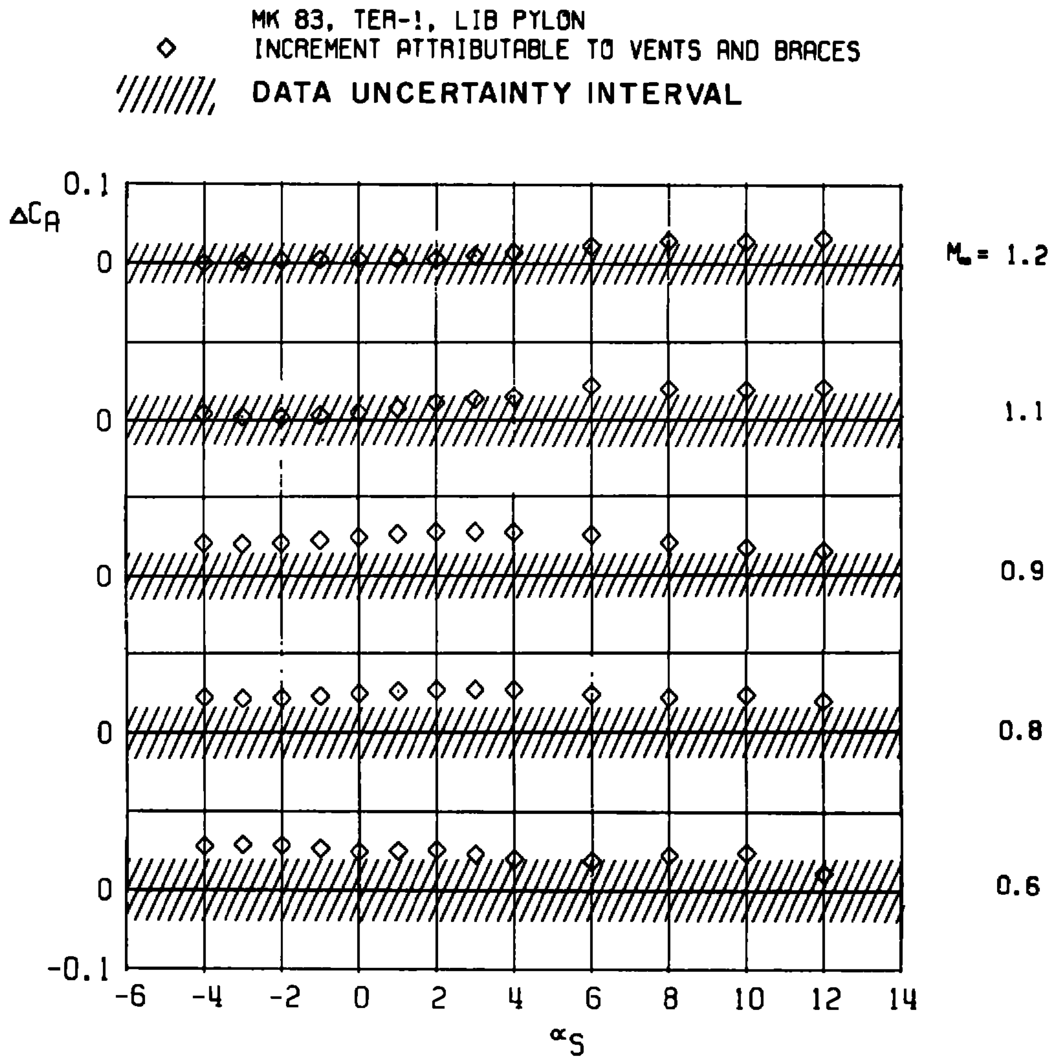

f. Increment in axial-force coefficient
Figure 19. Continued.

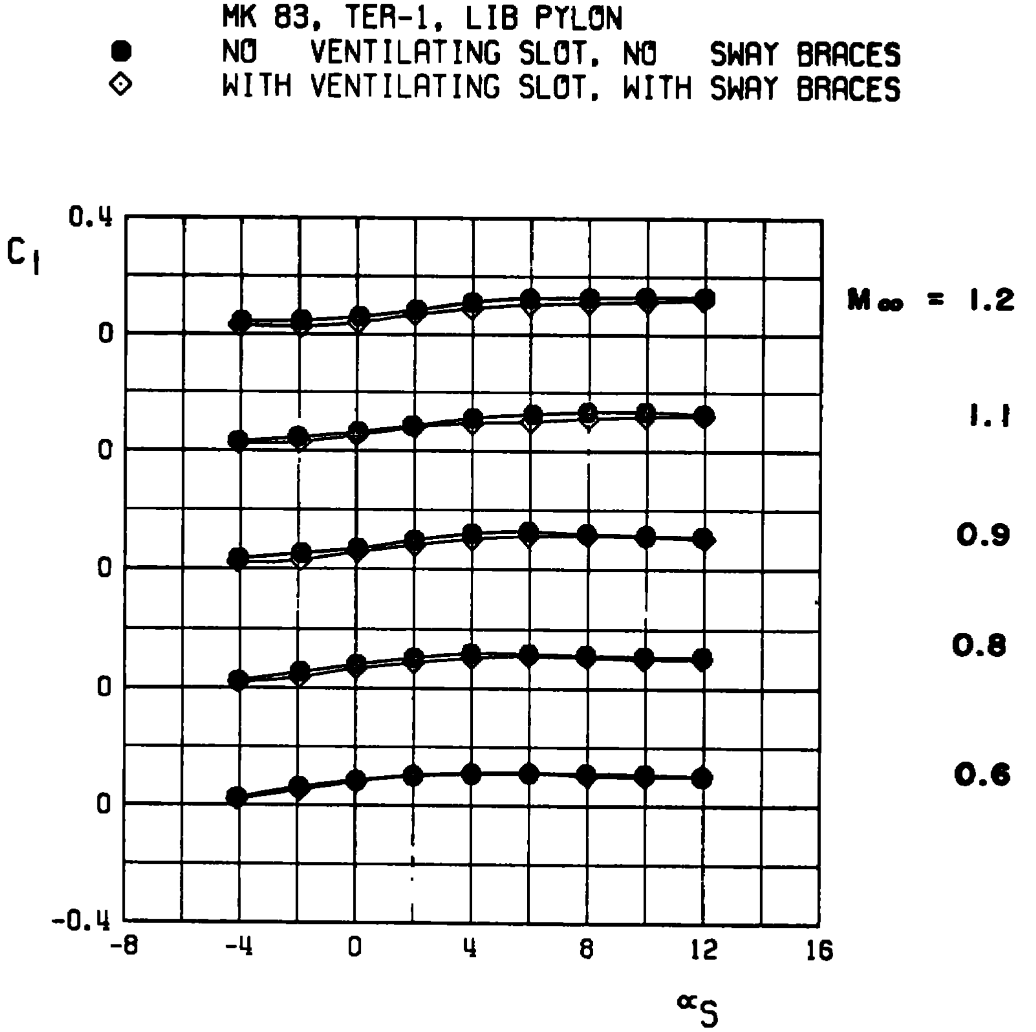

g. Rolling-moment coefficient
Figure 19. Continued.

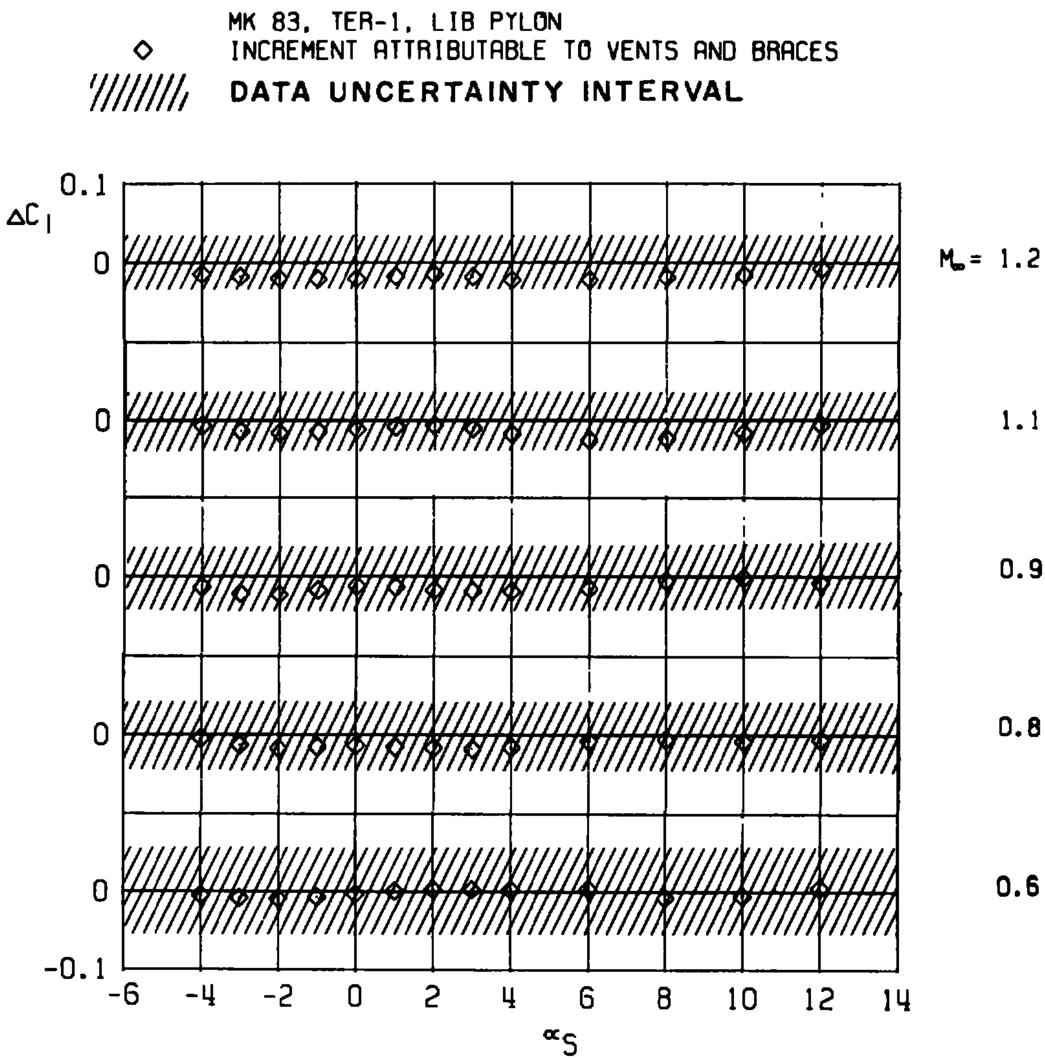

h. Increment in rolling-moment coefficient.
Figure 19. Continued.

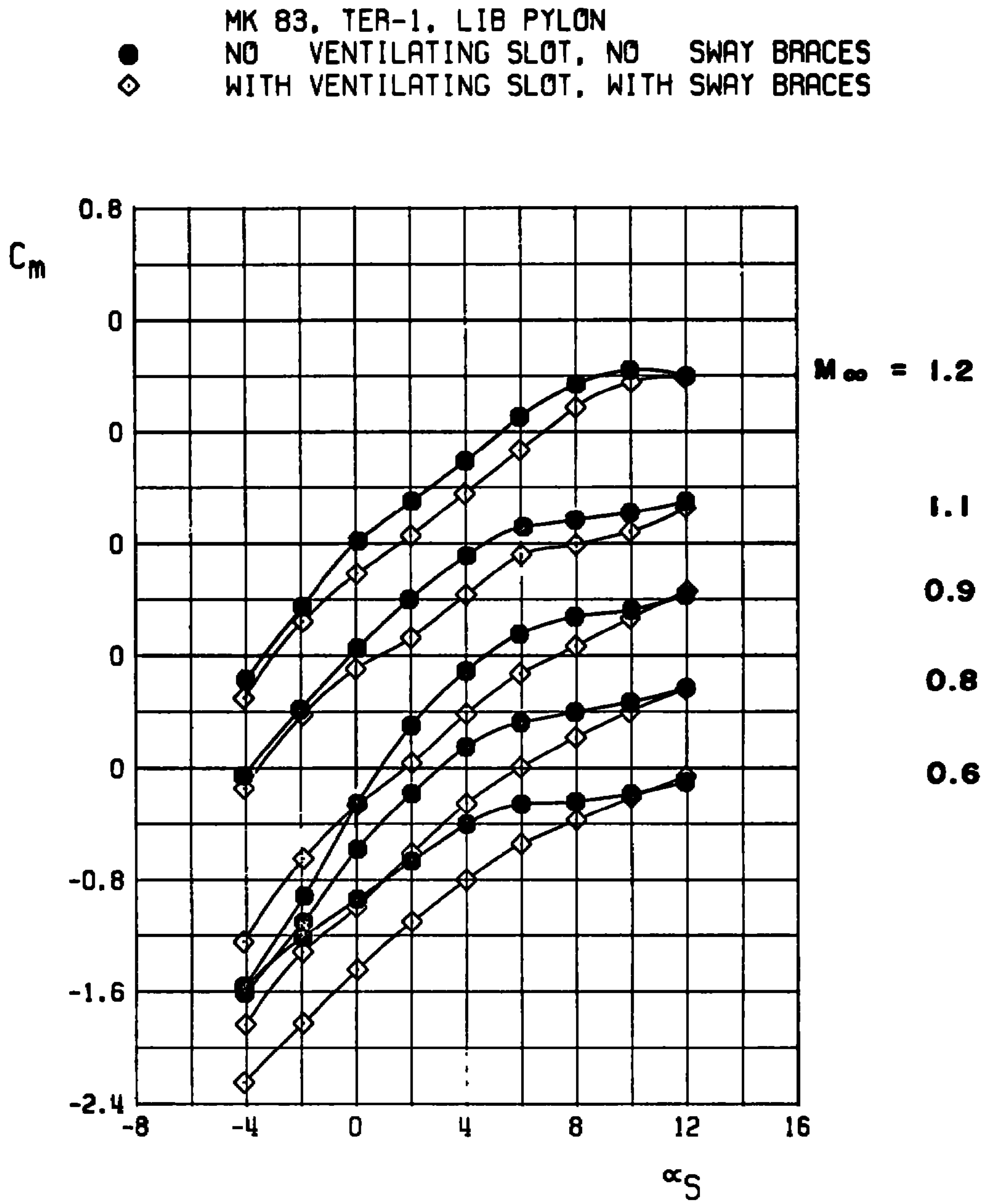

i. Pitching-moment coefficient
Figure 19. Continued.

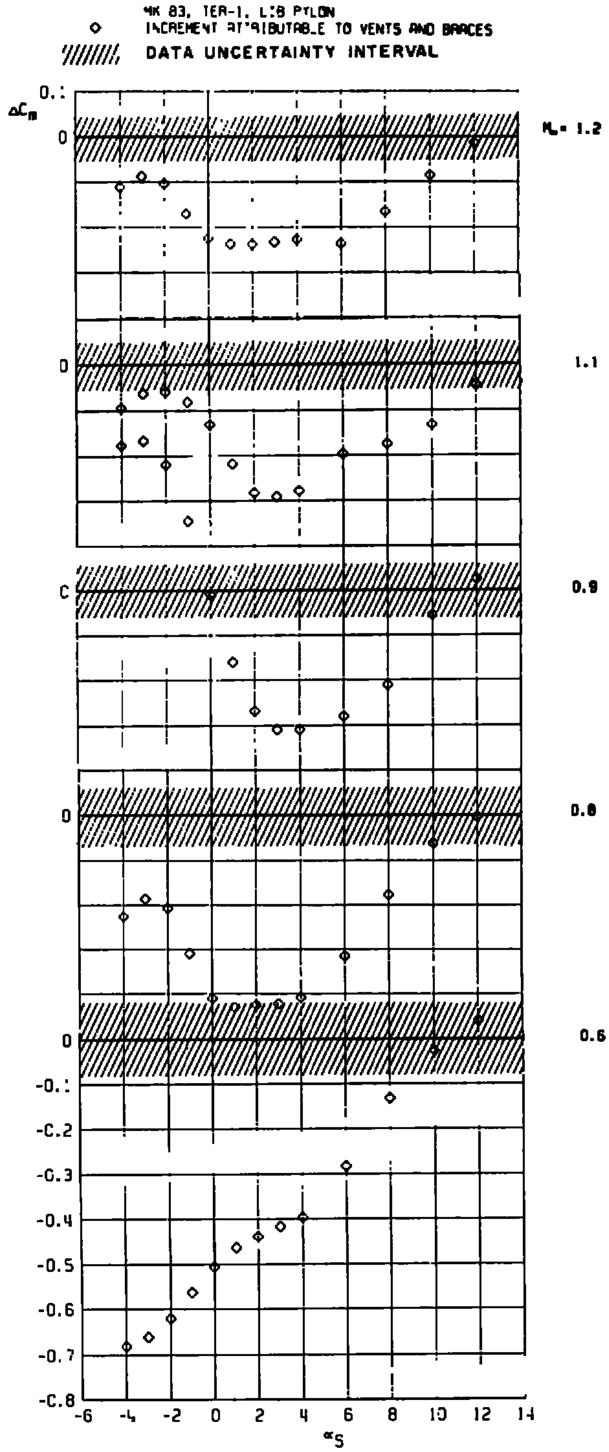

j. Increment in pitching-moment coefficient
Figure 19. Continued.

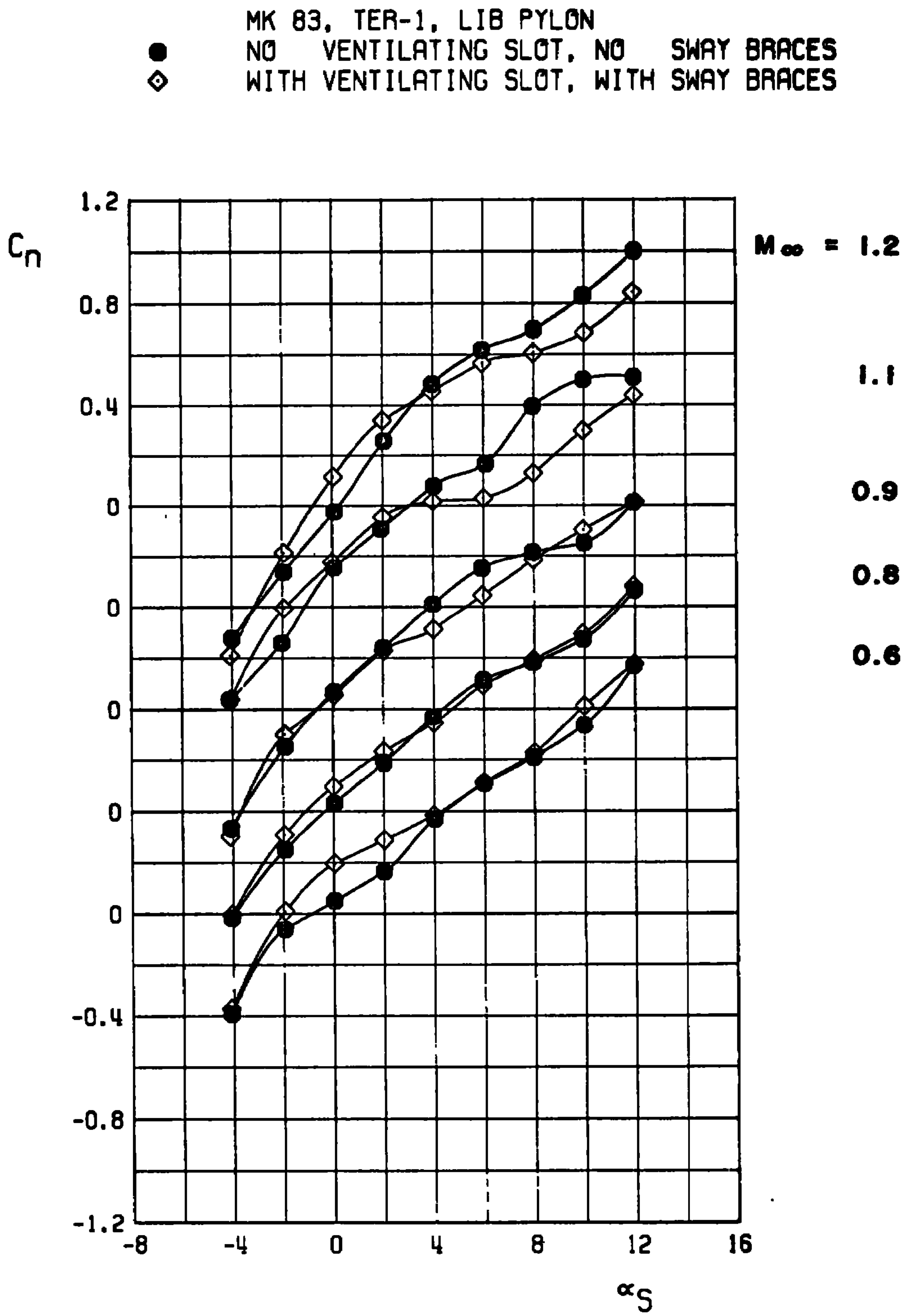

k. Yawing-moment coefficient
Figure 19. Continued.

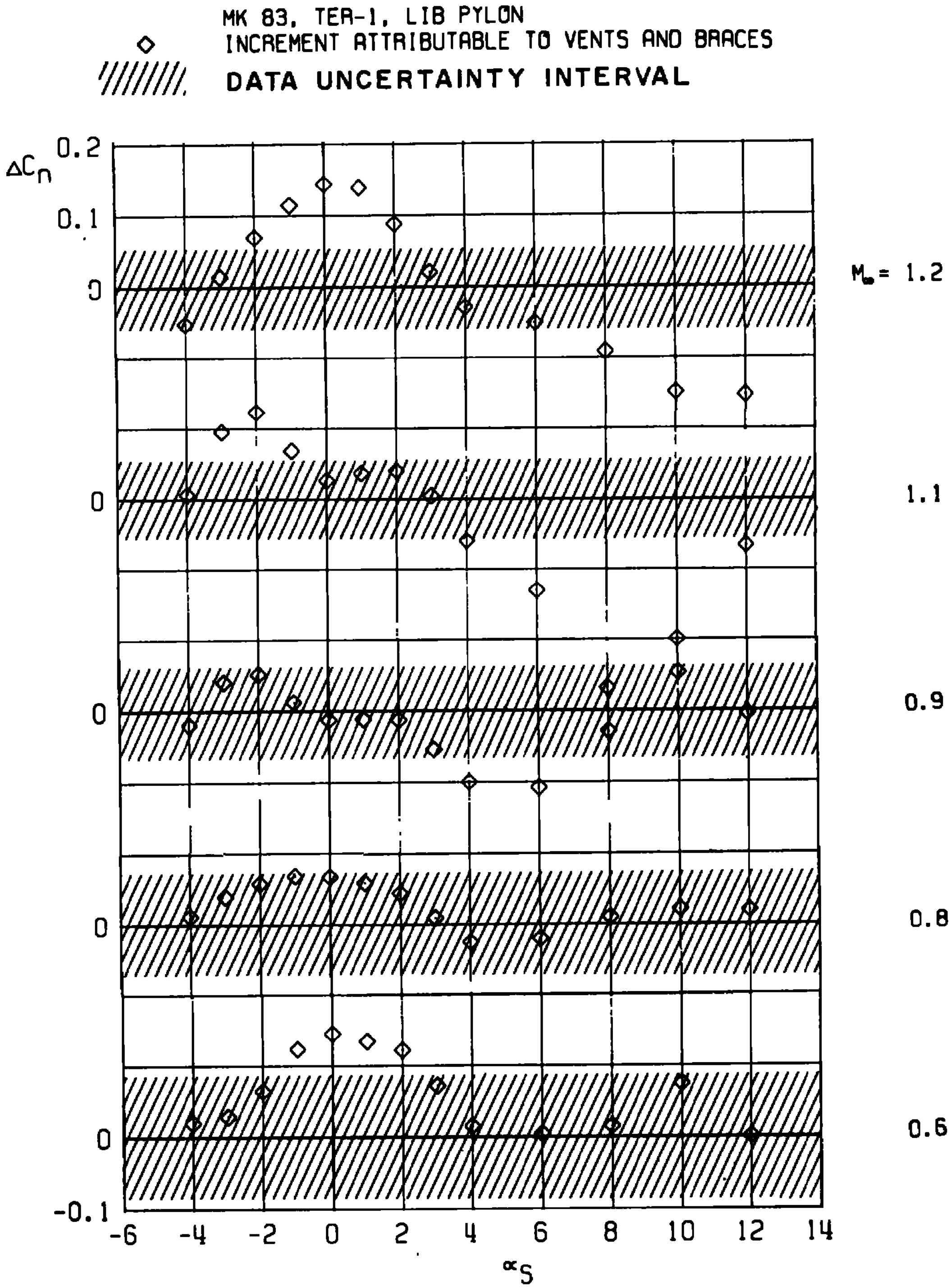

l. Increment in yawing-moment coefficient
Figure 19. Concluded.

Table 1. Miscellaneous Dimensions of Store Models

Full-Size Dimensions

Store	L, ft	D, ft	S, ft^2	X_{FL}, ft	X_{CG}, ft	Weight, lb
Black Crow	14.560	1.8333	2.6398	7.577	8.827	659
M-118	15.188	2.0100	3.1731	3.457	4.683	3049
MK 83	9.898	1.1667	1.0690	3.625	4.208	985

Full-Size Dimensions

Store	I_{xx}, slug-ft^2	I_{yy}, slug-ft^2	I_{zz}, slug-ft^2	I_{xz}, slug-ft^2	C_{ℓ_p}	C_{m_q}	C_{n_r}
Black Crow	11.9	260.2	259.8	0	0	-60.5	-60.5
M-118	50.7	685.0	685.0	0	-4.0	-70.0	-70.0
MK 83	5.4	114.0	114.0	3.73	-0.75	-75.0	-75.0

Table 2. Uncertainty Intervals in Force and Moment Coefficients for Store Models

Store	M_∞	$\varepsilon(C_N)$	$\varepsilon(C_Y)$	$\varepsilon(C_A)$	$\varepsilon(C_\ell)$	$\varepsilon(C_m)$	$\varepsilon(C_n)$
Black Crow	0.6	±0.033	±0.063	±0.042	±0.045	±0.082	±0.054
	0.8	±0.026	±0.050	±0.034	±0.036	±0.066	±0.043
	0.9	±0.024	±0.046	±0.031	±0.033	±0.060	±0.039
	1.1	±0.021	±0.041	±0.027	±0.029	±0.053	±0.035
	1.2	±0.020	±0.039	±0.026	±0.028	±0.051	±0.033
M-118	0.6	±0.026	±0.050	±0.033	±0.032	±0.059	±0.038
	0.8	±0.021	±0.040	±0.027	±0.026	±0.047	±0.031
	0.9	±0.019	±0.037	±0.025	±0.024	±0.044	±0.029
	1.1	±0.017	±0.033	±0.022	±0.021	±0.039	±0.025
	1.2	±0.016	±0.031	±0.021	±0.020	±0.037	±0.024
MK 83	0.6	±0.042	±0.048	±0.039	±0.053	±0.078	±0.086
	0.7	±0.038	±0.042	±0.035	±0.047	±0.069	±0.076
	0.8	±0.034	±0.038	±0.031	±0.043	±0.063	±0.069
	0.9	±0.031	±0.035	±0.029	±0.039	±0.058	±0.063
	1.1	±0.028	±0.031	±0.026	±0.035	±0.051	±0.056
	1.2	±0.027	±0.030	±0.025	±0.033	±0.049	±0.054

APPENDIX A
EFFECT OF SWAY BRACES ON STORE SEPARATION TRAJECTORIES

As part of the program of experiments discussed herein, a few separation trajectories were predicted using the CTS. Only the effects of the sway braces could be studied, since there were no internal brackets required for the sting-supported CTS experiments. It was not within the scope of the study to completely define the effect of sway braces on separation trajectories, but to simply determine whether or not effects existed. Therefore, only a few uncomplicated cases were investigated.

The effects of simulating pylon sway braces for the M-118 separating from the left inboard pylon of the F-4C are presented in Fig. A-1. Release conditions included an angle of attack of the aircraft of 1 deg, no ejector force, and level flight. The presentation of pitch angle as a function of vertical travel of the store is one indication of store clearance. Termination of the trajectories was caused by a limitation of travel permitted the CTS within the test section of the wind tunnel rather than a contact between the store and aircraft models. While the effect of sway braces at a Mach number of 0.6 is negligible, the effect at a Mach number of 0.9 is significant (approximately 15 percent at a travel of 2 ft).

Significant effects of the sway braces on the trajectory of the MK 83 separating from TER station 1 on the left inboard pylon of the F-4C are also apparent in Fig. A-2. An ejector force of 1,200 lb was used for a level-flight release at an angle of attack of the aircraft of 3.3 deg for a Mach number of 0.6, and 1.1 deg for a Mach number of 0.9. At a Mach number of 0.6, at least a 25-percent effect is evident at a travel of 4 ft. Even though the trajectory for Mach number 0.9 was terminated by an early contact of the store sting with the aircraft (attributable to the rapid pitchdown of the store), both with and without the sway braces, the presence of the sway braces evidently aggravated the already severe pitchdown. (The more severe pitchdown is consistent with the large negative effect of the sway braces on the pitching moment acting on the store in the captive position, observed in Fig. 17e.) Concern over the validity of separation trajectories predicted without TER sway braces appears warranted. Further study of the effect of sway braces on separation trajectories derived from wind tunnel experiments, either CTS or grid, seems necessary.

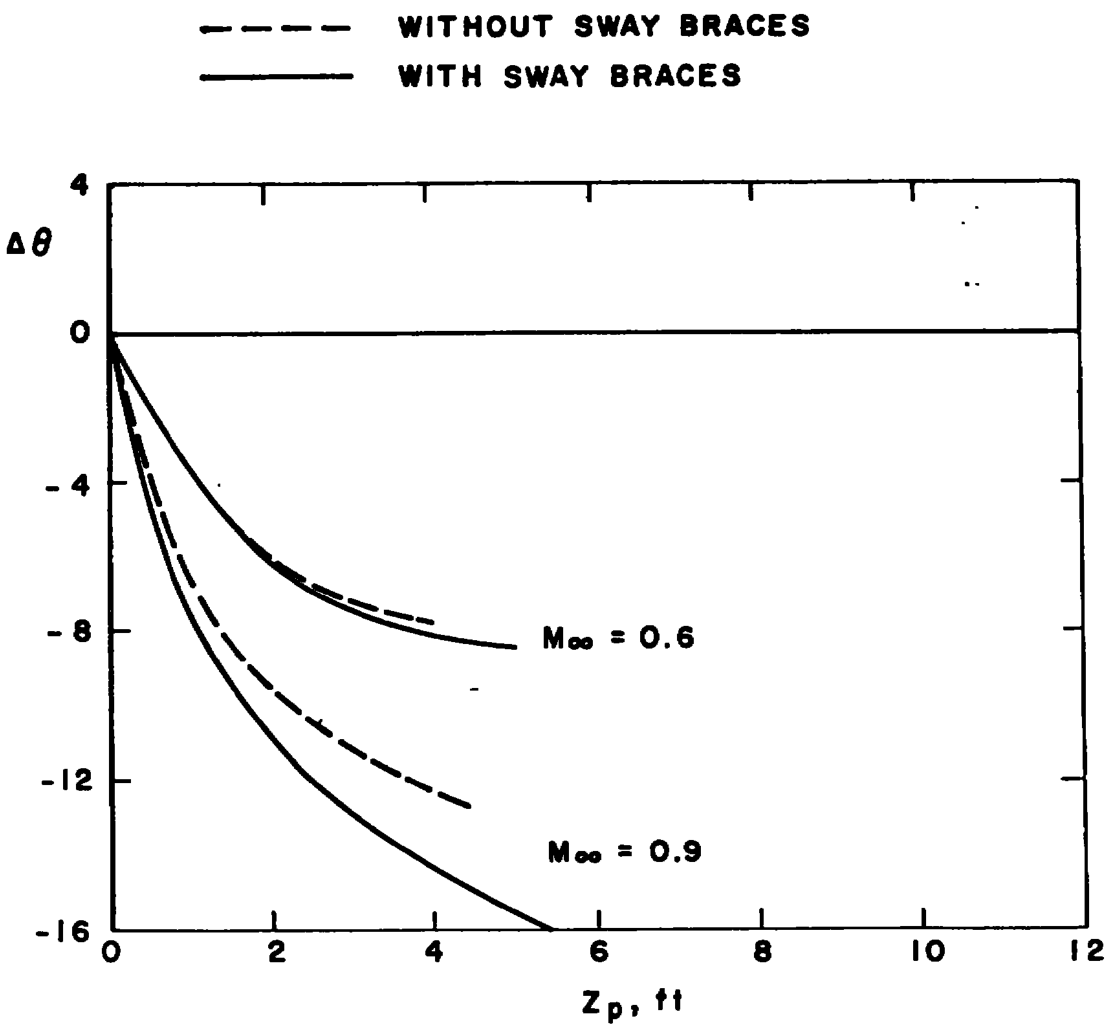

Figure A-1. Effect of sway braces on the separation trajectory of the M-118 bomb, left inboard pylon, level flight, zero ejector force.

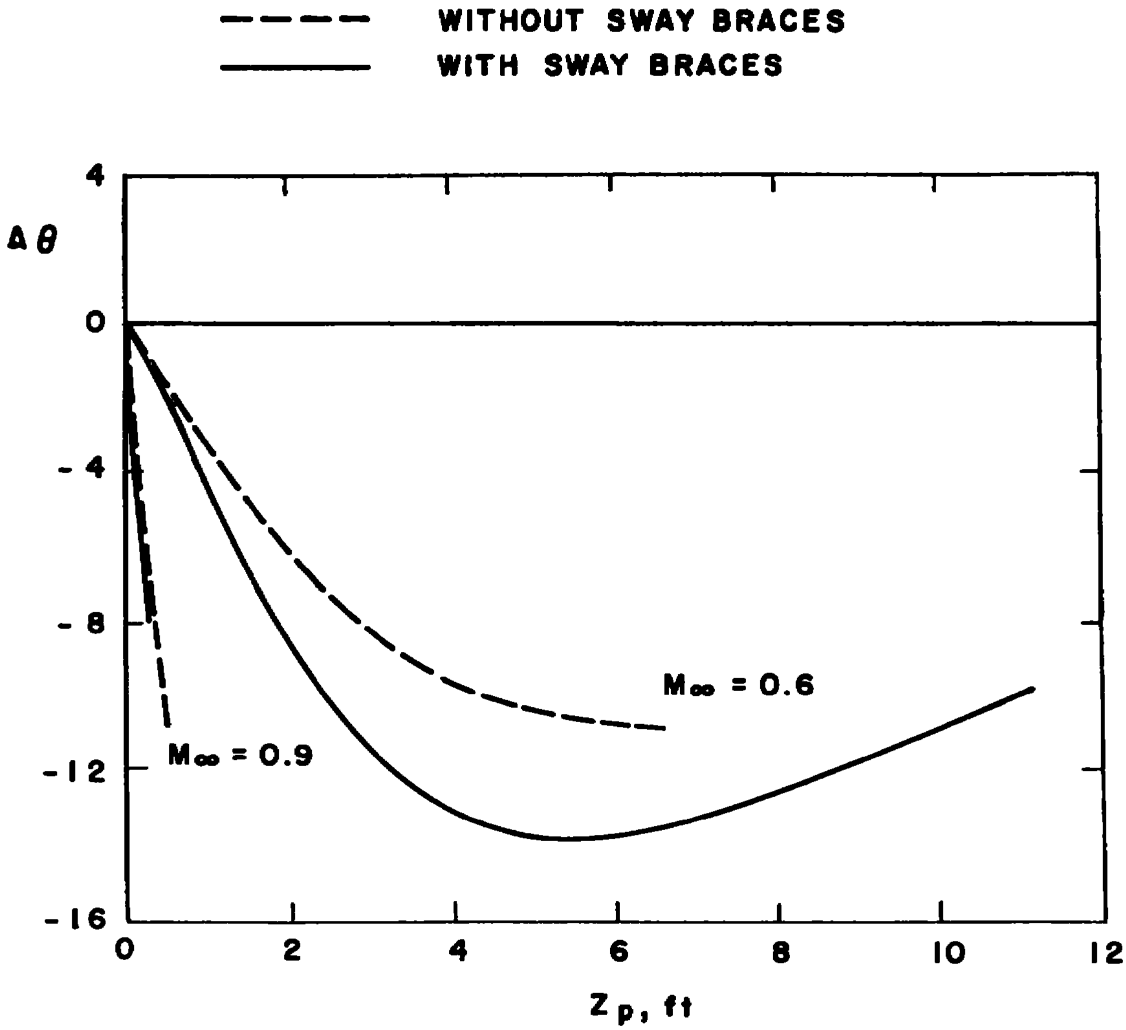

Figure A-2. Effect of sway braces on the separation trajectory of the MK 83 low-drag bomb, left inboard pylon, TER station 1, level flight, 1,200-lb ejector force.

APPENDIX B
COMPARISON OF FLIGHT TEST DATA WITH WIND TUNNEL DATA INCLUDING SWAY BRACES

Another indication of the advisability of simulating sway braces in wind tunnel experiments can be inferred from Fig. B-1. A series of flight tests of the same MK 83/TER/F-4C configuration as used in the wind tunnel experiments discussed herein was conducted at the Naval Air Test Center, Patuxent River, Maryland, June 1976. It is beyond the scope of this report to discuss the results of the flight test in detail, but a brief comparison of wind tunnel and flight data is instructive.

From Fig. B-1, comparing the current wind tunnel data with the flight data at the same nominal Mach numbers, it is clear that simulating sway braces on the wind tunnel model did improve the correlation of flight and wind tunnel data. It should be noted that the unit Reynolds number in both wind tunnel and flight tests was approximately 3.5×10^6 per foot, with, of course, a factor of 20 between the values of the total Reynolds numbers of the two tests. Notwithstanding the large discrepancy in true dynamic similarity of the test flows, the correlation between test results is good. Of primary importance, however, is the improvement in correlation attributable to the presence of sway braces on the model.

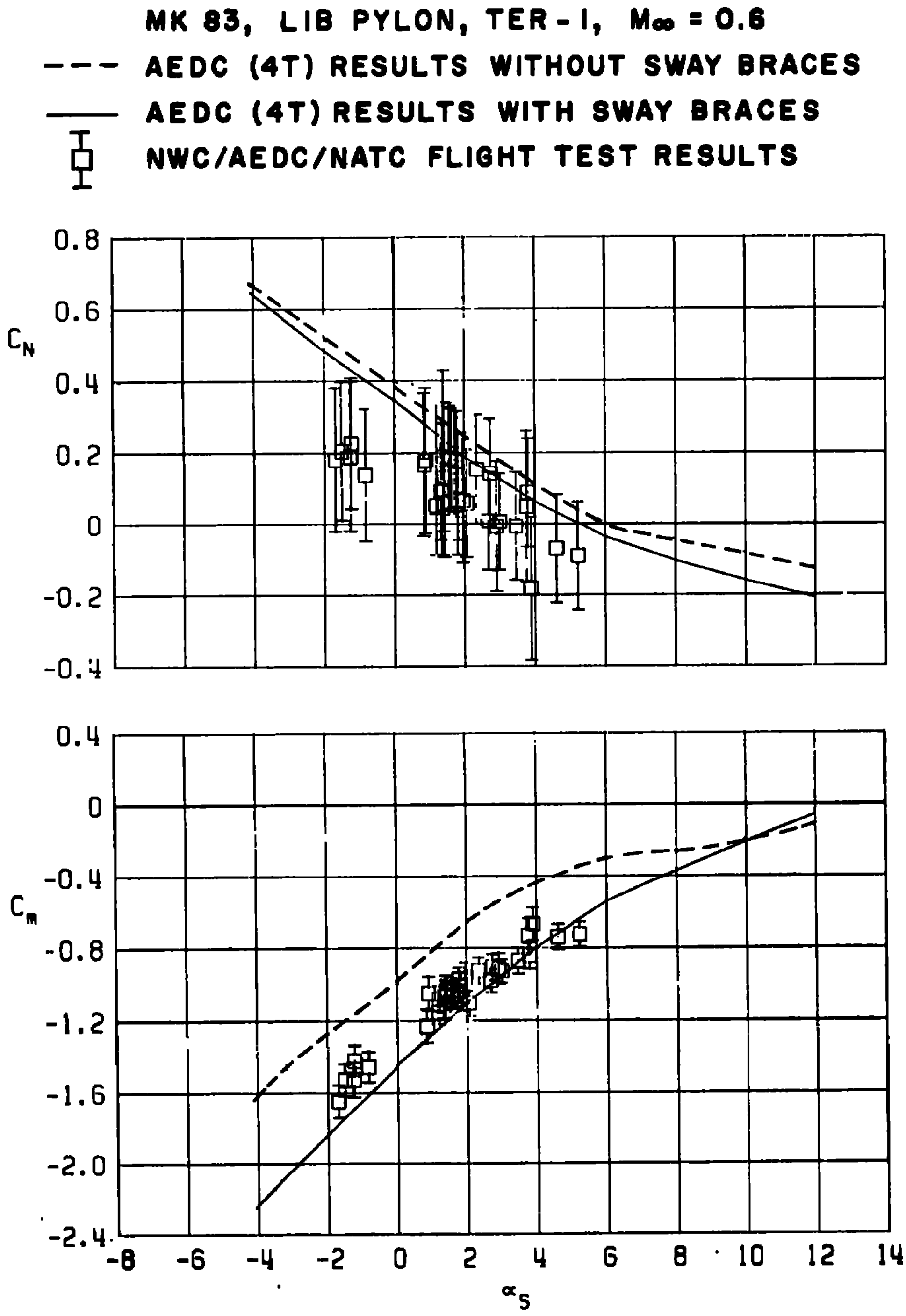

Figure B-1. Effect of sway braces on the comparison of wind tunnel and in-flight measurements of captive-position store loads for the MK 83 low-drag bomb.

NOMENCLATURE

BL	Aircraft buttock line, measured from the plane of symmetry of the model, in., model scale
C_A	Coefficient of measured axial force acting on a store model, measured axial force/$q_\infty S$
C_ℓ	Coefficient of measured rolling moment acting about the axis of symmetry of a store model, measured rolling moment/$q_\infty SD$
C_{ℓ_p}	Roll-damping derivative of a store, $dC_\ell/d(pb/2V_\infty)$
C_m	Coefficient of measured pitching moment acting about the cg of a store model, measured pitching moment/$q_\infty SD$
C_{m_q}	Pitch-damping derivative of a store, $dC_m/d(qD/2V_\infty)$
C_N	Coefficient of measured normal force acting on a store model, measured normal force/$q_\infty S$
C_n	Coefficient of measured yawing moment acting about the cg of a store model, measured yawing moment/$q_\infty D$
C_{n_r}	Yaw-damping derivative of a store, $dC_n/d(rD/2V_\infty)$
C_Y	Coefficient of measured side force acting on a store model, measured side force/$q_\infty S$
D	Maximum diameter of a store model, in., model scale
FS	Fuselage station of the aircraft model, in., model scale
I_{xx}	Moment of inertia of the full-scale store about the longitudinal body axis of the store, slug-ft^2
I_{xz}	Product of inertia of the full-scale store with respect to the longitudinal and vertical body axes of the store, slug-ft^2
I_{yy}	Moment of inertia of the full-scale store about the lateral body axis of the store, slug-ft^2
I_{zz}	Moment of inertia of the full-scale store about the vertical body axis of the store, slug-ft^2

L Maximum length of a store model, in., model scale

M_∞ Free-stream Mach number

p Angular rolling velocity of a store about the longitudinal body axis of the store, radians/sec

p_{t_∞} Free-stream total pressure, psfa

p_∞ Free-stream static pressure, psfa

q Angular pitching velocity of a store about the lateral body axis of the store, radians/sec

q Free-stream dynamic pressure, $0.7p_\infty M_\infty^2$, psfa

r Angular yawing velocity of a store about the vertical body axis of the store, radians/sec

S Reference area of a store model (maximum cross-sectional area), $\pi D^2/4(144)$, ft^2

V_∞ Free-stream velocity, ft/sec

WL Waterline of the aircraft model, measured from the horizontal reference plane of the aircraft, in., model scale

X_{CG} Location of the cg of a store, measured from the extreme tip of the nose of the store and along the longitudinal body axis of the store, in., model scale

X_{FL} Location of the forward suspension lug of a store, measured from the extreme tip of the nose of the store and along the longitudinal body axis of the store, in., model scale

Z_P Travel of the cg of the store in the pylon-axis system Z_P direction, ft, full scale, measured from the captive position of the store

α_s Gravimetric angle of attack of a store model, degrees

ΔC_x Increment in a measured force or moment coefficient attributable to use of a ventilated bracket, sway braces, or both, as applicable (coefficient with a feature) (coefficient without the feature)

$\Delta\theta$ Difference in θ at a point in the trajectory and the value of θ in the captive position

$\epsilon(C_x)$ Uncertainty interval of a measured force or moment coefficient

θ Angle between the longitudinal axis of a store and the projection of the longitudinal axis in the X_P-Y_P plane

FLIGHT-AXIS SYSTEM COORDINATES

Directions

X_F Parallel to the free-stream wind vector, positive direction is forward as seen by the pilot

Y_F Perpendicular to the X_F and Z_F direction, positive direction is to the right as seen by the pilot

Z_F Parallel to the aircraft plane of symmetry and perpendicular to the free-stream wind vector, positive direction is downward

The flight-axis system origin is coincident with the aircraft cg and remains fixed with respect to the aircraft during store separation. The X_F, Y_F, and Z_F coordinate axes do not rotate with respect to the initial flight direction and attitude.

STORE BODY-AXIS SYSTEM COORDINATES

Directions

X_B Parallel to the store longitudinal axis, positive direction is upstream in the captive position

Y_B Perpendicular to the store longitudinal axis, and parallel to the flight-axis system X_F-Y_F plane when the store is at zero roll angle, positive direction is to the right looking upstream when the store is at zero yaw and roll angles

Z_B Perpendicular to both the X_B and Y_B axes, positive direction is downward as seen by the pilot when the store is at zero pitch and roll angles

The store body-axis system origin is coincident with the store cg and moves with the store during separation from the parent aircraft. The X_B, Y_B, and Z_B coordinate axes rotate with the store in pitch, yaw, and roll so that mass moments of inertia about the three axes are not time-varying quantities.

PYLON-AXIS SYSTEM COORDINATES

Directions

X_P Parallel to the store longitudinal axis in the captive position, positive direction is forward as seen by the pilot

Y_P Perpendicular to the X_P axis and parallel to the flight-axis system X_F-Y_F plane, positive direction is to the right as seen by the pilot

Z_P Perpendicular to both the X_P and Y_P axes, positive direction is downward

The pylon-axis system origin is coincident with the store cg in the captive position. The axes are rotated with respect to the flight-axis system by the pitch angles of the aircraft. Both the origin and the direction of the coordinate axes remain fixed with respect to the flight-axis system throughout the trajectory.